AN RF-ISOLATED REAL-TIME MULTIPATH TESTBED FOR PERFORMANCE ANALYSIS OF WLANS

A Thesis submitted to the Faculty of

WORCESTER POLYTECHNIC INSTITUTE

in partial fulfillment of the requirements for the degree of

Master of Science

in

Electrical and Computer Engineering

by

_____

Leon Teruo Metreaud

(leonm@qualcomm.com)

August 17th 2006

APPROVED:

_____   _____

Prof. Kaveh Pahlavan, Thesis Advisor   Prof. Fred J. Looft, Department Head

_____   _____

Prof. Allen Levesque, Thesis Committee   Prof. Wenjing Lou, Thesis Committee

For Supatra

Abstract

Real-time performance evaluation of wireless local area networks (WLANs) is an extremely challenging topic. The major drawback of real-time performance analysis in actual network installations is a lack of repeatability due to uncontrollable interference and propagation complexities. These are caused by unpredictable variations in the interference scenarios and statistical behavior of the wireless propagation channel. This underscores the need for a Radio Frequency (RF) test platform that provides isolation from interfering sources while simulating a real-time wireless channel, thereby creating a realistic and controllable radio propagation test environment. Such an RF-isolated testbed is necessary to enable an empirical yet repeatable evaluation of the effects of the wireless channel on WLAN performance.

In this thesis, a testbed is developed that enables real-time laboratory performance evaluation of WLANs. This testbed utilizes an RF-isolated test system, Azimuth™ Systems 801W, for isolation from external interfering sources such as cordless phones and microwave ovens and a real-time multipath channel simulator, Elektrobit PROPSim™ C8, for wireless channel emulation. A software protocol analyzer, WildPackets Airopeek NX, is used to capture data packets in the testbed from which statistical data characterizing performance such as data rate and Received Signal Strength (RSS) are collected. The relationship between the wireless channel and WLAN performance, under controlled propagation and interference conditions, is analyzed using this RF-isolated multipath testbed.

Average throughput and instantaneous throughput variation of IEEE 802.11b and 802.11g WLANs operating in four different channels – a constant channel and IEEE 802.11 Task Group n (TGn) Channel Models A, B, and C – are examined. Practical models describing the average throughput as a function of the average received power and throughput variation as a function of the average throughput under different propagation conditions are presented. Comprehensive throughput models that incorporate throughput variation are proposed for the four channels using Weibull and Gaussian probability distributions. These models provide a means for realistic simulation of throughput for a specific channel at an average received power. Also proposed is a metric to describe the normalized throughput capacity of WLANs for comparative performance evaluation.

Acknowledgements

First, I would like to express my everlasting thankfulness to my wonderful, lovely wife Supatra for her support and encouragement in my studies. I send my continued appreciation to my parents and my entire family for their support and encouragement.

Thanks to Prof. Wenjing Lou and Prof. Allen Levesque for their guidance and review of my thesis. My appreciation goes out to all my colleagues at the Center for Wireless Information Network Studies for their help and pointers, in particular Dr. Bardia Alavi for examining my thesis.

Thanks also to Prof. Fred Looft for reviewing my thesis and to the ECE Department of Worcester Polytechnic Institute for providing me the opportunity to undertake my Masters degree at WPI.

Additional thanks go to Charles Wright and others at Azimuth™ Systems in Acton, MA for helping me in designing the testbed and understanding the operation of the Azimuth™ Systems 801W test platform.

I would like to express my sincere gratitude to all my colleagues at QUALCOMM, Inc. for their understanding, encouragement, and help while I completed my Masters degree.

Last but not least, my heartfelt appreciation goes out to Prof. Kaveh Pahlavan for all the wisdom and knowledge he has endowed on me over the past few years – this work is as much yours as mine.

Table of Contents

List of Figures

List of Tables

Glossary

ACK	Acknowledgement
AP	Access Point
ASD	Application Specific Device
BB	Base Band
BS	Base Station
CA	Collision Avoidance
CCK	Complimentary Code Keying
CD	Collision Detection
CDF	Cumulative Distribution Function
CDMA	Code Division Multiple Access
CFP	Contention-Free Period
CIR	Channel Impulse Response
CLI	Command Line Interface
CP	Contention Period
CSMA	Carrier Sense Multiple Access
DCF	Distributed Coordination Function
DIFS	DCF IFS
DLR	Data Link Rate
DSP	Digital Signal Processing
DSSS	Direct Sequence Spread Spectrum
DUT	Device Under Test
FFT	Fast Fourier Transform
FHSS	Frequency Hopping Spread Spectrum
GUI	Graphical User Interface
IFS	Inter-Frame Space
ISI	Inter-Symbol Interference
ISM	Industrial, Scientific, and Medical
LAN	Local Area Network
LOS	Line of Site
MAC	Medium Access Control

MIMO	Multiple Input, Multiple Output
MS	Mobile Station
MT	Mobile Terminal
MTH	mini Test Head
NLOS	Non-LOS
OFDM	Orthogonal Frequency Division Multiplexing
PCF	Point Coordination Function
PDP	Power Delay Profile
PHY	Physical
QoS	Quality of Service
RF	Radio Frequency
RFM	RF Port Module
RSS	Received Signal Strength
RX	Receiver
SIFS	Short IFS
SISO	Single Input, Single Output
SNAP	Sub-Network Access Protocol
STA	Station
STM	Station Test Module
Tcl	Tool Command Language
TDL	Tapped Delay Line
TDMA	Time Division Multiple Access
TGn	Task Group n
TMM	testMAC™ Module
TX	Transmitter
UDP	User Datagram Protocol
WLA	WLAN Analyzer
WLAN	Wireless LAN
WM	Wireless Medium

Chapter 1:   Introduction

The increasing popularity of WLANs and the resulting need for performance prediction has shown thee to be a lack of specific guidelines for comparative performance evaluation of WLANs, a process which has yet to be fully defined. The issue at the heart of the problem is that specifying metrics for and modeling the performance behavior of WLANs is significantly more challenging than doing so for wired networks, such as LANs, due in large part to the complexity of communication over the highly variable wireless medium (WM). In the case of WLANs, there are more factors that need to be taken into account.

Unlike their wired counterparts, wireless communication devices use a highly varying channel that is impossible to shield from interference sources such as microwave ovens, cordless phones, etc. Furthermore, IEEE 802.11 WLANs use a multi-rate physical (PHY) layer that specifies multiple communication data rates that vary depending on the current link quality, typically measured by looking at the signal-to-noise-ratio (SNR). (Rate adaptation algorithms are proprietary to the device manufacturer.) These and other factors lead to a communication system whose performance is highly difficult to evaluate and model, especially when approached analytically.

Adopting an empirical performance evaluation methodology for WLANs allows for such complex systems to be analyzed and characterized in a more straightforward manner. However, the data gathered must be collected in such a way that they represent a set of common environments where such devices are commonly used. An alternative approach is to take a sufficiently high number of measurements in many different environments to cover a large portion of the range of possible usage scenarios. If such precautions are not taken, the data that is gathered will be environment specific, effectively making them unrepeatable by others and not particularly well suited as a basis for drawing conclusions.

A method employed to overcome such obstacles, as well as eliminate the need to go to many different locations for data collection, is to use a wireless channel emulator for channel simulation, as has been implemented in [SIL04] and [STE03]. A testbed incorporating channel emulation has the benefit of creating any environment in the laboratory for performance analysis. However, the previous studies noted that utilized channel emulators to examine WLAN performance have utilized them not to characterize and model performance in everyday usage scenarios, but to examine how WLANs behave under harsh conditions, such as high velocity or large delay spread. Although these are interesting areas

to probe, WLANs were specifically designed for use indoors as portable devices and would logically have less than suitable performance under such operating conditions.

In this thesis, an RF-isolated testbed utilizing channel emulation is used for modeling the performance of WLANs for different indoor channels. The IEEE 802.11n channel modeling document is used as a basis for defining the channel models to be implemented in the channel emulator [IEE04]. The channel modeling specification describes single-input single-output (SISO) and multiple-input multiple-output (MIMO) models, of which the SISO models are used for the purposes of this thesis. The Power Delay Profiles (PDPs) defined in the document describe a wide range of indoor environments, ranging from residential areas to large open warehouses. Each of these environments has a specific PDP; representative PDPs were selected for use as the channel models.

By using the channels models put forth by the IEEE 802.11n channel modeling task group, a testbed environment is created that can be repeated and expanded on by others. The results presented here are based on channel models that are available to anyone. Although not all the models were used (Channel Models A-C were implemented and performance for these channels examined), further work can expand on the results presented here, for example additionally implementing models D-F as well as for MIMO WLANs. However, it may not be necessary to go through the process of developing and building a testbed as MIMO WLAN channel emulators are currently available on the market (e.g., from Azimuth™ Systems and LitePoint).

Section 1.1 gives some background on the project and Section 1.2 provides a summary of previous work relevant to the scope of the thesis, including a description of an undergraduate study performed by the author and two colleagues under Prof. Kaveh Pahlavan's guidance in 2003. In Section 1.3 and Section 1.4, the motivation for and contributions by the thesis are described. An outline of the thesis is provided in Section 1.5.

1.1   Background

Due to variations in the wireless channel, the received power can vary dramatically at the receiver. The predominant metric for determining when to change the Data Link Rate (DLR) is the SNR because the SNR has a direct impact on the probability of correctly demodulating the received symbols. Even when the WLAN terminal is kept in a constant location, the channel varies, causing the RSS to change, thus changing the SNR and resulting in DLR variations. Figure 1-1 shows a two-second snapshot of the

RSS and the corresponding DLR (per packet) for a single-tap Rayleigh fading channel. Note that the RSS fading in time causes changes in the DLR.
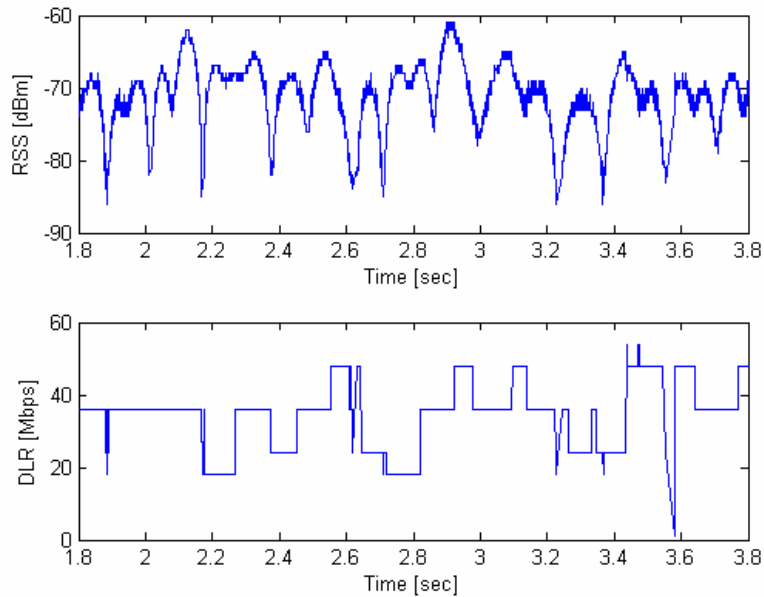
Figure 1-1 The variability of the wireless channel causes fading in the RSS, as shown in the upper half of the figure, resulting in changes to the DLR utilized, as can be seen in the lower half of the figure.

The variations in DLR caused by channel variations, which arise from the conditions of the propagation channel, have an effect on both the average throughput attainable for a given average RSS but also on variation in throughput observed. To date, the performance/channel relationship for WLANs has not been modeled in the literature using an empirical methodology, emulated channels, and actual WLAN devices[*]. Determination of capacity limits for wireless channels can be performed analytically, but to examine actual performance of WLANs, it is necessary to utilize simulation or empirical measurements. Analytical evaluation of WLAN performance in multipath fading channels is extremely complex and is best kept for simple cases.

---

[*] Throughput modeling as a function of SNR using empirically gathered data has been performed in [HEN01]. However, the measurement campaign consisted of gathering data in the "real world." This inherently makes results non repeatable and environment specific.

1.2   Previous Work

There is limited literature on systematic modeling of the throughput behavior of WLANs as a function of the received power or distance. This section provides an overview of this literature and WLAN performance evaluation. Section 1.2.1 gives an overview of research into WLAN performance found in the literature. Section 1.2.2 provides a summary of an empirical throughput measurement/modeling study performed at the Center form Wireless Information Network Studies (CWINS) at Worcester Polytechnic Institute (WPI) in 2003 by the author and two colleagues under the guidance of Prof. Kaveh Pahlavan.

1.2.1   WLAN Performance in the Literature

Early theoretical analysis of WLAN performance was performed at CWINS and is available in [ZHA90]. In this work, performed long before completion of the IEEE 802.11 standard, an analytical study of WLAN throughput in multipath fading channels was performed and compared with Monte Carlo simulation results. Later work at CWINS on WLAN performance evaluation used empirical measurements and ray-tracing techniques to analyze various performance issues for WLAN applications [ZAH97, ZAH00, BRO93, FEI99].

In [WIJ05] and [GOP04], methods are presented for predicting and calculating the maximum User Datagram Protocol (UDP) throughput in IEEE 802.11g WLANs and results compared with empirical measurements. However, the measurement approach used in [WIJ05] does little to take into consideration the propagation/interference environment that ultimately reduces the attainable throughput and causes significant variations in the measurement results obtained. The throughput prediction method described in [GOP04] does consider environmental impact on performance, incorporating path-loss and shadow fading effects, but any results are consequently environment dependent (due to the received power sampling methodology used for distance-power relation prediction, which involves the use of a path-loss model) and multipath fading effects are not incorporated in their technique.

In [SIL04], the PROPSim™+ was used for channel emulation in one signal direction, with isolators, a circulator, and attenuators used in the test setup to prevent loopback (circling) of the RF signal. This testbed was used to examine the performance of IEEE 802.11b WLANs with respect to the delay spread. A simple two-tap channel model was used to this extent and no fading was introduced. This study examined the delay spread bounds for 802.11b WLANs, but no models are presented relating

throughput/Packet Error Ratio (PER) performance to delay spread. Due to the simplicity and predictability of the channel, this study only looks at the performance impact of delay spread.

The Spirent Communications TAS4500 FLEX RF channel emulator was utilized to examine the impact of emulated mobile channels on IEEE 802.11b WLAN performance in [STE03]. The effects of mobility and delay spread were examined using a 6-tap channel model. It was shown that performance degrades as the velocity increases and additionally for large delay spreads, but models are not presented to relate these metrics to WLAN performance. [SIL04] and [STE03] both use testbeds with channel emulation to examine WLAN performance under extreme conditions that are not experience in everyday use with no WLAN performance models being put forward.

Throughput modeling as a function of SNR was performed in [HEN01]. Their approach involved taking a large number of empirical throughput measurements in three different environments (open/large office, closed/small office, and a long hallway) in the "real world" and developing models relating throughput to SNR that fit to these measurements. Measurements and modeling were performed for single client as well as multi-client network configurations. Piecewise linear and exponential modeling approaches were taken. The throughput modeling approach taken in [HEN01] is similar to that performed in this thesis with the following differences:

1) Measurements were taken in different, but non-repeatable environments whereas an RF-isolated, repeatable testbed with channel emulation is utilized here, thus making results applicable as a baseline

2) Variations in throughput were not modeled as it done here; this is important as throughput variations have a significant impact on performance and need to be modeled for accurate throughput modeling and simulation

3) Multi-client network configurations are considered in [HEN01], whereas they are not in this thesis; however, this thesis aims to examine and model the maximum achievable throughput for different channels, in which case a single client single AP network configuraiotion is desirable

4) Average throughput modeled as a function of SNR, not RSS; this is a minor difference as the relation between the two is a scalar

In their piecewise linear model, a maximum throughput region, for SNRs greater than a cutoff SNR is defined, as well as a dropoff region with a vendor/application (and channel) specific throughput decay slope given in Mbps/dB. The modeling performed in [HEN01] is more comprehensive in nature, examining performance with different WLAN devices, for multi-client scenarios as well as under interference. However, despite the more focused examination of WLAN performance performed in this thesis, the results presented here can be more generally utilized as they were performed in a controlled laboratory environment with channel emulation using publicly available IEEE WLAN channel models.

An undergraduate study performed by the author and two colleagues under the guidance of Prof. Kaveh Pahlavan set out to model and compare the throughput-distance relationship of IEEE 802.11b and 802.11g WLANs based on empirical measurements, and can be found in [BHA03] (see Section 1.2.2 below for more details). This study was unique in its attempt to model average throughput as a function of distance. It should be noted that all the papers mentioned above (except [SIL04] and [STE03]) describe results of either simulation or empirical data collected in non-repeatable environments.

The empirical results found in these papers were obtained (for the most part) from actual WLAN installations that are inherently prone to unpredictable interference. These may ultimately provide insight into the *overall* performance behavior of WLANs, but cannot be used as a performance baseline that relates the propagation environment to performance. For results that can be utilized to analyze and develop an understanding of the impact of different wireless channels on WLAN performance and for comparative performance evaluation of WLANs, a repeatable test environment with high levels of isolation from RF interference is necessary.

1.2.2 Empirical Throughput Study at CWINS

A group of undergraduate students performed an empirical analysis of throughput at CWINS in 2003 [BHA03]. The purpose of the study was to measure and model the throughput/distance relationship of IEEE 802.11b and IEEE 802.11g WLANs in a typical office environment[†]. The throughput modeling approach for WLANs undertaken in this project is the precursor of the measurement and analysis campaign described in this thesis and consequently will be described here. Figure 1-2 shows the

---

[†] The 3rd floor of the Atwater Kent building at Worcester Polytechnic Institute, Worcester, MA, USA was used as the testbed for this measurement campaign.

throughput data for IEEE 802.11b and 802.11g versus distance with the models generated by curve fitting overlaid. The throughput-distance models for average throughput are given by (1.1) and (1.2) for IEEE 802.11b and 802.11g, respectively.
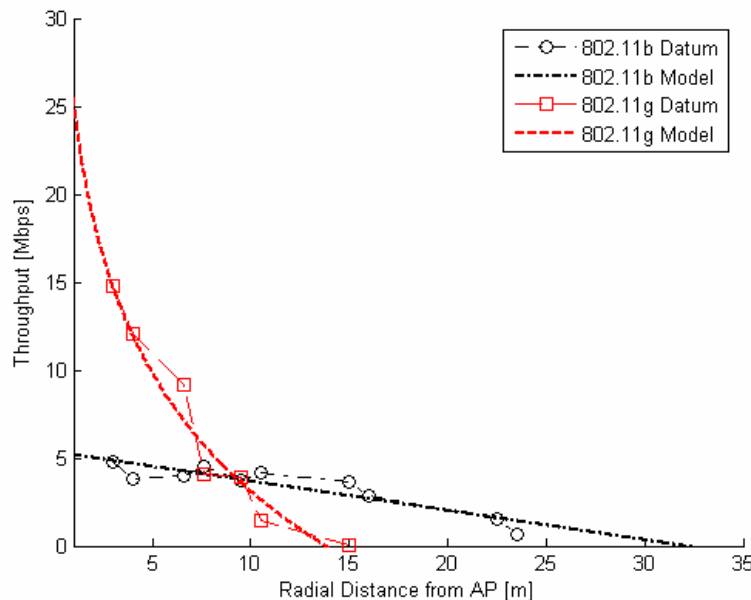
Figure 1-2 Models of throughput versus distance for IEEE 802.11b and 802.11g WLANs. The empirical throughput data is shown with the linear and logarithmic models overlaid. (From [BHA03].)

$$S_b(r) = -0.17r + 5.34 \quad ,0 < r < R_b \qquad \text{[Mbps]} \qquad \textbf{(1.1)}$$

$$S_g(r) = -22.34\log_{10}r + 25.48 \quad ,1 < r < R_g \qquad \text{[Mbps]} \qquad \textbf{(1.2)}$$

where r is the radial distance, and R_b and R_g are the maximum coverage radii (where the throughput becomes 0 Mbps) for a given Access Point (AP). It should be noted that these models do not incorporate variations in throughput and merely give the average throughput for a given distance. The research on testbed design and performance modeling presented in this thesis is a continuation of the effort at CWINS to characterize the performance of WLANs.

The downside of the previous study was that it was performed in only one interference-prone environment. A more thorough measurement campaign to model throughput was needed and is addressed in this thesis. Comprehensive throughput models for IEEE 802.11b and 802.11g WLANs in four different channels are presented. An RF-isolated real-time multipath testbed is a means for

7

evaluating performance in various environments because it is a practical approach to channel characterization/specification. The existence of multiple propagation paths is a fundamental wireless channel characteristic that defines WLAN performance and performance must be better understood in this context. This research tackles this issue by analyzing the throughput/power relationship.

1.3   Motivation

This work was motivated by the need for throughput models describing the channel/performance relationship of IEEE 802.11b and 802.11g WLANs. The frequency selective multipath fading radio channel is a highly variable medium that causes variations in the RSS, which is a very complex statistical phenomena. IEEE 802.11 WLANs have a multi-rate implementation, with the selected data rate dependent on the RSS. The variations in the DLR caused by the wireless channel directly impacts the achievable throughput for a given channel and average RSS.

The models proposed in this thesis provide relationships between average throughput and average power as well as modeling instantaneous throughput variation. Researchers working in the higher layers (e.g., the application layer) need models that describe throughput as a function of RSS, which can be utilized to accurately simulate throughput behavior. This thesis strives to present practical models, which can be utilized in research and industry that describe how WLAN performance is affected by common usage environments such as residential homes.

1.4   Contribution

An RF-isolated real-time multipath testbed utilizing emulated channels was designed and implemented using the Elektrobit PROPSim™ C8 channel emulator, Azimuth™ Systems 801W WLAN test platform, an WildPackets Airopeek NX WLAN protocol analyzer. Using this multipath testbed, a large measurement database of performance metrics for IEEE 802.11b and 802.11g WLANS operating in four channels was compiled. This database of measurements was utilized for modeling the average throughput behavior and instantaneous throughput variation behavior of WLANs as a function of the average RSS.

Practical models that relate average throughput to average RSS for four different channels are presented. Throughput variation for these channels is modeled using two different methods utilizing Weibull and Gaussian distributions. It is observed that average throughput has a piecewise linear relationship to the average RSS and that this relationship is more pronounced for multipath fading

channels. Throughput variation modeling shows that two approaches can be utilized: one yielding a Weibull distributed instantaneous throughput variation whereas the other a Gaussian distribution. The Weibull approach accounts for changes in the distribution as a function of the average throughput. The Gaussian approach combines all instantaneous throughput variations measured for many different received powers into one distribution.

Using the average throughput and throughput variation models, a comprehensive model for simulation of throughput was developed. For the Weibull case, given the average throughput and Weibull parameters derived from the average throughput, the Weibull distributed Random Variable (RV) is the comprehensive throughput sample. For Gaussian throughput variation modeling, the RV drawn from a Gaussian distribution with standard deviation determined by the channel and 802.11 operational mode is added to the average throughput for a given average RSS. The sum yields the comprehensive throughput sample when using this approach. The Gaussian modeling approach is reminiscent of path-loss models where a lognormal distributed RV describes shadow fading.

The average throughput data, as a function of the average RSS can be utilized to determine the comparative throughput performance metric proposed. This metric yields the normalized throughput capacity of a WLAN operating in a given channel with a given operational mode with respect to the manufacturer specified cutoffs and per-DLR throughputs. Such a metric is useful for comparative performance evaluation of WLANs, to quantize a WLAN devices effectiveness in performing under given channel conditions for different operational modes. The comparative analysis of how well two different WLANs perform can be conducted using this metric, even when their respective maximum performance is drastically different (as is the case for IEEE 802.11b and 802.11g WLANs).

1.5   Thesis Outline

In Chapter 2, background on the wireless channel, including descriptions of the TGn channel models utilized in this thesis, and IEEE 802.11b and 802.11g WLANs is provided. In Chapter 3, a description of the equipment used in the multipath testbed and a description of the design of the testbed, including implementation and traffic generation can be found. Chapter 4 presents performance evaluation of WLANs, and results of data collection and analysis that was performed to look at average throughput and throughput variation in four channels. Models for average throughput, throughput variation, and an overall comprehensive throughput model are provided. Chapter 5 concludes the thesis and proposes ideas for future work that would expand on the research undertaken for this thesis.

Chapter 2:   Wireless Channels and WLANs

In this chapter, the behavior of the wireless channel and an overview of IEEE 802.11 WLANs are presented as they underlie the research and performance modeling performed. Section 2.1 gives an overview of the characteristics of wireless propagation and Section 2.2 describes multipath channel models and presents the three IEEE TGn channel models utilized in this thesis. Sections 2.3 and 2.4 describe multi-rate wireless data networks and the IEEE 802.11 WLAN standard, which is the *de-facto* standard utilized for wireless access to LANs and the Internet.

2.1   Wireless Channel Characteristics

The wireless channel is characterized by path-loss, which is a function of distance and the materials that the electromagnetic waves propagate through; slow fading, which arises from movements of the terminals of objects around the terminals; and fast fading, which is the result of multiple propagation paths with different phases summing together destructively upon arrival at the receiver. These three characteristics of wireless propagation are described in Sections 2.1.1-2.1.3.

2.1.1   Path-Loss

As electromagnetic waves propagate through the wireless medium (air), the energy spreads out and at any given distance is inversely proportional to a power α of the distance. The simplest form of the path-loss model (in dB) is given by (2.1) [PAH05].

$$L_p = L_0 + 10\alpha\log_{10}d \qquad\qquad (2.1)$$

where $L_0 = -10\log_{10}G_t G_r \left(\frac{\lambda}{4\pi}\right)^2$ (in dB) is the path-loss in the first meter, α is the distance-power gradient, and d is the distance in meters. The distance-power gradient α is a propagation parameter that depends on the environment and is equal to 2 in free-space. This means that for every decade increase in distance, there is a 10α dB increase in the path-loss. For indoor environments, the distance-power gradient varies widely, from less than 2 (waveguide effect in hallways) to 6 (when the building is constructed of metal) [PAH05]. However, to more accurately describe indoor environments, a more environment specific path-loss model is appropriate. The partition dependent path-loss model describes the total path-loss as free-space path-loss with an additional path-loss component contributed by walls and floors, as given by (2.2) [PAH02].

10

$$L_p = L_0 + 20\log_{10}d + \sum_{type} m_{type}W_{type} \qquad \text{(2.2)}$$

where m_{type} is the number of partitions of a particular type and W_{type} is the loss (in dB) for the given partition type. There are more complex models that, for example incorporate breakpoints (piecewise models), where the path-loss up to a certain distance d_{bp} has a smaller distance-power gradient than after the breakpoint. The IEEE 802.11n channel modeling document [IEE04] uses such models for each of the six channel models that are proposed. More information on various path-loss models can be found in [PAH02, PAH05, IEE04].

2.1.2   Shadow Fading

For a given average path-loss there is variation in the actual path-loss over time. Long term fading, otherwise referred to as "slow fading" or "shadow fading," is caused by changes in the environment, either from terminal movements (e.g., behind a wall) or external movements (e.g., movement of people). An example of slow fading occurs if a line-of-sight connection between two terminals is broken by the movement of a person across this direct path. The person in effect causes the momentary addition of an extra partition, thus increasing the path-loss. Shadow fading is modeled using a lognormal distribution, which is added to the distance and partition dependent path-loss model as shown in (2.3) [PAH05].

$$L_p = L_0 + L_f(n) + 10\alpha\log_{10}d + l \qquad \text{(2.3)}$$

where $L_f(n)$ is the loss incurred as a result of propagation through floor(s) and l is a random variable (RV) with a lognormal distribution representing the shadow fading. Figure 2-1a shows an example lognormal PDF and Figure 2-1b gives an example of shadow fading in time causing long-term slow variations in received power.

(a)   (b)
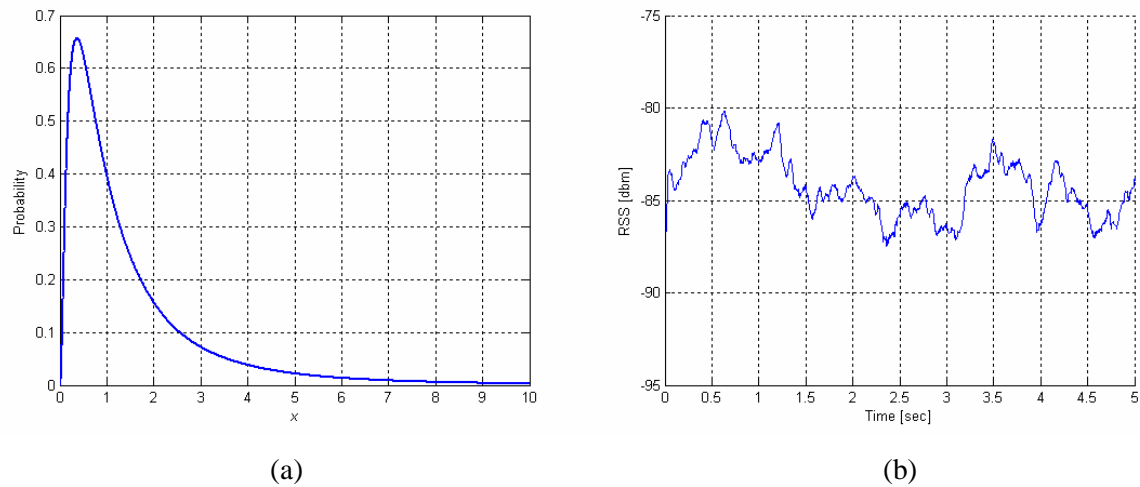
Figure 2-1 Shadow fading distribution and slow fading example: (a) sample lognormal PDF and (b) example of slow fading in time.

2.1.3   Multipath Fading

Multipath fading is a variation in the signal strength caused by multiple propagation paths combining at the receiver, each having varying amplitudes and phases. This is best visualized with narrowband signals, where it is most prominent. A narrowband signal can be described as a sinusoidal wave having a magnitude and a phase (i.e., a phasor). When multiple propagation paths exist, the propagation time amongst the various paths will differ, resulting in each signal arriving at the receiver potentially having a different phase. If these signals are in phase alignment, they will add constructively and make the resulting sum larger than if only a single path existed. However, if two signals are 180° out of phase, they will combine destructively, resulting in a deep fade for that given location. In indoor environments, multipath fading is prevalent as many propagation paths exist due to transmission, reflection, and diffraction off various surfaces.

For broadband and ultra-wideband signals, multipath fading is not as big of a concern. This is because greater bandwidth translates to narrower width pulses in time, allowing for multipath components to be isolated. Consequently, multipath can be exploited by using a RAKE receiver to constructively add the signals propagating along separate paths. In IEEE 802.11a/g/n WLANS, which use Orthogonal Frequency Division Multiplexing (OFDM) technology, multiple narrowband subcarriers, each acting as flat fading narrowband signals, allow deep fading due to multipath to exist, but in such a way that it does not significantly affect the overall transmission mechanism. If even several subcarriers go into

12

deep fade, the chances are they will not be adjacent and convolutional source coding allows the bits lost due to fading to be recovered.

There are three main phenomena that encompass multipath propagation: transmission, reflection, and diffraction. Additionally, the scattering phenomenon occurs when small scale variations in a surface result in a wave being scattered in different directions. Figure 2-2 shows the four wireless propagation phenomena that occur as radio waves propagate from the transmitter (TX) to the receiver (RX). Note that reflections of higher order occur than those shown in the figure. Figure 2-3 shows an Ultra-Wide Band (UWB) example of frequency selective fading caused by multipath.
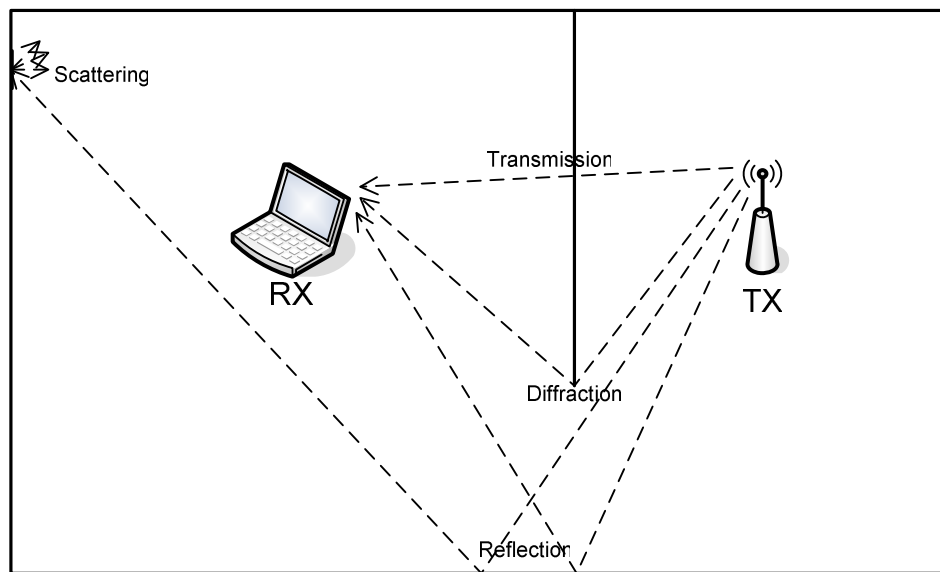
Figure 2-2 Wireless channel propagation factors: transmission, reflection, diffraction, and scattering.

A Sample Frequency Response of an Indoor Environment
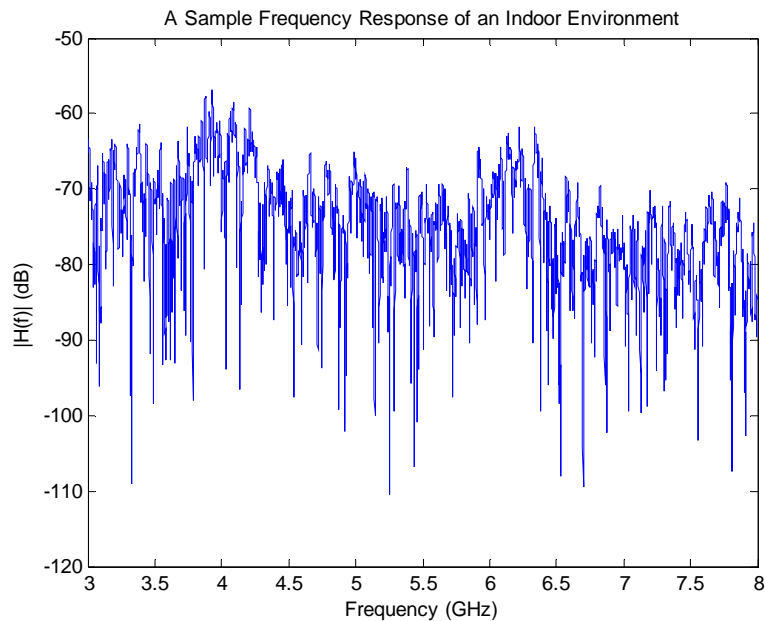
Figure 2-3 UWB example of frequency selective multipath fading in an indoor environment. Note the deep fades in the frequency spectrum at select frequencies. (Courtesy: Dr. Bardia Alavi.)

2.2 WLAN Multipath Channel Models

Wireless multipath channels are modeled using a PDP that can be implemented using a Tapped Delay Line (TDL) for channel emulation, which specifies the relative delay and average power at a receiver of one or more propagation paths with respect to the first path. Additionally, a fading distribution and Doppler spectrum is specified for the taps. Amplitude fading has a Rayleigh amplitude distribution for Non Line-of-Sight (NLOS) scenarios and a Rician amplitude distribution for Line-of-Sight (LOS) scenarios with a flat or bell shaped Doppler power spectrum for indoor environments [PAH05, IEE04]. An example Rayleigh amplitude distribution and flat Doppler spectrum are shown in Figure 2-4a and Figure 2-4b, respectively.

14

(a)   (b)
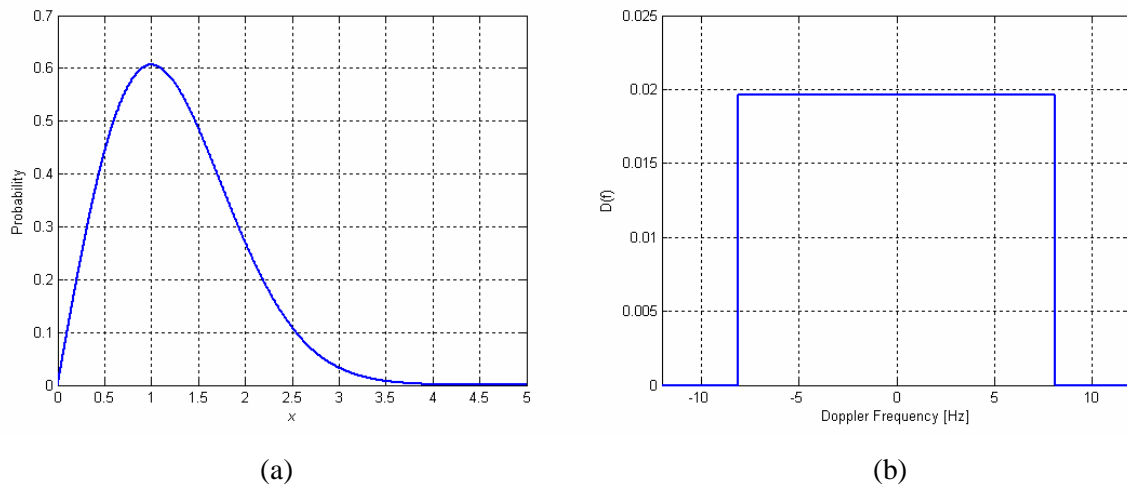
Figure 2-4 Amplitude fading and Doppler spectrum examples: (a) Rayleigh PDF and (b) flat Doppler spectrum.

The IEEE provides SISO and MIMO channel models for the IEEE 802.11n standard that specify the PDP for various environments [IEE04]. Three of the six channel model PDPs (TGn Channel Models A-C) are utilized in this thesis as they describe a range of typical indoor propagation environments, each having different RMS multipath delay spreads. For channel models B and C, a bell-shaped Doppler power spectrum is defined in [IEE04], where the Doppler frequency f_d (the frequency where the spectrum is 10% of the peak value) is calculated assuming a velocity of 1.2 km/hour [IEE04][‡]. The maximum frequency shift is defined as being $5f_d$. However, this Doppler power spectrum is not utilized in the testbed as the PROPSim™ C8 utilized does no support specification of arbitrary Doppler spectra. Instead, the flat Doppler power spectrum was used in the testbed implementation. The channel model PDPs are described in Sections 2.2.2-2.2.5 with the tap specifications given in Appendix A.

2.2.1   Justification for Using IEEE TGn Channel Models

The WLAN channel models presented in [IEE04] were created to describe a wide range of environments in which WLANs are used. These include residential and large office scenarios as well as a channel model describing a large indoor and outdoor space. The different channel models are defined as multiple clusters of taps, each having a delay and average power. The channel models have

---

[‡] The TGn channel models describe indoor environments and a velocity of 1.2 km/hour is representative of human movement in an indoor setting.

a range of delay spreads, thus modeling different environments. Although the document specifies channel modeling for IEEE 802.11n MIMO WLANs, the channel model PDPs can be used to emulate channels for SISO WLANs.

As [IEE04] is the first channel modeling document released by the IEEE for 802.11 WLANs, it seems the logical source for channel models when exploring performance/channel behavior. Additionally, these models can act as a framework for comparison of performance results, as the models are publicly available. No claim is made as to their accuracy in describing the specified environments; instead they act as a foundation. Specific residential/office environments will likely have a different PDP. The tradeoff here is that they will likely have a similar RMS delay spread, which gives an overall metric for the type of environment. The other approach would have been to take measurement in the various environments, but this would have resulted in environment specific multipath models.

TGn Channel Models B and C have a bell shaped Doppler power spectrum per tap whereas the single tap TGn Channel Model A has a flat Doppler power spectrum. For the multipath tesbed described in this thesis, the flat Doppler spectrum was used for TGn Channel Models A-C. This is because of the limitations of the PROPSim™ C8. See Section 3.3.2 for details on why the bell shaped Doppler spectrum was not implemented and what Doppler spectrum was utilized in its place.

2.2.2   Constant Channel

The constant channel has no multipath, no fading, and no Doppler spread. It describes a constant channel with one tap (thus an RMS multipath delay spread of zero) with an average power of 0 dB and no fading. It is essentially equivalent to a cable connecting the transmitter and receiver of the WLAN devices. This channel model is included for the sole purpose of having a baseline for the devices utilized in data collection upon which measurements taken in other channels can be compared. It is also used as a reference to compare results obtained using the IEEE TGn channel models.

2.2.3   IEEE TGn Channel Model A

The IEEE 802.11n Channel Model A [IEE04] is the simplest of the three IEEE channel models used in the multipath testbed. Channel Model A describes a one tap (thus an RMS multipath delay spread of zero) channel with an average power of 0 dB and Rayleigh fading on the single tap. The IEEE channel modeling document specifies a flat Doppler spectrum for the single tap.

2.2.4   IEEE TGn Channel Model B

The IEEE 802.11n Chnnel Model B is a two cluster model used to model the propagation conditions of residential homes. Channel Model B has an RMS delay spread of 15 ns [IEE04] and is shown in Figure 2-5. The Doppler spectrum specified by the TGn channel modeling document for Channel Model B is bell-shaped.
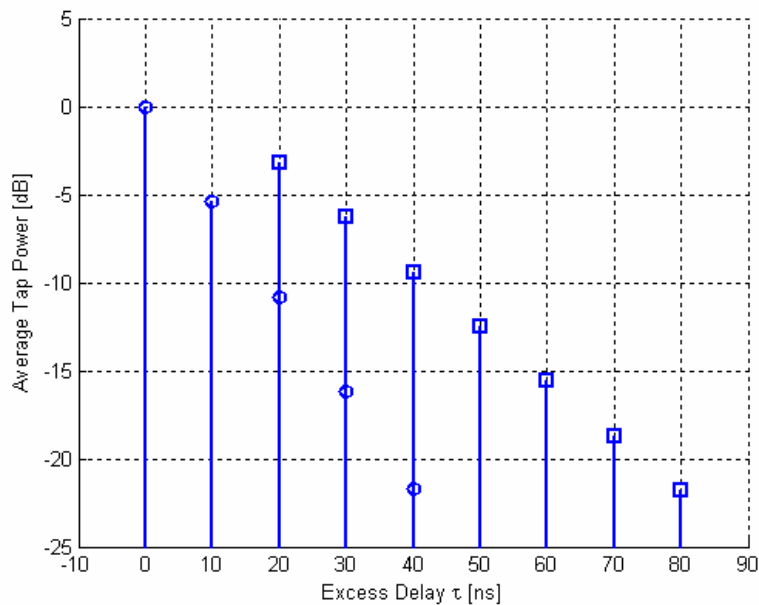
Figure 2-5 PDP of IEEE TGn recommended Channel Model B, which has two clusters with multiple taps.

2.2.5   IEEE TGn Channel Model C

The IEEE 802.11n Channel Model C is a two cluster model that models the channel in a small office environment. Channel Model C has a RMS multipath delay spread of 30 ns [IEE04] and is shown in Figure 2-6. The Doppler spectrum specified by the TGn channel modeling document for Channel Model C is bell-shaped.
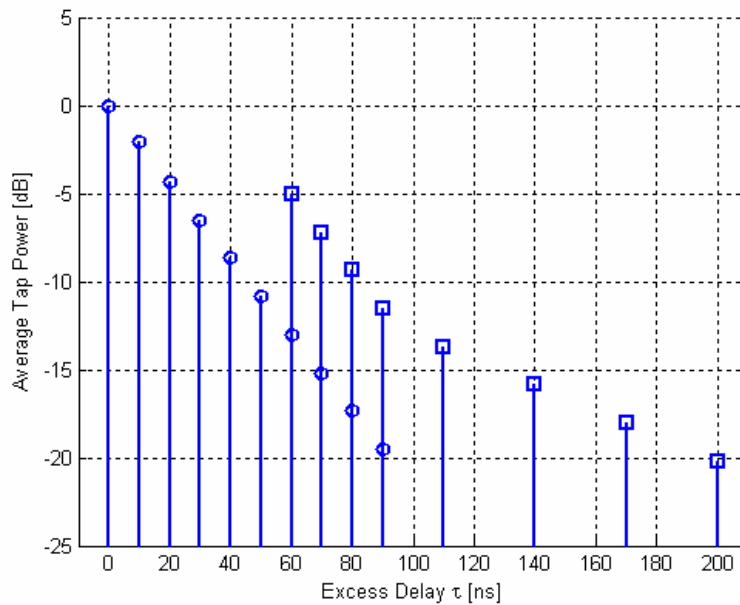
Figure 2-6 PDP of IEEE TGn recommended Channel Model C, which has two clusters with multiple taps.

2.3   Multi-Rate Wireless Data Networks

The use of multiple PHY layer data rates by utilizing different modulation schemes and coding rates is an effective method for maximizing the average data rate that can be obtained through the WM in the coverage area of a given Base Station (BS)/AP. This method is based on the principle that the probability of error is lower at higher SNRs, thus allowing higher order symbol constellations to be utilized for transmission. TDMA and CDMA digital cellular networks utilize this method to provide higher data transfer rates for data services to Mobile Terminals (MTs) closer to the BS. Figure 2-7 gives an example data rate topology for a multi-rate wireless device, in this case showing concentric circles representing regions over which the wireless device will achieve the given data rate.
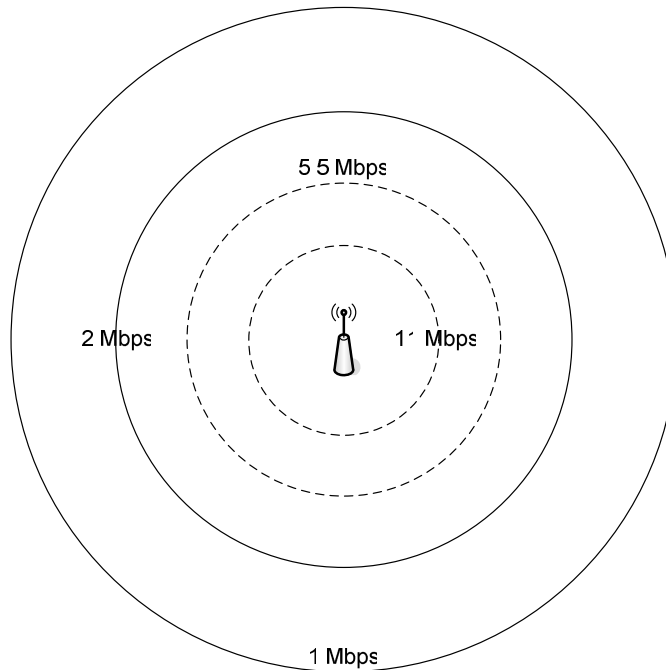
Figure 2-7 Example topology showing the multiple PHY layer data rates of an IEEE 802.11b WLAN, which decrease as the distance from the AP increases resulting in a lower RSS.

This thesis focuses on WLANs, a multi-rate wireless network designed primarily for data services. Given the high data rates utilized in the more recent revisions of 802.11 (802.11g and the upcoming 802.11n), it is critical that a multi-rate system be implemented to provide the maximum possible average throughput in a given AP's coverage area. The use of a multi-rate OFDM modulation scheme enables high data rates close to the AP while still maintaining connectivity at low SNRs.

2.4 IEEE 802.11 WLANs

WLANs have seen a dramatic growth in popularity with the introduction of the IEEE 802.11b and successive standards, which currently provide LAN and Internet access at PHY layer rates of up to 54 Mbps in a 20 MHz band, with at least 100 Mbps at the MAC data services AP using only mandatory features specified in the upcoming IEEE 802.11n standard [IEE06]. The growth in the WLAN market for wireless data access was partly fueled by the parallel growth in Internet usage. WLANs were designed as an extension to wired LANs, thus providing tether-less access to the local LAN and worldwide Internet while being less physically confined.

Sections 2.4.1 and 2.4.2 describe the Medium Access Control (MAC) and PHY layers of the original IEEE 802.11 standard. The PHY layer and overhead calculation for IEEE 802.11b and IEEE 802.11g are given in Sections 2.4.3 and 2.4.4. Section 2.4.5 presents an overview of the upcoming IEEE 802.11n standard. The following sections are an overview of the IEEE 802.11 standard and summarize material contained in [IEE99a, IEE99b, IEE99c, IEE03, IEE06].

2.4.1   MAC Layer

The IEEE 802.11 MAC layer is primarily comprised of the mandatory contention-based Carrier Sense Multiple Access (CSMA)/Collision Avoidance (CA) Distributed Coordination Function (DCF). There are two other optional medium access methods that can be implemented on top of the DCF: the Point Coordination Function (PCF) and Request-to-Send/Clear-to-Send (RTS/CTS) virtual carrier sense mechanism. The PCF is provided for Quality of Service (QoS) and RTS/CTS as a way to improve transmission reliability by ensuring channel reservation for a given frame, in particular to mitigate the hidden terminal problem and increase the probability of transmitting a long frame succesfully. Figure 2-8 shows the structure of the IEEE 802.11 MAC, depicting the PCF as built on top of the DCF.
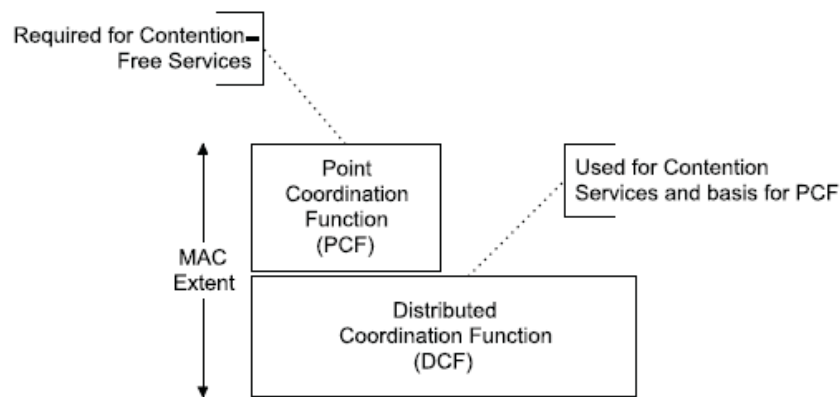
Figure 2-8 The overall IEEE 802.11 MAC structure showing the mandatory DCF and optional PCF, which is implemented on top of the DCF. (From [IEE99a].)

The fundamental access method of IEEE 802.11 is a DCF that utilizes CSMA/CA. This is based on the CSMA/Collision Detection (CD) used for LANs, while substituting CD with CA due to the highly varying nature of the wireless channel, which makes CD impossible. For each frame that is transmitted there are Inter-Frame Spaces (IFSs), an Acknowledgment (ACK), and backoff(s) associated with it to ensure successful transmission. The overall access method for the IEEE 802.11 MAC, showing the IFSs and backoff is given in Figure 2-9.
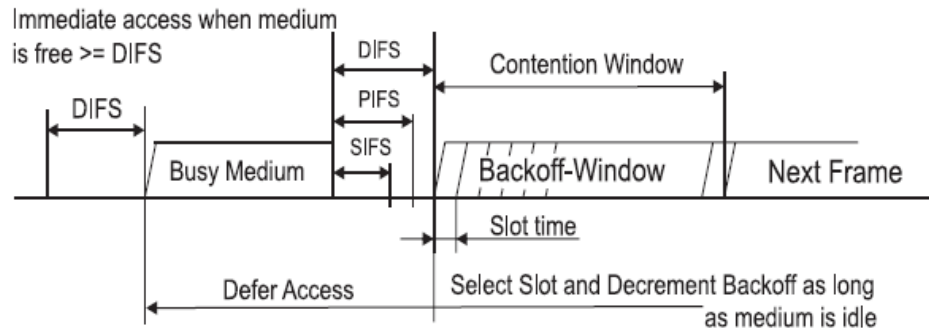
Figure 2-9 The general access method for IEEE 802.11 WLANs. For frame transmission, there are IFSs and backoffs to facilitate priority and reduce the probability of collisions occurring. (From [IEE99a].)

The IEEE 802.11 DCF operates via a backoff algorithm that runs an all Stations (STAs) and APs. Whenever a packet is queued up for transmission, the medium is sensed to determine if it is busy. If a busy medium is detected, a random backoff is set. Transmission proceeds when the backoff counter reaches zero after the medium is sensed to be idle for a DCF IFS (DIFS) period. The backoff is selected from a uniform distribution of integers in the range [0,CW], where the Contention Window (CW) size is an exponentially increasing value (2^n-1) and depends on the retransmission state [IEE99a]. Figure 2-10 shows the exponential increase in backoff window size with each successive retransmission.
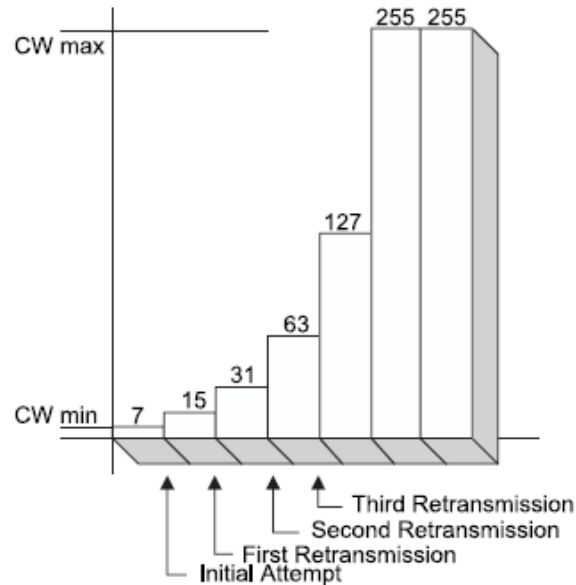
Figure 2-10 An example of the binary exponential backoff mechanism showing the maximum contention window size increasing with each successive retransmission. (From [IEE99a].)

This backoff procedure is implemented to reduce the probability of collisions occurring. With a CSMA/CA system, collisions would occur with highest probability directly after an STA has finished a transmission as other STAs would be waiting for the medium to become free [IEE99a]. By implementing a random backoff before accessing the WM, the probability of collision is greatly reduced by having all STAs wait different periods of time (random backoffs) before attempting a transmission, following a WM idle period of DIFS. The STA whose backoff counter first reaches zero will transmit while the other STAs will have to wait until the WM is once again idle. STAs restart their backoff counters from where they left off in the previous attempt, as shown in Figure 2-11. Only after a transmission attempt is the backoff counter reset[§].

[§] If the transmission is unsuccessful, the backoff counter is still reset but selected from a bigger CW.
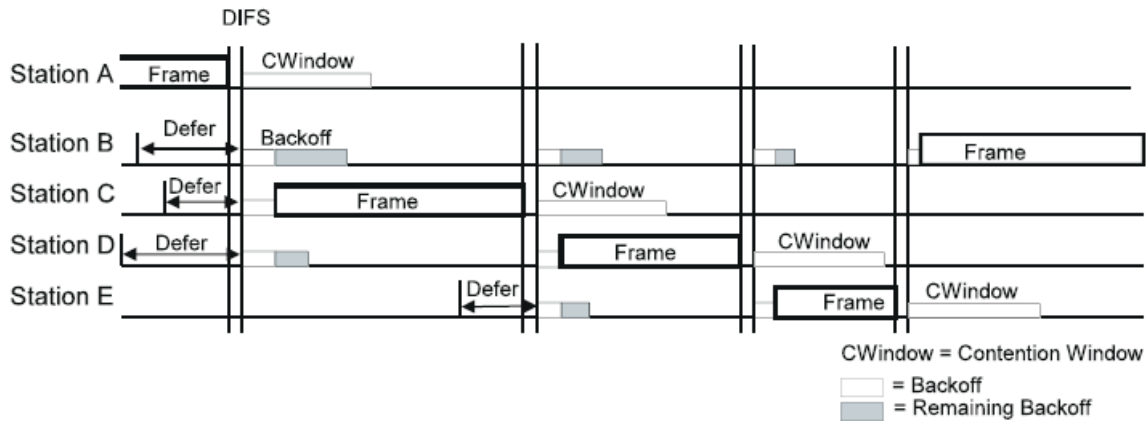
Figure 2-11 An example of the process of multiple STAs contending for access to the WM with the DCF access mechanism. Each STA has an independent backoff timer that counts down before the STA can transmit a queued frame. (From [IEE99a].)

Because the wireless medium is subject to significant variation and is highly prone to interference, it is also critical to have a method for informing the transmitting STA that a transmitted frame has been successfully received. This is done though immediate positive acknowledgement, which means that all received frames (of a certain type) are confirmed using an ACK frame, which is transmitted after a Short IFS (SIFS). If either the original frame or the ACK is lost or corrupted (i.e., no transmission confirmation), the transmitting STA schedules the frame for retransmission. When a retransmission is necessary, the CW is increased and a new backoff selected. The ACK procedure of the IEEE 802.11 is illustrated in Figure 2-12.
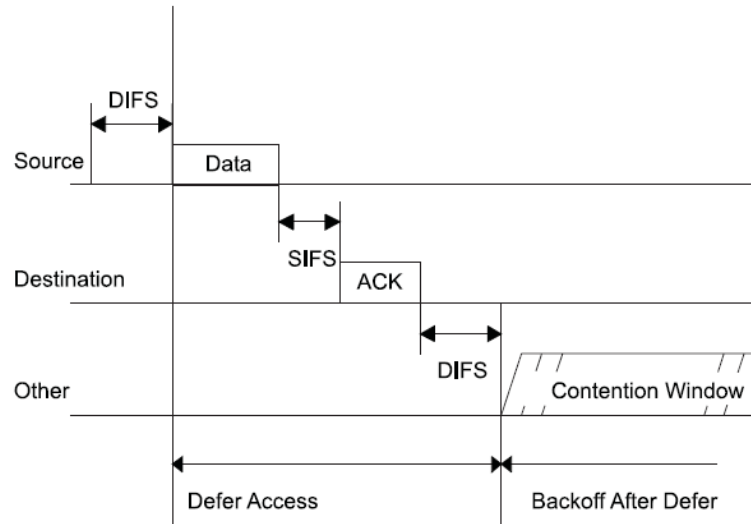
Figure 2-12 The transmission of a data frame with the DCF access mechanism showing the immediate positive ACK frame. (From [IEE99a].)

To ensure proper frame transmission in highly varying channels, RTS/CTS can be used as a method for checking the transmission path. This is particularly useful for transmission of long frames. Ordinary frame transfer continues following an RTS/CTS frame exchange. The RTS/CTS mechanism is not a means for bypassing contention but merely a method for checking the transmission path as control frames are still subject to contention.

The optional PCF is a "contention-free" access method that is only available in infrastructure network configurations and operates via a point coordinator (PC) located at the AP. The PC controls channel access within a Contention-Free Period (CFP). STAs request access to the medium CFP by sending Contention-Free (CF) polls. The PCF mechanism was included for time-bounded services for QoS by applying tighter bounds on contention. However, it should be noted that it is still subject to contention, utilizing the shorter PCF IFS (PIFS) to increase the likelihood that it will be able to access the WM. Figure 2-13 shows the WM being shared between the PCF CFPs and DCF Contention-Periods (CPs). Note that the Network Allocation Vector (NAV) is set during a CFP.

Figure 2-13 The PCF and DCF access mechanisms sharing the WM; each CFP of the PCF is followed by a CP of the DCF. (From [IEE99a].)

The overall access to the WM is determined by examining the current states of the backoff counter, NAV, and Clear Channel Assessment (CCA) result. If either of these functions indicates that the WM is busy, frame transmission is deferred. This ensures that collisions are minimized and increases the reliability of frame transmission. Whenever a frame must be retransmitted, the previous attempt was a wasted instance of WM use and has an accumulative impact on the overall throughput performance.

2.4.2   DSSS PHY Layer

Direct Sequence Spread Spectrum (DSSS) is a spread spectrum technology that is one of the three PHY layer options in legacy IEEE 802.11. Spread spectrum techniques are suitable for wireless communications as they help to mitigate channel effects (being wideband) and can be used in conjunction with a RAKE receiver to increase stability of the received power, consequently increasing coverage. The 802.11 DSSS PHY layer takes an input bit stream of 1 or 2 Mbps, maps the bits to symbols using Differential Binary Phase Shift Keying (DBPSK) or Differential Quadrature Phase Shift Keying (DQPSK) modulation, then multiples each bit with a length 11 Barker sequence (PN code) to generate a spread spectrum signal with a chip rate of 11 Mcps. The use of a pseudo-random noise (PN) code whitens the input bit stream alleviating the need for scrambling. A SYNC field in the Physical Layer Convergence Procedure (PLCP) preamble of 128 bits is necessary for synchronization. See [PAH02, IEE99a] for more details on the IEEE 802.11 DSSS PHY layer.

2.4.3   IEEE 802.11b

The IEEE 802.11b extension to the 802.11 standard is a high throughput addendum to support 5.5 and 11 Mbps PHY layer data rates on top of the original 1 and 2 Mbps data rates. In IEEE 802.11b, a new

Complimentary Code Keying (CCK) PHY layer is specified, whereas the original 802.11 PHY layer included Frequency Hopping Spread Spectrum (FHSS), DSSS, and Infra-Red (IR). The 802.11b PHY layer uses the same PLCP preamble and header as 802.11 for backward compatibility.   Both a decoder for the 802.11 Barker coded data and 802.11b CCK coded data (using 64 correlators) are implemented for demodulation.

The data rates support by IEEE 802.11b are given in Table 2-1 with RSS cutoffs [CIS05b].

Table 2-1 IEEE 802.11b Supported Data Rates (Cisco Aironet 802.11a/b/g CardBus Client Card [CIS05b])

RSS [dBm]	*Data Rate [Mbps]*
-94	1
-93	2
-92	5.5
-90	11

2.4.3.1   CCK PHY Layer

The CCK PHY layer allows the data rate to increase to 5.5 and 11 Mbps, or 1:2 and 1:1 ratios with respect to the chip rate of the DSSS PHY layer. This is done by mapping bit pairs to points in a Quadrature Phase Shift Keying (QPSK) constellation, and then mapping the respective symbol phases to an 8 element complex code (yielding 256 orthogonal codes) using the mapping given by (2.4).

$$c = \{e^{j(\varphi_1+\varphi_2+\varphi_3+\varphi_4)}, e^{j(\varphi_1+\varphi_3+\varphi_4)}, e^{j(\varphi_1+\varphi_2+\varphi_4)}, -e^{j(\varphi_1+\varphi_4)},$$
$$e^{j(\varphi_1+\varphi_2+\varphi_3)}, e^{j(\varphi_1+\varphi_3)}, -e^{j(\varphi_1+\varphi_2)}, e^{j(\varphi_1)}\} \tag{2.4}$$

For 5.5 Mbps operation, groups of four bits are broken into two pairs, each pair being mapped to one of four orthogonal complex codes. In 11 Mbps operation, 6 bits are encoded to one of 64 orthogonal complex codes with the remaining 2 bits being directly mapped to a phase (each element in the mapping equation has a common $e^{j(\varphi_1)}$ term). A symbol rate of 1.375 Msps gets mapped to an air interface chip rate of 11 Mcps using 8 chips (codes) [PAH02]. The occupied bandwidth per channel of IEEE 802.11b is 26 MHz. See [IEE99c] for the bit to symbol mapping for 5.5 and 11 Mbps modes and other details on the CCK PHY layer.

2.4.3.2   IEEE 802.11b Overhead Calculation

If a transmission protocol is assumed, the theoretical throughput can be calculated by taking into account all the 802.11 overhead as well as any higher layer overhead (e.g., TCP acknowledgements). Throughput calculation for one frame exchange sequence is sufficient to find the average throughput if the PHY layer data rate is fixed. This also assumes that there are no retransmissions, as this will have a detrimental impact on overall achievable throughput. In the calculations performed here, it is assumed that there are only two STAs (i.e., one STA and one AP) in an interference free environment, thus simplifying the calculations (since collisions do not need to be factored in) with only the average of the initial backoff window, within the range [0,aCWmin] and equal to aCWmin/2 needing to be factored in for backoff. This has the effect of providing the maximum achievable instantaneous throughput for the given protocol and data rate.

The per-DLR throughput is calculated by taking the data payload size (in bits) transmitted per frame and dividing by the duration of time required for transmission of that data. The inter-packet delay is the sum of SIFS, DIFS, and the duration of the frame and ACK for transmission of a UDP frame. Frame durations are calculated by taking data (in bits) per frame and dividing by the PHY layer data rate. The calculation of IEEE 802.11b per-DLR throughputs for UDP traffic in a one client/one AP infrastructure network configuration is given by (2.5) [CIS05a].

$$S_{th} = \frac{L_{data}}{\text{DIFS} + \text{SIFS} + {aCWmin}/{2} + {(L_{data} + H_{MAC} + H_{IP} + H_{UDP} + L_{ACK})}/{\text{DLR}} + 2\text{PLCP}_{\text{preamble}} + 2\text{PLCP}_{\text{header}}} \quad \text{[bps]} \quad \textbf{(2.5)}$$

where L_{data} is the data segment length (in bits), L_{ACK} is the ACK length (in bits), H_{MAC}, H_{IP}, and H_{UDP} are the MAC, IP and UDP header lengths (in bits), $\text{PLCP}_{\text{preamble}}$ and $\text{PLCP}_{\text{header}}$ are the PLCL preamble and header durations in microseconds, DLR the PHY layer data rate(s), and S_{th} the theoretical per-DLR throughputs at the given DLRs. Table 2-2 gives the per-DLR calculated throughputs for IEEE 802.11b with both the short and long preambles.

Table 2-2 Per-DLR Calculated Throughputs (IEEE 802.11b)

DLR [Mbps]	Throughput [Mbps]	
	short preamble	*long preamble*
1	0.9211	0.8965
2	1.7861	1.6957
5.5	4.4388	3.9195
11	7.7109	6.2681

2.4.4 IEEE 802.11g

The IEEE 802.11g amendment to IEEE 802.11 brought the higher data rates of IEEE 802.11a to the 2.4 GHz band, which would allow for backward compatibility with IEEE 802.11 and 802.11b, as well as greater coverage due to the lower frequency of operation. Additionally, due to market saturation of 802.11b WLANs, IEEE 802.11g would seem a natural upgrade, in part due to the added advantage of backward compatibility. This was indeed the case, and IEEE 802.11g has achieved far greater market saturation than IEEE 802.11a despite being released at a later date (in 2003 as opposed to 1999).

IEEE 802.11g utilizes the 802.11a OFDM PHY layer, which is a mandatory element of the standard, to achieve higher data rates over the WM. There are two optional PHY layers defined in addition to the IEEE 802.11a PHY layer. OFDM is inherently well suited for communication over a frequency selective fading communication channel since each subcarrier acts as a flat fading narrowband channel. By utilizing convolutional coding, data contained in tones that go into deep fade can be recovered. Another advantage of OFDM is the ability to have a Digital Signal Processing (DSP) based solution using Fast Fourier Transforms (FFTs).

The data rates support by IEEE 802.11g are given in Table 2-3 with RSS cutoffs [CIS05b].

Table 2-3 IEEE 802.11g Supported Data Rates (Cisco Aironet 802.11a/b/g CardBus Client Card [CIS05b])

RSS [dBm]	Data Rate [Mbps]
-86	6
-86	9
-86	12
-86	18
-84	24
-80	36
-75	48
-71	54

2.4.4.1   OFDM PHY Layer

OFDM technology increases the spectral efficiency by utilizing multiple subcarriers within a single 20 MHz channel (of which 16.6 MHz is occupied). Each subcarrier has a bandwidth of 312.5 kHz and acts as a narrowband fading channel. There are 52 subcarriers, of which 48 carry data and 4 are used as pilots. On each subcarrier, the input bit stream is modulated using BPSK, QPSK, 16-QAM, or 64 QAM with three different code rates (1/2, 2/3, and 3/4), thus yielding 8 different PHY layer data rates (6, 9, 12, 18, 24, 36, 48, and 54 Mbps) [IEE03]. Adjacent OFDM symbols are separated by a guard interval 800 ns to prevent ISI.

The modulation scheme (modulation and code rate) chosen for transmission of a frame is dependent on the quality of the link, which is generally ascertained using the SNR and is determined using proprietary algorithms. The IEEE 802.11g standard does not specify how the data rates are selected. However, the performance requirements on the transmitter and receiver for the different data rates are defined. Of the possible PHY layer data rates, 6, 12, and 24 Mbps as well as the legacy 1, 2, 5.5, and 11 Mbps data rates are mandatory. For more information on the OFDM PHY layer and IEEE 802.11g, see [IEE99b, IEE03]. Figure 2-14 shows the OFDM PHY layer, depicting the multiple orthogonal subcarriers with inter-carrier spacing of 312.5 kHz.
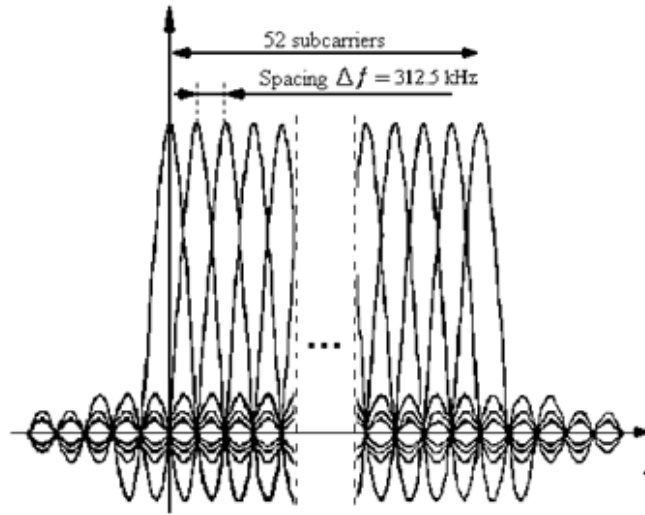
Figure 2-14 The spectra of the IEEE 802.11a/g OFDM PHY layer showing the multiple orthogonally spaced subcarriers. (From <http://www1.linksys.com/products/images/ofdm.gif>.)

2.4.4.2   IEEE 802.11g Overhead Calculation

In Section 2.4.3.2, the principle behind throughput calculation for WLANs was laid out for the IEEE 802.11b case with UDP traffic in a one client one AP infrastructure network configuration. Throughput calculation for IEEE 802.11g data rates is slightly different from that of IEEE 802.11b as an OFDM PHY layer is implemented, with the addition of and modification to some parameters in the calculation. However, the overall procedure of taking number of bits of data sent in a frame and dividing by the total duration of that frame exchange applies, as shown in (2.6) [WIJ05].

$$S_{th} = \frac{L_{data}}{\text{DIFS} + \text{SIFS} + {^{\text{aCWmin}}\!/_2} + {^{(L_{data} + H_{MAC} + H_{IP} + H_{UDP} + L_{ACK} + \text{TAIL})}\!/_{\text{DLR}}} + 2\text{PLCP}_{\text{preamble}} + 2\text{PLCP}_{\text{header}} + 2\text{SigExt}}$$
$$\text{[bps]} \quad \textbf{(2.6)}$$

where L_{data} is the data segment length (in bits), L_{ACK} is the ACK length (in bits), H_{MAC}, H_{IP}, and H_{UDP} are the MAC, IP and UDP header lengths (in bits), TAIL is the appended tail bits, PLCP$_{\text{preamble}}$ and PLCP$_{\text{header}}$ are the PLCL preamble and header durations in microseconds, SigExt is a pause following the transmission of a frame to ensure that the convolutional decoding process finishes, DLR the PHY layer data rate(s), and S_{th} the theoretical per-DLR throughputs at the given DLRs. Table 2-4 gives the per-DLR calculated throughputs for IEEE 802.11g.

Table 2-4 Per-DLR Calculated Throughputs (IEEE 802.11g)

DLR [Mbps]	Throughput [Mbps]
6	5.2804
9	7.6376
12	9.8321
18	13.7963
24	17.2798
36	23.1165
48	27.8141
54	29.8350

2.4.5   IEEE 802.11n

The IEEE 802.11n standard is the most recent addendum to the original 802.11 standard. It specifies modifications to the MAC and PHY layers to support both QoS and MAC data services AP measured rates of 100 Mbps with only mandatory features. High throughput is achieved by taking advantage of multipath, a phenomenon previously considered to degrade channel capacity. This is done by using multiple antennas at either or both the transmitter and receiver. At the very least, extra antennas yield more diversity, resulting in a more stable channel; additionally, more antennas enables exploitation of multipath by using space-time block coding and transmit beam-forming.

Frame aggregation, block ACKs, and a short guard interval of 400 ns are all part of the standards effort to increase throughput. The IEEE 802.11n standard uses MIMO OFDM technology with multiple operational modes (legacy, mixed-mode, and Green Field) for use in different network settings. The Green Field operational mode is optional and utilizes non-backward compatible frame format. For more details on the IEEE 802.11n draft standard, see [IEE06].

Chapter 3: Design and Implementation of the Testbed

This chapter describes the design and implementation of the multipath testbed that was developed and utilized to collect data for the purpose of examining and modeling the effects of the wireless channel on WLAN performance. In Section 3.1, descriptions of the various hardware and software elements of the testbed are presented. Section 3.2 discusses the testbed design and Section 3.3 the implementation of the testbed. In Section 3.4, a description of traffic generation in the testbed and the software package (Airopeek NX) used for to capture packets in the testbed is provided.

3.1   Elements of the Multipath Testbed

The multipath testbed consists of two main components: the Azimuth™ Systems 801W RF-isolated WLAN test platform (chassis, modules, and isolation chambers) and the Elektrobit PROPSim™ C8 multipath channel emulator, which are described in Sections 3.1.1 and 3.1.2 respectively. Additional hardware utilized to implement the multipath testbed is described in Section 3.1.3.

3.1.1   Azimuth™ Systems W-Series

The Azimuth™ Systems 801W is a modular test solution for examining the performance of SISO WLANs. It utilizes RF isolation chambers to significantly reduce RF interference, with the Devices Under Test (DUTs) being cabled together. However, the 801W does not emulate wireless channels; it simply simulates changes in distance via digitally controlled attenuators, which can be increased or decreased in 1 dB steps. It is a system designed for validation and comparative performance evaluation of SISO WLANs in an ideal channel. The hardware components are controlled via the Azimuth™ DIRECTOR™ software, which operates on an external server and is connected to the 801W chassis/modules via the Bus-Net. A Test-Net is used for traffic, which is generated using Ixia IxChariot[**], Iperf[††], or the Azimuth™ traffic generator (part of the Azimuth™ DIRECTOR™ software package).

[**] Ixia IxChariot is a professional solution for network testing with realistic loads, such as video streaming and file transfer. See <http://www.ixiacom.com/solutions/display.php?skey=ixchariot> for more details.
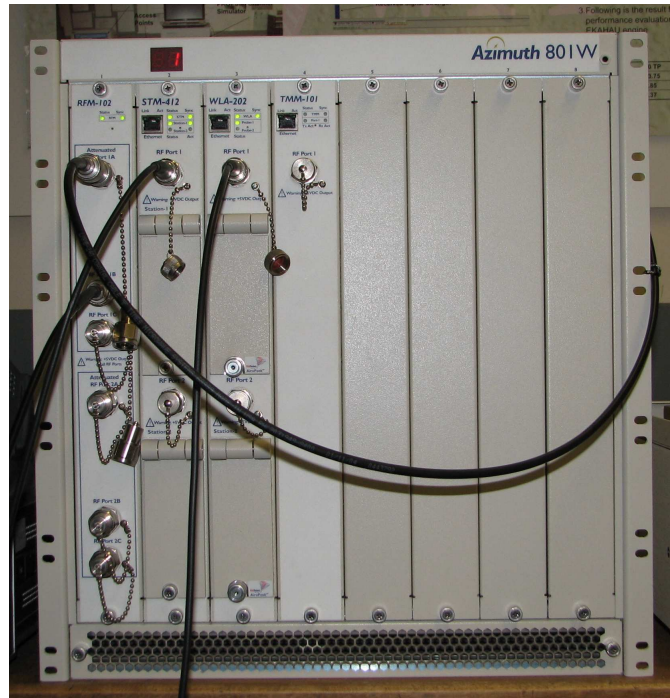
Figure 3-1 The front panel of the Azimuth™ Systems 801W, which is the chassis for the various test modules offered by Azimuth™ Systems.

A typical test setup involving one client and one AP using the Azimuth™ Systems 801W is given in Figure 3-2. Note that this configuration would yield results that would not represent performance in an actual environment as no channel is emulated in the Azimuth™ Systems 801W.

[††] Iperf is a free utility for measuring TCP and UDP network performance that reports metrics such as bandwidth and jitter. See <http://dast.nlanr.net/Projects/Iperf/> for more details.
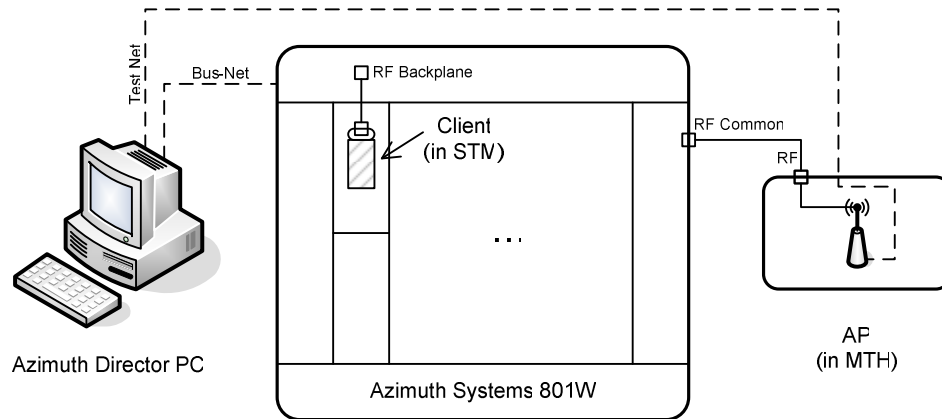
Figure 3-2 Typical client/AP test setup using the Azimuth™ Systems 801W and STM module. The WLAN client is installed inside the STM and the WLAN AP is isolated inside the MTH. The AP is cabled to the 801W RF backplane, which is connected to the WLAN client in the STM. The Bus-Net and Test-Net facilitate control and testing. This test setup allows for basic rate vs. range testing in an ideal channel.

3.1.1.1   Azimuth™ DIRECTOR™ Software

The Azimuth™ DIRECTOR™ software acts as a Graphical User Interface (GUI) for the hardware modules. It should be noted that all control of the Azimuth™ hardware can be achieved through Tool Command Language (Tcl) scripting. The Azimuth™ DIRECTOR™ allows for manual control of the various attenuators, setup of the DUTs, and remote desktop capability for the various modules that have an internal computer. Figure 3-3 shows a screenshot of the Azimuth™ DIRECTOR™ software with the Topology View tab selected. Although not shown in this network topology, the PROPSim™ C8, which would be connected in between the AP and client. See [AZI05] for more details on the Azimuth™ DIRECTOR™ software.
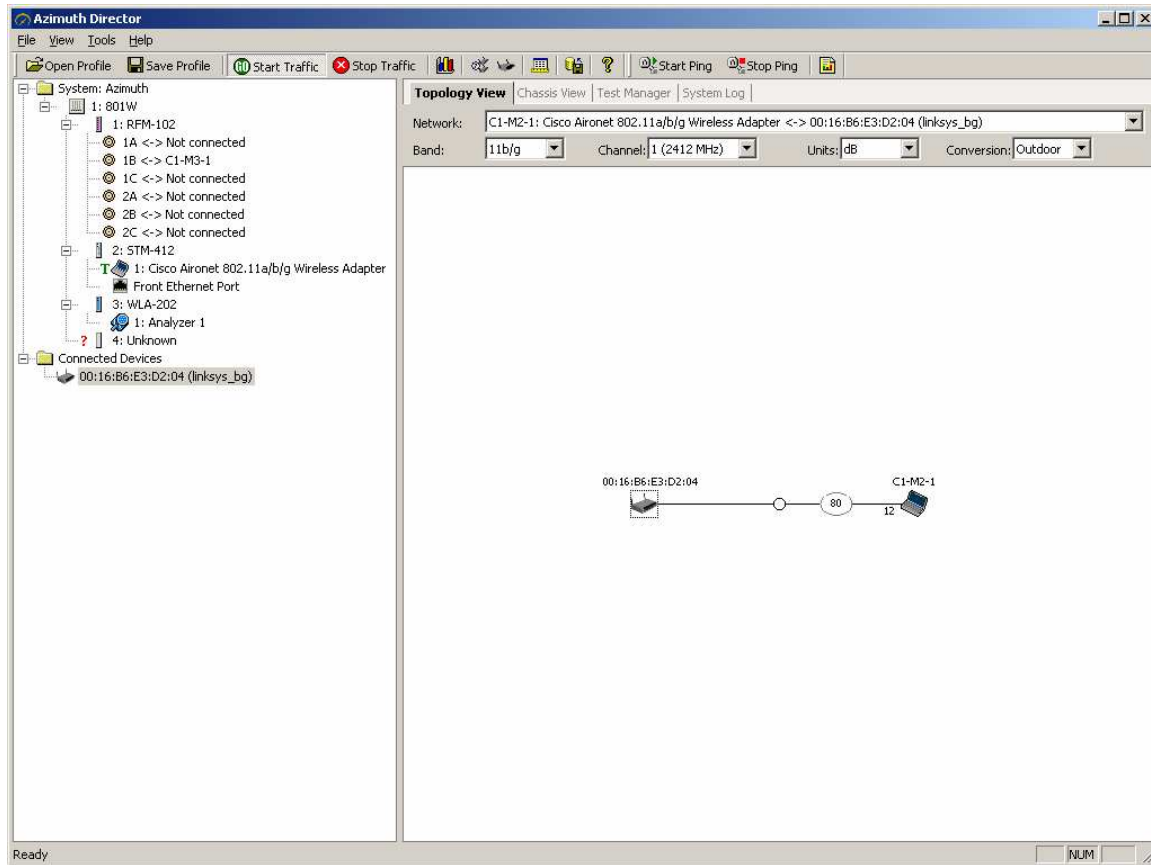
Figure 3-3 An example screenshot of the Azimuth™ Systems DIRECTOR™ software. The left half of the window shows the modules/clients/APs connected. The right half of the screen has multiple tabs for viewing the current network topology, system log, etc. Various functions such as starting/stopping traffic and pings can be performed from the toolbar provided.

3.1.1.2   Module/Hardware Descriptions

There are four modules in the Azimuth™ 801W chassis used for this research. These modules are the RF Port Module (RFM), the Station Test Module (STM), the WLAN Analyzer (WLA), and the testMAC™ Module (TMM). Of these four, only the RFM, STM, and WLA were used in the multipath testbed. These are described in more detail below, along with reasons for their use or non-use in the testbed. Additionally, a brief description of the 801W chassis and mini Test Head (MTH), which is used to house the AP, are given.

801W Chassis

The 801W chassis houses the various test modules that Azimuth™ provides. It is comprises an RF backplane, which the modules plug into (all of the module's RF components are connected via the RF backplane) and digital circuitry to interface with the Azimuth™ DIRECTOR™ software, modules, and to connect all of the modules to the common Bus-Net, which is used for modular control. Connectors for the RF backplane (named RF common) and Bus-Net are provided at the back of the chassis. The modules draw power from the chassis when they are inserted. Each chassis (and other Azimuth™ components that are part of the test platform) is assigned an ID number, starting with 1. For the system at CWINS, the chassis ID was 1, as there was only one unit in the lab. Multiple chassis can be utilized for which synch in and synch out (RJ-45) connectors are provided at the rear of the chassis.

RF Port Module

The RFM is a bank of attenuators that is connected to the 801W chassis RF backplane. There are 6 RF connectors at the front of the panel. These connectors and attenuators are connected as illustrated in Figure 3-4. The attenuation of each attenuator can be individually set via the DIRECTOR™ software's GUI configuration window for the RFM, or set via Tcl commands.
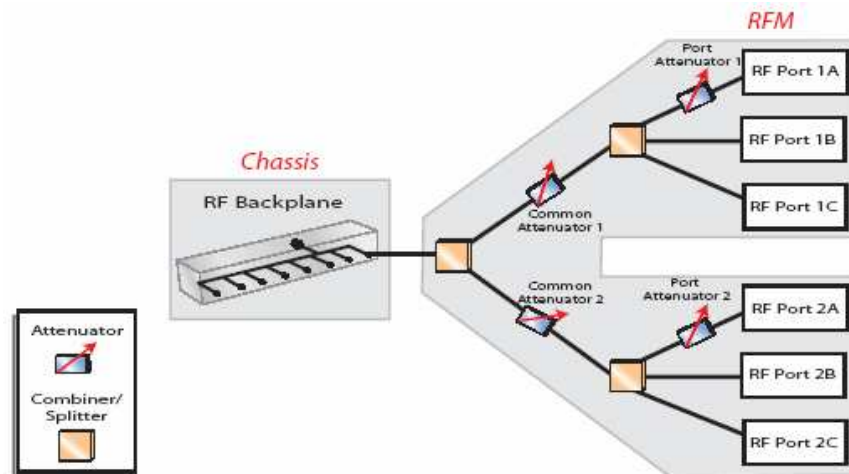
Figure 3-4 The RF configuration of the RFM; two banks have three RF ports each, with an RF combiner/splitter and attenuator. All ports of the RFM are connected to the RF backplane of the Azimuth™ Systems 801W. (From [AZI04b].)

Station Test Module

The STM houses up to two STAs in RF-isolated chambers. A Carrier Card (of which several types exist) is needed to mount the STA card onto. The RF output of the STA is cabled to the upper front panel RF port (there are two front panel RF ports, one for each STA bay) of the STM. A computer running Windows XP is part of the STM and interfaces with the DIRECTOR™. Remote Desktop is used to access the computer, which is necessary for configuring the STA for setup and when collecting data in different wireless modes. A Test-Net connector is located at the front panel of the STM. For the multipath testbed, the STA RF was routed to the front panel RF connector of the STM. One of the bays of the STM houses the WLAN client in the multipath testbed.

WLAN Analyzer

The WLA houses two IEEE 802.11a/b/g clients in RF-isolated chambers. These clients are configured with Airopeek drivers to be in promiscuous mode, meaning that they do not associate with any other STAs and receive all packets. The WLA has a computer running Windows XP that has a copy of Wildpackets Airopeek NX[‡‡] installed on it. Like the STM, the WLA has a Test-Net connector on the front panel and an RF connector on the front panel (to which Analyzer 1, in the top chamber, is connected), which is used for sniffing the packets after they have passed through the emulated channel. An attenuator between the front panel RF ports (of which there are two) and Analyzers 1 and 2, respectively, allow the signal levels at the WLA Analyzers to be adjusted. In the multipath testbed, the WLAN sniffer inside the WLA was used to capture the data packets after they had propagated through the PROPSim™.

testMAC™ Module

The TMM is a module used for testing the MAC of DUTs. It has a single WLAN client and emulates multiple STAs by using multiple IP and MAC addresses. It is used for stress testing APs to see how many STAs can be associated at a single time. A Test-Net connector and a single front panel RF port are available. The TMM does not have a built-in computer because its sole purpose is to generate the

---

[‡‡] See <http://www.wildpackets.com/products/airopeek/airopeek_nx/overview> for more information on Wildpackets Airopeek NX.

appearance of multiple WLAN clients. No configuration of clients or data save is necessary and all configuration of the TMM can be done via the DIRECTOR™. The TMM was not used for the multipath testbed as we were examining the effects of the channel on maximum achievable performance, focusing on throughput as a performance metric. This meant that we needed only one STA and one AP for data collection, and having multiple emulated STAs would not have been useful for our purposes.

mini Test Head

The MTH is a dual RF islation chamber that is used to house APs and ASDs. It has filtered Ethernet, RF, and power pass-throughs in the back panel. The chamber provides 90 dB of radiated isolation [AZI04a], which means that there will effectively be no interference from outside sources, allowing for repeatable performance testing. The RF ports, Ethernet ports, and power port in the rear panel of the MTH are filtered to minimize RF leakage through these sources. In the multipath testbed, the MTH was used to house the single WLAN AP.

3.1.2   Elektrobit PROPSim™ C8

The Elektrobit PROPSim™ C8 is a multichannel multipath channel emulator. It allows wireless channels to be emulated using a TDL with the delay, average power, and fading all user-settable. Each channel of the PROPSim™ C8 is unidirectional. It utilizes either a GUI or Command Line Interface (CLI) for control. Due to the general implementation of the PROPSim™ C8, it can be used to emulate channels for many purposes including WLANs. Figure 3-5 shows the front panel of the PROPSim™ C8. The software used for specifying the channel, simulation control, etc. is described in Section 3.1.2.1 and the PROPSim™ C8 hardware is described in Section 3.1.2.2.
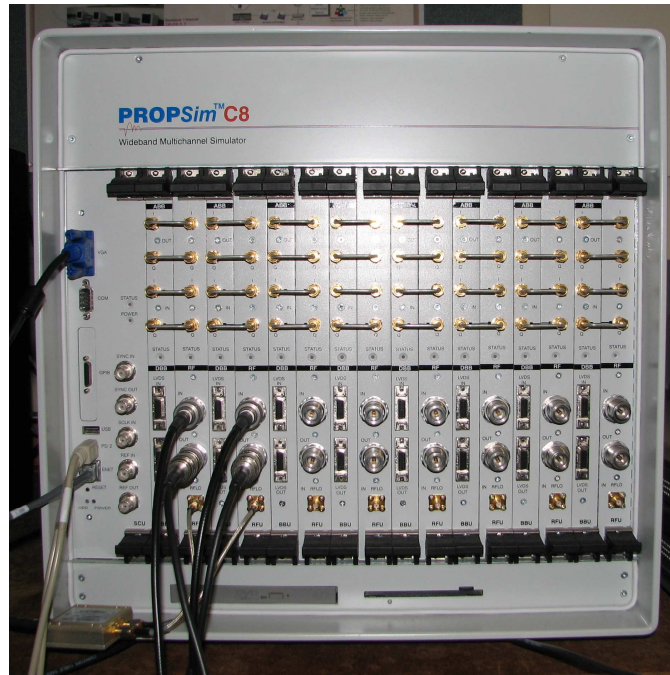
Figure 3-5 The front panel of the Elektrobit PROPSim™ C8. The PROPSim™ C8 has eight unidirectional channels, each having RF and digital inputs and outputs, as well as an RF local oscillator input. An internal computer is used for control of the PROPSim™ C8.

A tutorial on setting up the PROPSim™ C8 is given in Appendix C. Further documentation on the PROPSim™ C8 can be found in [PRO02].

3.1.2.1   PROPSim™ C8 Software

There are four GUI-based programs that are used to control the PROPSim™ C8. These allow the PDP and fading characteristics of the emulated channel to be defined, and correlation between the channels of the PROPSim™ C8 to be specified before the channel is generated and simulated. These software programs make up the PROPSim™ C8 Channel Modeling Toolbox and are used when defining and emulating wireless channels are described in more detail below. All tap specification and channel emulation can be controlled without the use of the PROPSim™ GUI via a library of commands that can be executed remotely.

Channel Model Editor

The Channel Model Editor is where the multipath channel is specified. This is done by specifying the channel PDP. Individual tap spacing, average power, and amplitude fading (e.g., Rayleigh) can be

entered. For each tap, a Doppler spectrum (e.g., flat Doppler spectrum) for frequency variation is entered. Tap modes, such as fixed delay or random hopping can be specified. Additionally, parameters such as center frequency and model precision (i.e., how many hardware taps should be used for interpolation of channel model taps) are entered using the Channel Model Editor. Figure 3-6 gives a screenshot showing the Channel Model Editor window.
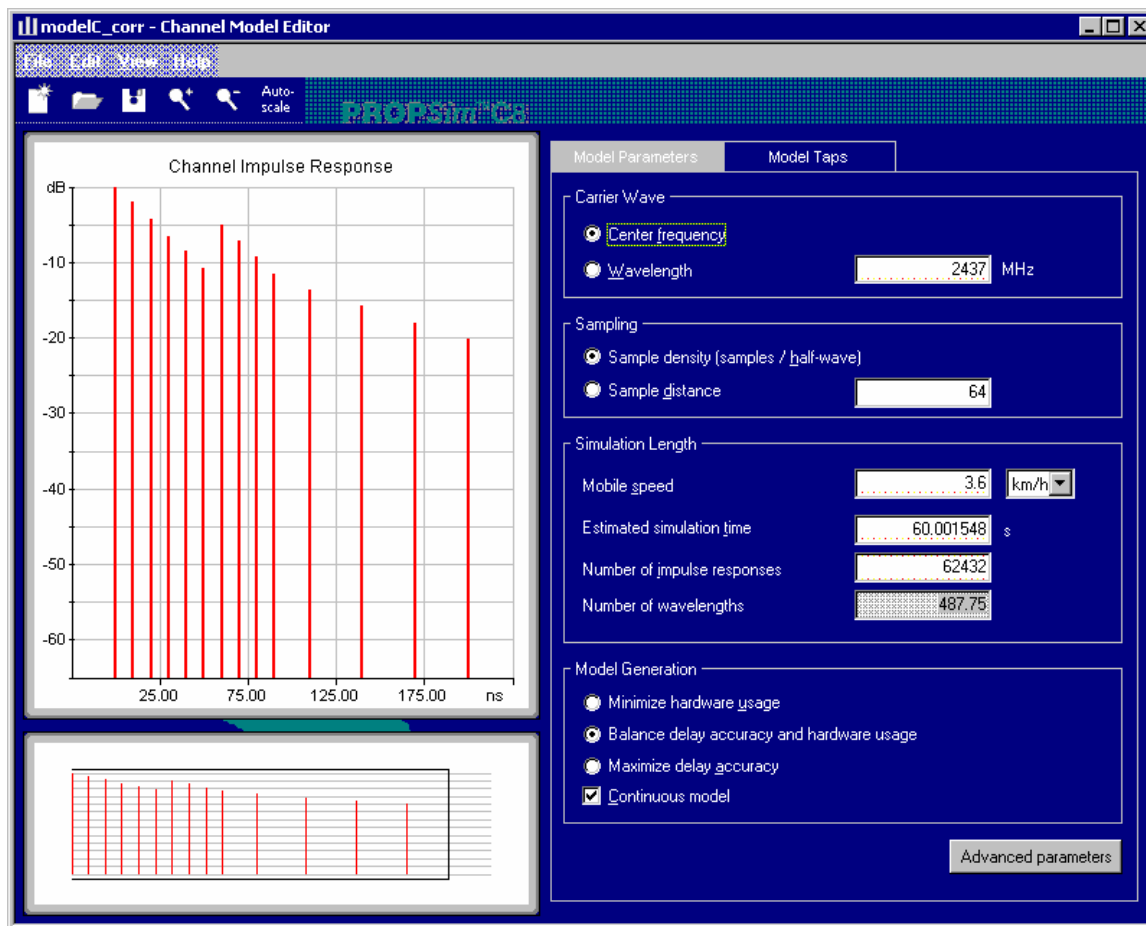
Figure 3-6 A screenshot of the PROPSim™ Channel Model Editor with the channel model PDP shown on the left and emulation factors such as center frequency and mobile speed shown on the right.

Correlation Editor

The Correlation Editor is used to specify correlation between the PROPSim™ C8's eight channels. Either amplitude or complex (amplitude and phase) correlation can be specified. Channel correlation is done by specifying a correlation matrix, where the lower triangular portion of the correlation matrix is the cross correlation coefficient values that are specified. The upper triangle is the complex conjugate

of the lower triangle. Naturally, the diagonal elements are unity, since they represent an autocorrelation. For the multipath tested, a 2x2 complex correlation matrix is configured with cross correlation coefficients of 1, which specifies the perfect correlation between uplink and downlink channels.

Simulation Editor

The Simulation Editor allows the specific channel configuration to be set up. This includes specifying then number of channels to use and which channels to use, as well as the average input power per channel, the crest factor per channel, and the specific configuration of which input goes to which output. Previously defined channel models (specified using the Channel Model Editor) are selected for given input/output combinations. Phase adjustment can be performed on the inputs and outputs if necessary. Additional attenuation can be set using the Simulation Editor. Some parameters, such as the average input power and channel attenuation can be set "on the fly" while simulating the channel using the Simulation Control software package. A noise source can be added to the output if desired. After the simulation setup is configured and saved, the channel model can be generated. Figure 3-7 shows a screenshot of the Simulation Editor with the PROPSim™ setup used for the multipath testbed.
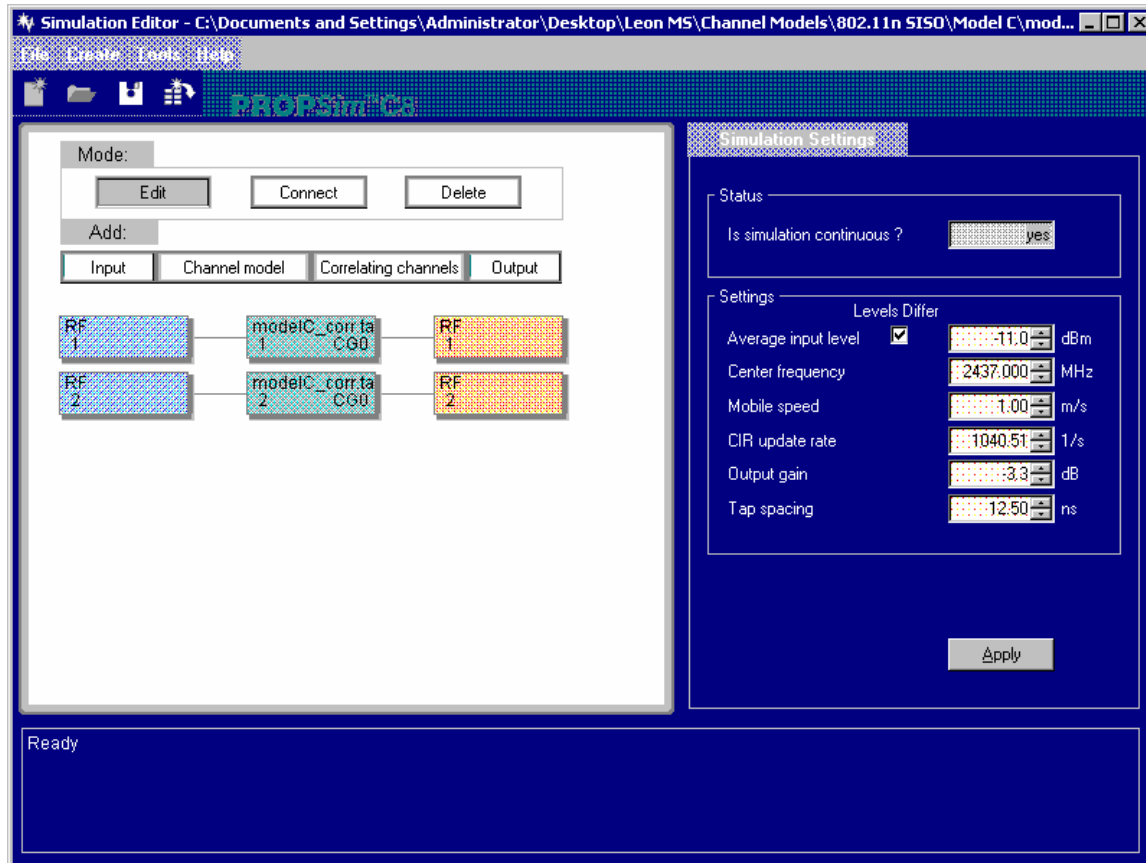
Figure 3-7 A screenshot of the PROPSim™ Simulation Editor showing the RF port(s) and channel model(s) utilized on the left-side of the window and the model generation specifications on the right-side of the window.

Simulator Control

The PROPSim™ Simulator Control is the program used to control simulation runtime. Parameters such as the input TX power level and output attenuation (gain) can be varied here, while the channel is being emulated. A previously generated simulation (using the PROPSim™ Simulation Editor) is opened for emulation. The channel emulation can be started, stopped, and paused. From the Window tab, the user can navigate to view the simulation settings, the Channel Impulse Response (CIR), which is shown in Figure 3-8, or the ports currently in use on the PROPSim™ C8. Figure 3-8 shows a screenshot of the Simulator Control program with emulation paused showing the CIR of IEEE 802.11n Channel Model C. Notice that the taps for the two channels (uplink and downlink) are correlated. Note that the taps shown here are at multiples of the PROPSim™ hardware tap spacing of 12.5 ns; the emulate channel uses interpolation to achieve the tap spacing of 10 ns used for the IEEE 802.11n channel models.
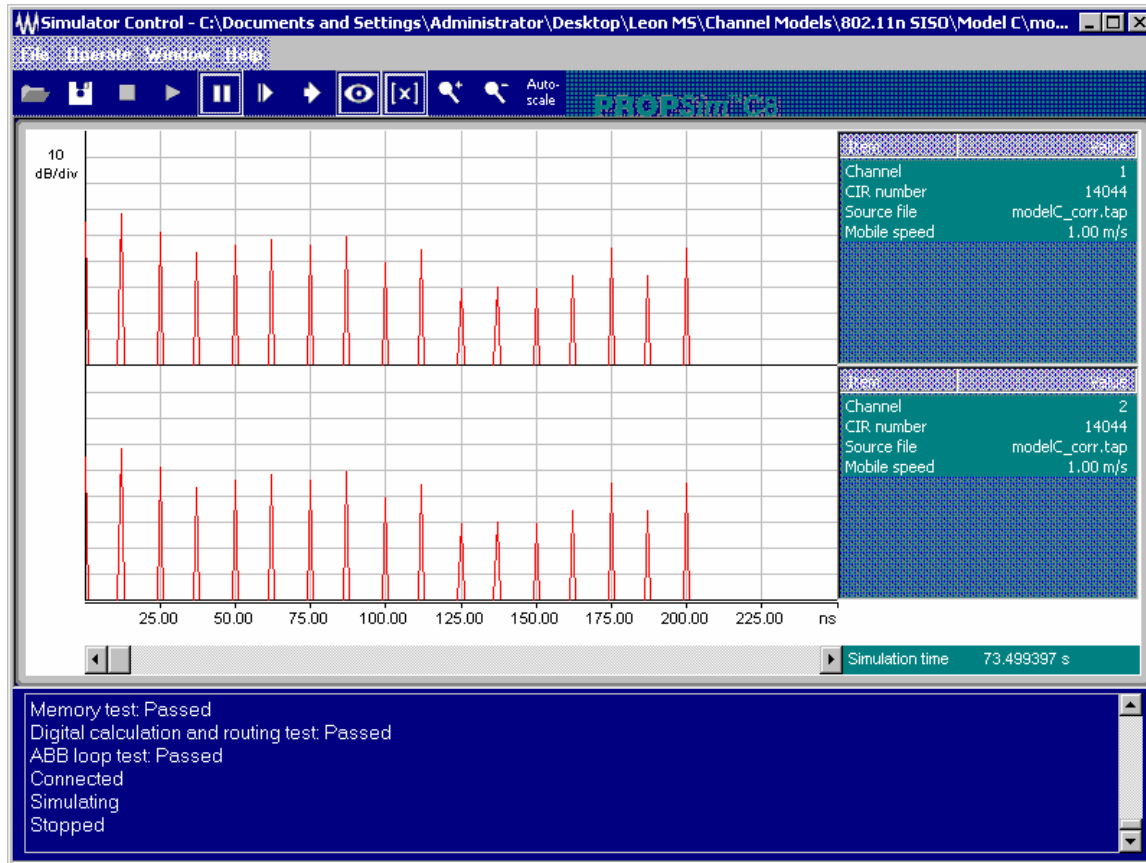
Figure 3-8 A screenshot of the PROPSim™ Simulator Control showing the emulated channel PDP(s) and current parameters of the channel(s) being simulated.

PropSoft

PropSoft is a software package that allows a terrain to be entered and time-variant channel models to be generated for a receiver traversing through that terrain. This is a software program that is more geared towards performance evaluation for Wide Area Network (WAN) applications. As the mobile moves through an environment, the channel models that represent the propagation environment between the base station and mobile are generated, allowing emulation of mobility in an environment without actual deployment in the environment. This software is not utilized in the multipath testbed as predefined indoor multipath channel models were used and no performance measurements were taken in actual environments, only the IEEE recommended channels.

3.1.2.2   PROPSim™ C8 Hardware

The PROPSim™ C8 is a self contained unit with eight RF/Base Band (BB) module pairs, each unidirectional, that emulate independent or correlated multipath channels modeled with a PDP. Each baseband unit can support 24 hardware taps for a total of 192 taps. If utilizing the RF inputs, the input signal is first downconverted then sampled, after which Digital Signal Processing (DSP) is applied (as a TDL) to emulate the channel, and the result converted back to an analog signal and upconverted. The center frequency range of the PROPSim™ C8 is from 350 MHz to 6 GHz, with a bandwidth of 70 MHz. An external local RF oscillator is necessary to use the RF ports. For RF signals having a center frequency less than or equal to 3 GHz, the RF local oscillator must be 300 MHz above the center frequency; for RF inputs with a center frequency greater than 3 GHz, the RF local oscillator must be 300 MHz below the center frequency [PRO02].

3.1.3   Other Hardware

An HP 8672A synthesized signal generator was used as the RF local oscillator for the PROPSim™ C8. Accompanying the Azimuth™ Systems 801W is a dual testhead (the MTH) where the AP is contained. This is an isolation chamber that effectively eliminates interference from outside sources, thus creating a repeatable test environment. Two MECA Electronics CN-2.500 RF circulators were used to separate and combine downlink and uplink RF signals. The circulators are required because the PROPSim™ C8 has unidirectional channels. Additionally, miscellaneous cables and RF pads were used for interconnection between the various components and signal level balancing purposes, respectively.

3.2   Multipath Testbed Design

Section 3.2.1 discusses the design considerations that went into the design of the multipath testbed. In Section 3.2.2, the functional and system level block diagrams of the multipath testbed are presented.

3.2.1   Design Considerations

Several considerations had to be taken into account during the design of the testbed and are outlined below. Once a design for the testbed was created and implementation attempted, adjustments were made to the design as needed to ensure proper forward/reverse channel isolation as well as correct channel emulation and balance of power levels.

- Loopback of RF signal (forward/reverse channel isolation)

- Input power to and output power from the PROPSim™

- How to cope with the unidirectionality of the PROPSim™?

- How should attenuation be varied to emulate distance changes?

- Specification of the multipath channel and which channel models to use

- How should WLAN packets be captured?

Several configurations were attempted, such as having only the traffic channel (granted that UDP traffic was used) having multipath and fading, while the reverse channel was constant. Another factor was channel attenuation. Originally this was to be done with the Azimuth™ RFM, which is a bank of attenuators. However, this was not the ideal design as the range was limited (due to insertion losses) and possible RF signal leakage occuring across the two banks of the RFM, despite maximizing attenuation across the banks. In the final testbed, the RFM was used but for the purpose of attenuating the signal to and from the AP so that path losses to the WLA analyzer and AP would match.

3.2.2   Block Diagram

The resulting functional block diagram for the multipath testbed is given in Figure 3-9. Both forward and reverse channels of this design have emulated channels, which have a one-to-one correlation, implementing a reciprocal channel. Distance is emulated by attenuating the output signal level of both the forward and reverse channels of the PROPSim™ in unison. Circulators are used to separate and combine signal propagation directions. UDP traffic is generated at the STA flows from the STA to the AP. Note that this testbed design is for a SISO communication system, but could be expanded for use with MIMO communication systems.
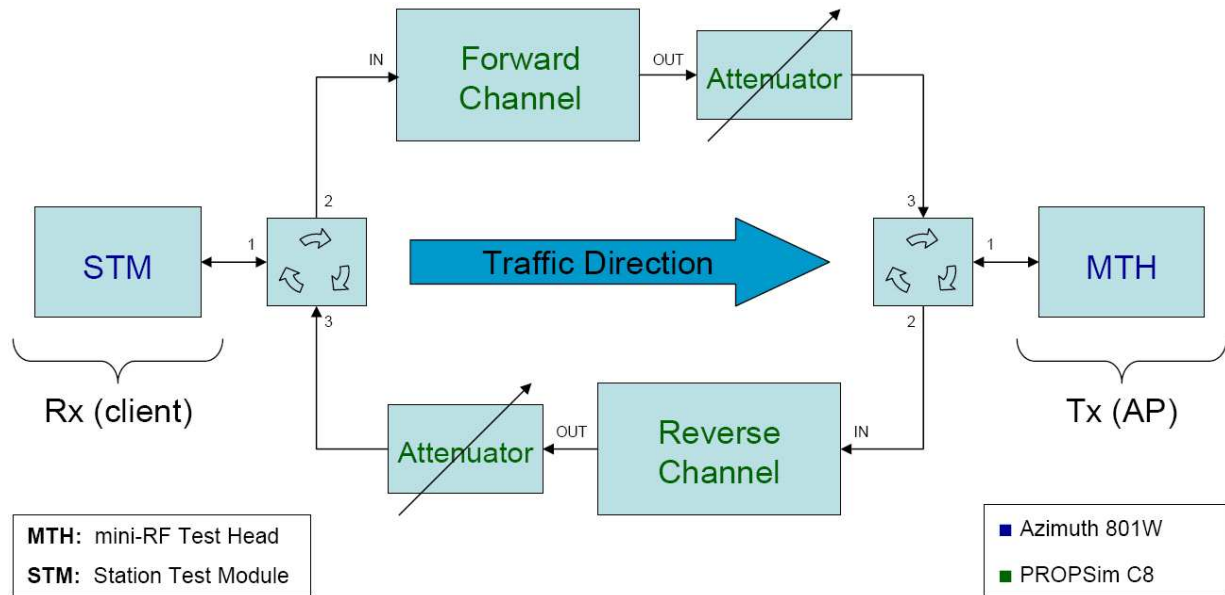
Figure 3-9 Functional block diagram of multipath testbed. Both the WLAN client and AP are housed in RF-isolation chambers, with the uplink and downlink signals going through separate PROPSim™ channels. Traffic is pumped from the client to the AP and distance emulated by varying the gain (attenuation) at the PROPSim™ RF output ports.

This design is not susceptible to the RF signal looping back as each channel of the PROPSim™ is unidirectional and acts as a terminator for an RF signal entering output port. This means that an RF signal will not be able to bypass the fading channel, which would skew the results. The reverse direction could be kept as a constant channel, but we instead opted for a time-varying channel to better emulate the wireless propagation environment.

3.3   Testbed Implementation

The multipath testbed was first implemented in the CWINS lab on the third floor of the Atwater Kent Electrical Engineering building at Worcester Polytechnic Institute in the Spring of 2005 and modified during 2006. Initial assembly took place following the development of the first draft of the block diagram. However, this particular implementation, which had only signals propagating in one direction going through the emulated channel, did not work. Consequently, further testing of that configuration and a redesign resulted in a working testbed. The final multipath testbed functional block diagram is show in Figure 3-9. Assembly and verification of the testbed involved several steps, outlined below.

1) Cabling together various components (DUTs, Azimuth™, PROPSim™)

2) Checking the power levels at PROPSim™ C8 inputs, WLAN STA, and WLAN analyzer (sniffer)

3) Adjusting received power levels using attenuators (RF pads) to balance the uplink and downlink channels as well as balance the RSS seen at the WLAN analyzer with that seen at the STA (to within a few dB)

4) Use a network analyzer to check the signal path and attenuation of the path for both uplink and downlink; verify that the channel was fading/exhibiting frequency selectivity (for multipath channel models)

5) Verifying that the client was associating with the AP and that disabling the PROPSim™ C8 (done by turning off the RF local oscillator) terminated the link

6) Increasing the path attenuation using the PROPSim™ output attenuators on both the uplink and downlink (in unison) to verify that the RSS was decreasing

7) Emulating a fading channel and examining the RSS across many packets to verify that the channel was varying

8) Performing a comparison between measured and theoretical fade duration and fade rate for a single-tap Rayleigh fading channel to verify correct channel emulation

9) Configuring traffic generator/WLAN sniffer for data collection

3.3.1   Assembly

Testbed assembly involved cabling together the various components (Azimuth™, PROPSim™, etc.) and validating the signal levels at several points along the RF chains. The overall testbed was verified using a network analyzer, which enabled the channel variation to be visualized. Assembly is as indicated in the block diagram shown in Figure 3-9. Attenuators were used as necessary to adjust the signal levels so that the uplink and downlink path losses were within a few dB. It should be noted that the PROPSim™ output level is fixed for different PROPSim™ channels with the same channel model given that the PROPSim™ input power level is set correctly, given that the PROPSim™ output

attenuation is equal across channels. The PROPSim™ input power level setting needs to be set such that no clipping occurrs at the PROPSim™ input during channel emulation.

Antenna diversity is not considered in this testbed implementation. The primary antenna is connected for the AP (with the secondary antenna terminated) and a splitter/combiner is used at the STA. The Azimuth™ 801W does not facilitate evaluation of antenna diversity unless both the AP and STA were placed in external isolation chambers. In this testbed, the client was inserted into the STM, which only has a single RF port for each chamber. Because antenna diversity is not examined, worst case results are obtained for deep fades, as antenna diversity is not available to help mitigate fading. With more RF ports available, antenna diversity could be examined since there are extra unused channel on the PROPSim™ C8.

The Azimuth™ Carrier Card with the Cisco Aironet client inserted and cabled for use in the testbed is shown in Figure 3-10. Figure 3-11 shows the Linksys WRT54G AP in the MTH cabled for use in the testbed. The antenna ports of the Linksys WRT54G have RTNC connectors; an RTNC to SMA male cable was used to cable the AP to the testbed. The circulators, splitters, and attenuators used for the testbed can be seen in Figure 3-12.
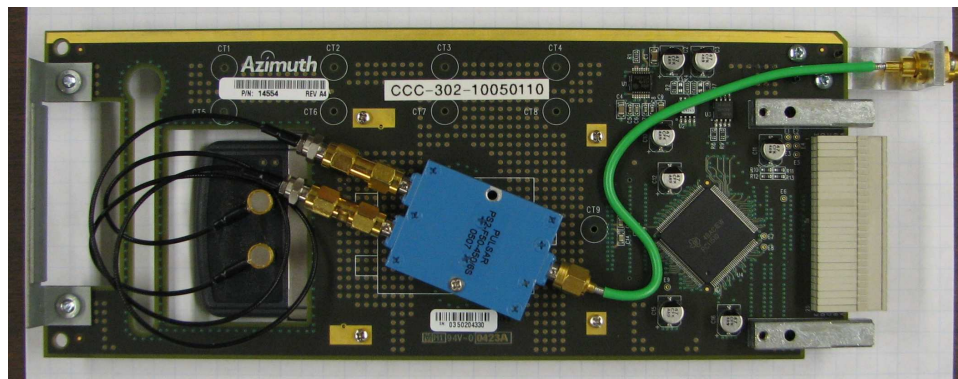
Figure 3-10 The Azimuth™ Systems Carrier Card with Cisco Client inserted and cabled using a splitter. The Carrier Card is inserted into the STM.
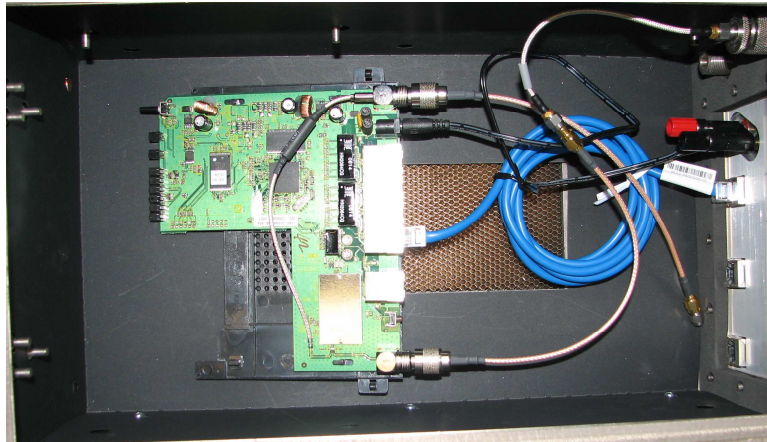
Figure 3-11 A chamber of the Azimuth™ Systems MTH, which is housing the Linksys AP that is cabled and connected to the testbed.
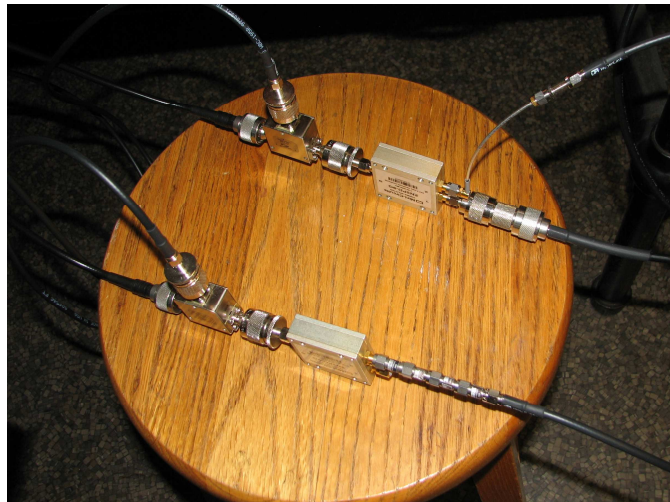
Figure 3-12 A close-up view of the circulators and attenuators used in the testbed.

Pictures showing the assembled multipath testbed are given in Figure 3-13 and Figure 3-14. The PROPSim™ is on the left and the Azimuth™ Systems 801W is on the right. The HP signal generator is in between while the MTH housing the AP is at the far right. The black computer at the far left is the Azimuth™ DIRECTOR™ computer.
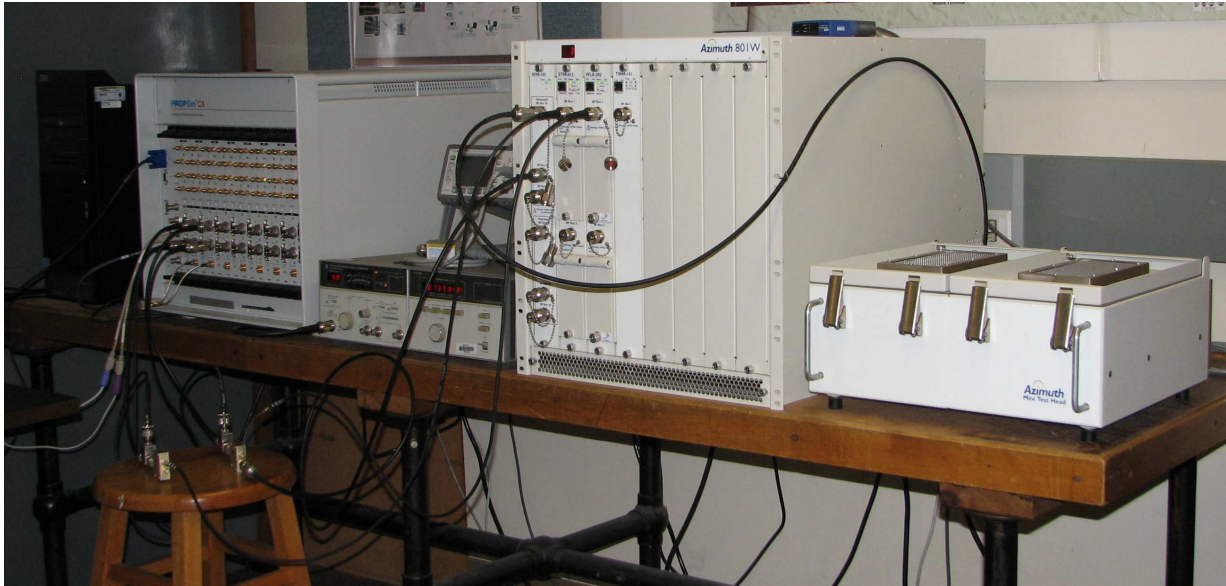
Figure 3-13 The assembled multipath testbed; from left to right: Azimuth™ DIRECTOR™ computer, Elektrobit PROPSim™ C8, HP signal generator, Azimuth™ Systems 801W, and Azimuth™ Systems MTH.

Figure 3-14 The multipath testbed control terminal; the screen on the left is for controlling the PROPSim™ C8 and the screen on the right is for controlling the Azimuth™ Systems 801W, modules, etc.

Testbed configuration involved setting up channel models, adjustment of attenuation levels, setting the RF local oscillator to the correct frequency, traffic generation setup, and Airopeek capture setup. The local oscillator for the PROPSim™ must be set to 300 MHz above the center frequency of the channel that is being used, when using equipment operating in the 2.4 GHz ISM band. Since channel 6 (2.437 GHz) was used during data collection, the signal generator was set to generate a 2.737 GHz continuous wave. The power of the RF local oscillator signal at the PROPSim™ RF local oscillator input should

be 0 dBm. For the testbed, the signal generator was set to generate a ~3 dBm signal, with a splitter being used to feed the signal into the RF local oscillator ports of the two PROPSim™ channels used.

3.3.2 Configuration of Channel Models

IEEE TGn Channel Models A-C were utilized for the multipath testbed, with RMS delay spreads of 0, 15, and 30 ns, respectively [IEE04]. Channel Models B and C represent two different environments that WLANs are commonly used in; namely the home and office. An overview of the PDPs of these channel models can be found in Section 2.2. The PDPs alone represent SISO channels and can thus be used for IEEE 802.11a/b/g WLANs. The channel modeling standard further defines the generation of correlation matrices for MIMO operation, but these are not needed for the work presented here. In addition to the four IEEE 802.11n channel models, a constant channel equivalent to an RF cable with attenuation was utilized as a baseline for comparison of results obtained using more realistic channels.

The IEEE TGn channel modeling document defines a new Doppler power spectrum for channel models B-F and is given by (3.1) [IEE04].

$$S(f) = \frac{1}{1 - A\left(\dfrac{f}{f_d}\right)^2} \tag{3.1}$$

where f_d is the Doppler frequency for the given velocity, A is a constant that shapes the spectrum to be 10% from the peak value at the frequency f_d [IEE04, PAH05], and $|f| \le 5 f_d$. The velocity recommended by the channel modeling standard is 1.2 km/hour, which is slower than the average human walking speed. However, this Doppler power spectrum includes greater Doppler shifts but with lower probability. The Doppler power spectrum defined by (3.1) is shown in Figure 3-15.
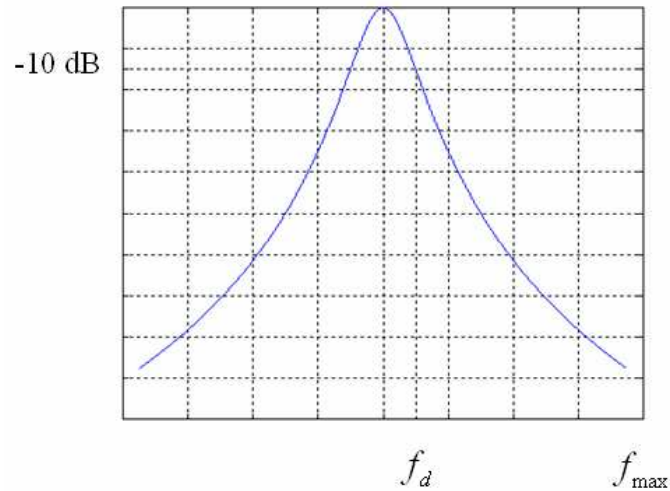
Figure 3-15 The bell-shaped Doppler power spectrum recommended in the IEEE 802.11n channel modeling document. (From [IEE04].)

However, the Doppler power spectrum specified in the channel modeling standard is not used in our testbed. Instead, a flat Doppler power spectrum with a Doppler spread (bandwidth) representing a velocity of 3.6 km/hour at 2.437 GHz ($f_d = \pm 8.12$ Hz), representing the lower range of human walking speeds is used [PAH05]. This is because the PROPSim™ C8 does not allow the user to define arbitrary Doppler power spectra, instead only letting the user choose from predefined Doppler power spectra. Despite being different from the IEEE channel modeling document, the flat Doppler power spectrum is noted in [PAH05] as simply but accurately modeling indoor channels.

3.3.3   Configuration of PROPSim™ C8

There are many PROPSim™ parameters that need to be set and others that are not set but must be specified. These define the channel that is emulated and are necessary for replication of the testbed and also to verify that the emulated channel is the same. The following are general PROPSim™ parameters:

- IEEE 802.11b PROPSim™ input power settings: -11 dBm and -9 dBm for PROPSim™ channel 1 and channel 2, respectively

- IEEE 802.11g PROPSim™ input power settings: -12 dBm and -11 dBm for PROPSim™ channel 1 and channel 2, respectively

- Crest factor of 6 dB per PROPSim™ channel

- No changes to input/output phase

- No additional noise source added/enabled

- CIR update rate is 1040.51 s^{-1}

- Sample density of 64 samples/half-wave

- Estimated simulation time of 60.001548 seconds

- Number of impulse responses: 62432

- Number of wavelengths: 487.75

- Continuous model used

- Random number (distribution) seed of 18467

Table 3-1 gives the PROPSim™ setup parameters for the four channel utilized.

Table 3-1 Per-Channel PROPSim™ Setup Parameters

Channel	Initial Gain [dB]	Expected Output [dBm]	Model Generation
Constant	-10.0	-26.0	Maximize delay accuracy
TGn Model A	-0.2	-26.0	Maximize delay accuracy
TGn Model B	-2.0	-26.0	Balance delay accuracy and hardware usage
TGn Model C	-3.3	-26.0	Balance delay accuracy and hardware usage

3.4   Traffic Generation and Data Collection

Traffic was generated in the testbed and pumped through the PROPSim™, with the frames being captured after they had propagated through the emulated channel. Section 3.4.1 and 3.4.2 explain why UDP traffic is generated for data collected and the utility used for traffic generation. In Section 3.4.3, an overview of WildPackets Airopeek NX, a WLAN protocol analyzer is presented.

3.4.1 Why UDP Traffic?

UDP traffic is used because it is the simplest form of IP traffic and for the maximum possible throughput to be achieved. There are no higher layer ACKs (such as in Transport Control Protocol (TCP)) that would result in higher layer retransmissions and reduction in throughput. To the higher layers, a UDP frame is either received or not. However, it should be noted that at the IEEE 802.11 MAC/PHY layer, retransmission will occur if a frame is not received or acknowledged properly. This enables channel effects on the maximum WLAN throughput to be analyzed and an upper bound on throughput performance determined. By using UDP traffic in the measurement campaign, we ensure that our results do indeed provide an upper bound on throughput performance for the different channel models that were analyzed.

3.4.2 Azimuth™ Traffic Generator

The Azimuth™ traffic generator generates low layer Sub-Network Access Protocol (SNAP) packets to be sent from STA to STA. These are effectively UDP packets because they are acknowledged at the IEEE 802.11 MAC layer and do no incur retransmissions. For the data collection campaign undertaken for this thesis, both IEEE 802.11b and 802.11g traffic was generated with 100% traffic density (back-to-back frames) and a frame length of 1536 bytes.
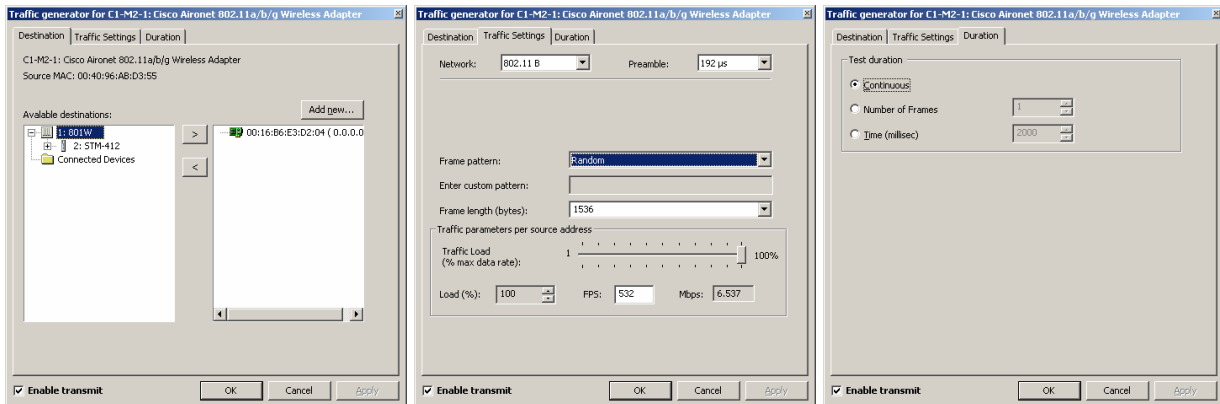
Figure 3-16 Screenshots showing the Azimuth™ Systems traffic generator utility; from left to right: destination tab, traffic settings tab, and duration tab.

3.4.3   Airopeek NX Packet Capture

To facilitate packet capture for data collection, the WildPackets Airopeek sniffer was utilized. The Azimuth™ Systems 801W at CWINS has a WLA module with two WLAN sniffers that are designed for this purpose. Analyzer 1 in the WLA was routed to the RF front panel port 1 and connected in parallel with the AP in the testbed. An additional 6 dB of attenuation in the WLA balanced the power seen by the WLAN client and WLAN analyzer. Data frames being pumped from the STA would thus be captured by Airopeek after they had passed through the channel emulated by PROPSim™. Figure 3-17 shows a screenshot Airopeek NX following a packet capture. Observe the RSS and DLR variation, with CRC errors on some of the packets.
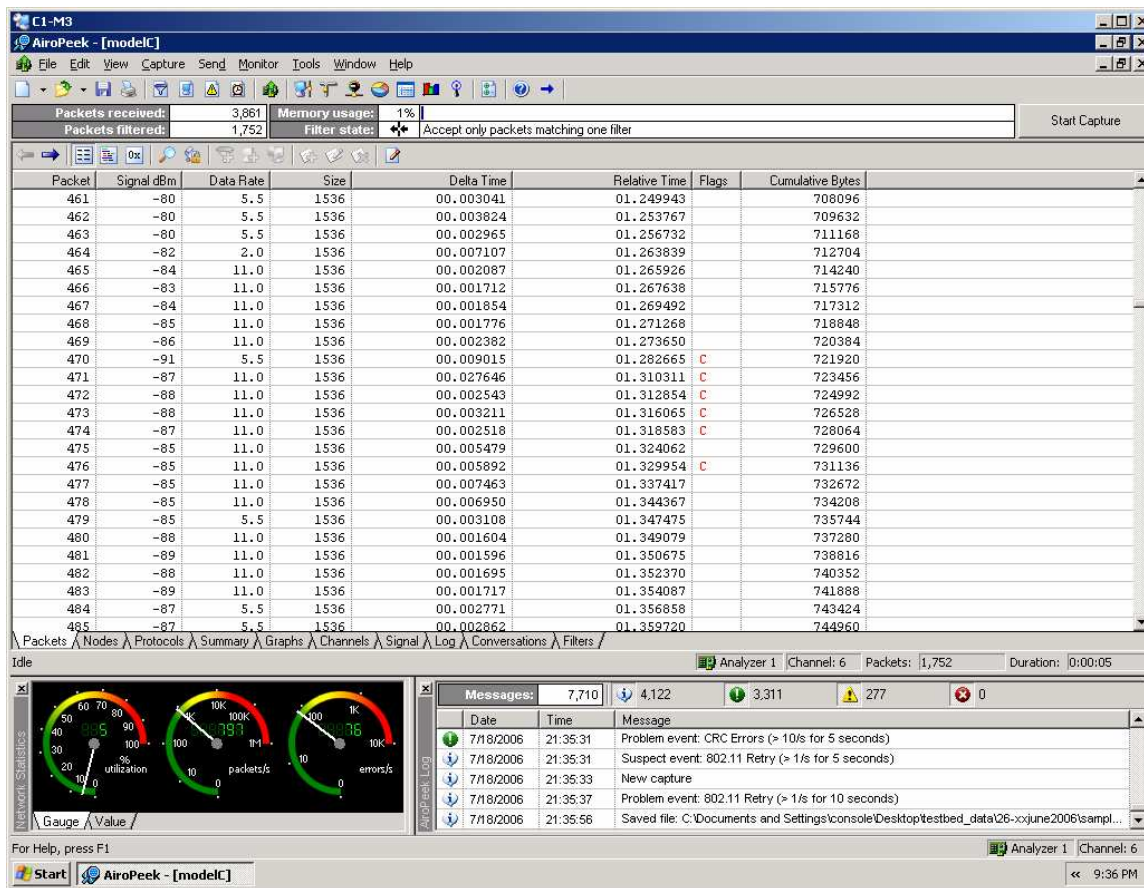
Figure 3-17 A screenshot of the Airopeek NX WLAN protocol analyzer showing a sample packet capture with per-packet information such as RSS and data rate.

An Airopeek filter was used to filter out the uplink UDP data packets. Information such as the RSS, DLR, and packet length were saved as tab separated files. A sample of the packet list file obtained for data collection for an IEEE 802.11b WLAN is given below:

```
57    -87    11.0    1536    00.004072    00.129213    C    87552

58    -88    11.0    1536    00.005080    00.134293    C    89088

59    -91    5.5     1536    00.006759    00.141052         90624

60    -90    5.5     1536    00.024210    00.165262         92160

61    -90    5.5     1536    00.004704    00.169966         93696

62    -87    2.0     1536    00.014211    00.184177         95232

63    -87    11.0    1536    00.002043    00.186220         96768
```

The first column gives the packet number, which begins with 1 for the first packet captured. The second column is the RSS and the third the DLR. The fourth and eighth columns show the total frame length (in bytes) and total cumulative bytes of data captured, respectively. Columns five and six give the time between successive packets and total time elapsed. Column seven gives any flags that were thrown for the given packet. In this sample, the 'C' flag for the first two packets shows that they had an invalid FCS. The exact format of the packet lists is up to the user. All of the above information was not directly used to generate results but was considered useful to have.

For data collected to analyze the average throughput, no triggers were utilized. For each sample, the packet capture was started and ended manually once the desired (fixed) number of packets had been collected. Measurements used for analyzing variations in instantaneous throughput were performed by manually starting packet capture and setting the trigger to stop after the 1 minute sample duration had elapsed for 1536, 512, and 128 byte frames.

Chapter 4:   Performance Evaluation, Results, and Analysis

This chapter presents the results and analysis of performance evaluation conducted with IEEE 802.11b and IEEE 802.11g WLANs using the multipath testbed that was developed as part of the thesis project and is described in Chapter 3. Section 4.1 explores what performance evaluation of WLANs means and the methods that are used for analyzing and characterizing WLAN performance. Section 4.2 give an overview of the WLAN devices that were utilized for data collection and Section 4.3 outlines the data collection and evaluation procedure. A comparison between theoretical and measured fade duration and fade frequency for a single-tap Rayleigh channel is presented in Section 4.4 as this relates the emulated channel to what should theoretically be occurring in the channel emulator.

Sections 4.5 and 4.6 show throughput versus power and throughput variation data for three channels, with models presented that relate throughput to received power and throughput variation to the average throughput. Section 4.7 provides a description a comprehensive throughput-power model developed using throughput measurements and that describes both the average throughput as a function of power and the throughput variation. In Section 4.9, a metric for comparatively examining WLAN throughput performance is proposed and a example calculation performed.

4.1   Performance Evaluation of WLANs

Performance evaluation is fundamental to understanding and characterizing networks. It is necessary to model the performance behavior of various types of networks. Development of models that describe how performance metrics behave in different environments enables the use of these models for performance comparison, comparative performance analysis, and integration into research and development work that will yield more accurate results and outcomes. The goal of performance evaluation and modeling is to better understand the limitations and behavior of the network/device on hand under various operational conditions and scenarios.   These specific network/condition configurations would then not require measurement campaigns to analyze given that models have previously been developed for that purpose.

Whereas in the case of LANs, where quantifying performance was easier because it was possible to accurately develop a model to describe throughput, PER, etc. given the stability of the medium (channel), it is much more difficult to do such an analysis for WLANs as a result of the channels variability. The statistical complexity of the wireless medium and inherent implementation complexity

required by WLAN devices to transmit data over the wireless channel is the source of the difficulties in performance evaluation of WLANs. At the core of the issue is the significant time and space varying nature of the wireless channel.

In wireless channels, there is never a single fixed path for signals, resulting in multiple paths each having different degrees of attenuation and taking different lengths of time to travel. This results in multipath fading, which is characterized by fast fading at various frequencies. For a narrowband signal, fast fading causes momentary decreases in received signal strength on the order of 20-30 dB [PAH05]. For wideband wireless communication systems such as WLANs, multipath (frequency selective) fading is mitigated by using RAKE receivers, transmission using OFDM (which utilizes multiple narrowband subcarriers), or MIMO technology.

However, to analytically model such a system would be a daunting task. Describing the throughput of a WLAN in a lognormal fading channel is a relatively straightforward task despite the multi-rate nature of WLANs, as lognormal fading is long-term variations in path-loss, where it can be assumed that a single packet will have a fixed path-loss associated with it (i.e., the path-loss will not change during the transmission of the packet. This is not the case for multipath fading, where fades can occur during a packets transmission, resulting in packets being lost despite a high average received signal strength. Analyzing these types of variations analytically, where fading is random is not the desired approach.

A more desirable method is to instead take empirical measurements of performance in given set of environments and use the measurement to model the nature of performance for the those environment. Picking environments that generalize typical usage scenarios helps to make results more applicable. A straightforward way of examining the throughput is by using Iperf or Chariot, which will yield the average throughput and throughput versus time that can be transmitted over a given channel. A more comprehensive approach is taken in this project, where DLR probability statistics, average throughput, and instantaneous throughput variations are examined as a function of average RSS in relation to standardized channel models.

Section 4.1.1 describes techniques for performance valuation of WLANs.

4.1.1 Evaluation Techniques

There are three techniques that are used when evaluating WLAN performance. These are empirical measurements, simulations, and analytical analysis. Combinations of these can be utilized as well –

they are not disjoint evaluation methods. Sections 4.1.1.1-4.1.1.3 summarizes these performance evaluation techniques. Certain methods are best applied to certain applications, where taking empirical measurements was the method chosen for the research described here. This method is desirable when considering the complexity of simulating or analytically analyzing the effects of a multipath fading channel on a multi-rate communication system.

4.1.1.1   Empirical Measurements

Collecting measurements in "real world" environments is the preferred method for analyzing the behavior of complex indoor channels. Indoor environments are subject to high degrees of multipath, which significantly increases the complexity of any analytical analysis or simulation. If sufficient sample sizes are gathered during a measurement campaign, the results are representative of the given wireless environment; if environments are carefully selected, the results provide a set of data that can be used to derive an idea of performance in all environments.

Empirical measurements of WLAN performance have traditionally been performed by moving WLAN clients around buildings (and when appropriate outdoors) and measurement performance metrics such as throughput, RSS, SNR, DLR, PER, and jitter are measured for multiple locations in the given measurement testbed. However, such results are location specific and, given the channel specific measurements that are observed, do no represent data that can be replicated by others. This emphasizes the need for a standard set of environments that can be utilized by anyone for performance evaluation.

Using an RF-isolated WLAN test platform ensured that interference is minimized making results repeatable. Additionally, utilizing standardized channel models proposed by the IEEE with a channel emulator, a testbed can be created whereby multiple wireless environments can be examined without having to travel to multiple locations, and results gathered that can be replicated as a result of the RF-isolation utilized and use of standard channel models. This is the approach taken in the project described in this thesis – taking empirical measurements utilizing an RF-isolated WLAN test platform with emulated channel for three channel models representing typical environments for WLAN usage.

4.1.1.2   Performance Simulations

Simulations of WLANs can be performed using MATLAB or Ns (<http://www.isi.edu/nsnam/ns/>). WLAN simulations are a good way to test new idea but when used for performance analysis, they tend to produce idealized results. This is because they typically do not factor in the non-idealities of actual

WLAN devices. These variations for a particular device and between devices mean that there may be performance degradation due to the device in addition to channel effects, interference, and overheads due to the MAC and PHY headers and IFSs.

4.1.1.3   Analytical Evaluation

Analytical evaluation of WLANs can be done up to a point. These typically involve analysis of the MAC, calculation of overheads to determine maximum possible throughput, and the effects of simple channels (e.g., single tap channel with lognormal fading). Analysis of multi-tap Rayleigh fading channels involves analytically examining the effects of fast fading on frame reception, which is a function of the frame length, frame period, etc. on top of characterizing the average power, which experiences lognormal fading. Additionally, all fading on taps is stochastic, which further complicates an analytical expression for throughput in multipath fading channels. WLAN performance evaluation in complex channels is best examined using simulations or empirical measurements, where sample sizes are sufficient to provide conclusive results.

4.2   Devices Utilized

Two WLAN devices were utilized for performance measurement: Cisco Aironet IEEE 802.11a/b/g WLAN PC card client and Linksys IEEE 802.11b/g WLAN AP. Only one AP and one client were utilized to examine the maximum achievable throughput. Channel effects on throughput performance were examined, which stressed the need for minimizing other performance factors, such as effects of the MAC. These WLAN devices were put in either IEEE 802.11b or IEEE 802.11g operational mode. Security was *disabled* for the measurements; the consequence of enabling security is that extra overhead is added, which slightly reduces the maximum achievable throughput, a factor that can be calculated given the bounds on throughput presented in this thesis. Table 4-1 gives the specifications of the WLAN equipment utilized for the data collection campaign.

Table 4-1 WLAN Equipment Setup Used for Data Collection

	Cisco Aironet Client	*Linksys AP*
Model Number	AIR-CB21AG-A-K9	WRT54G
Firmware Version	–	v1.00.9
Driver Version	2.5.0.22	–
Operational Mode	802.11b and 802.11g	802.11b and mixed
Channel	6 (2.437 GHz)	
Security	Disabled	
Transmit Power	Full power	(Not user settable)
Access Mechanism	DCF	
IP Address	192.168.3.1	192.168.3.12

4.3   Data Collection and Evaluation Procedure

Data collection was slightly different for throughput versus power and throughput variation results. For throughput versus power, a fixed number of packets were captured, namely >10,000 for 802.11b mode and >50,000 for 802.11g mode, of which 10,000 or 50,000 frame statistics were used. For throughput variation results, a fixed capture period of 1 minute was specified with a variable number of frames. The data files, in the form of tab separated packet lists, were consequently parsed using C into multiple single column numerical files, which were loaded into MATLAB for further post processing. For more details on data collection and evaluation for the specific throughput results, see Sections 4.5-4.6.

4.4   Fade Duration and Frequency

Theoretical and measured fade duration and frequency was examined for the single tap Rayleigh fading channel (IEEE 802.11n Channel Model A). With the WLAN device operating in 802.11b mode, packets were collected for 60 seconds. The RSS and relative time data (from the packet lists) was used to analyze the fade duration and frequency. A moving average with a window size of 10 samples was utilized for the measured RSS data as there is a measurement variation of approximately ±2 dB that would cause the fade frequency to increase dramatically and the fade duration to decrease, particularly when the threshold and RMS amplitudes are within the measurement variation range of ±2 dB. The theoretical and measured plots of fade duration and frequency are shown in Figure 4-1 (measured data using IEEE 802.11b mode).

(a)   (b)
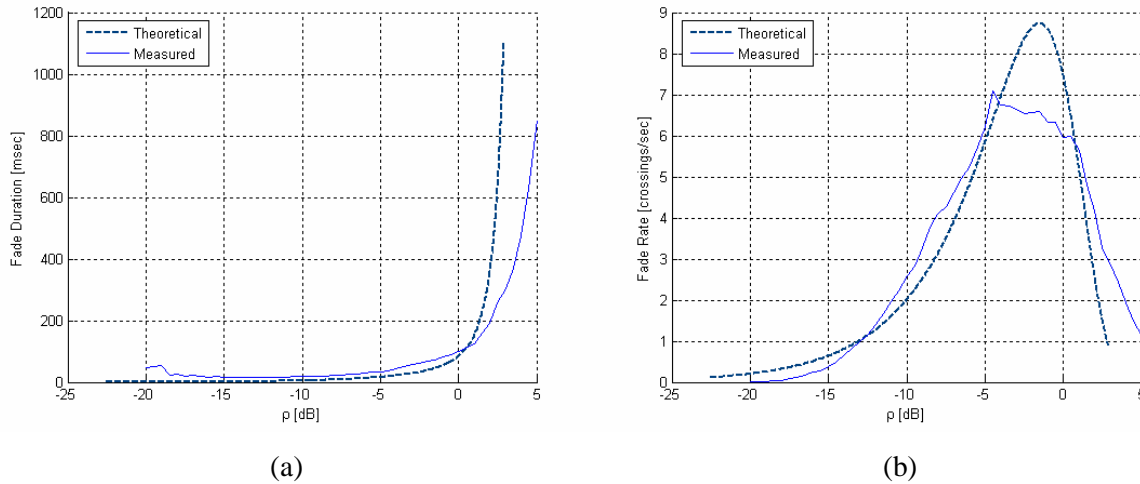
Figure 4-1 Comparison between theoretical and measured (using WLAN client RSS measurement in emulated channel) channel characteristics for a single-tap Rayleigh fading channel: (a) fade duration and (b) fade frequency.

As can be seen in Figure 4-1, the measured fade duration and fade frequency does not precisely match the theoretical results, as would be expected in an emulated channel. This is likely the results of RSS measurement inaccuracy on the part of the WLAN device as well as the RSS averaging that is necessary because of RSS measurement inaccuracy. The equations describing the theoretical fade duration $\tau(\rho)$ and fade frequency $N(\rho)$ area given by (4.1) and (4.2) [PAH05]. They are derived by relating a threshold amplitude to the RMS amplitude given that the amplitude is varying with a Rayleigh distribution.

$$\tau(\rho) = \frac{e^{\rho^2} - 1}{\sqrt{2\pi}\rho f_M} \tag{4.1}$$

$$N(\rho) = \sqrt{2\pi} f_M \rho e^{-\rho^2} \tag{4.2}$$

where $\rho = A/A_{RMS}$ (the ratio of the threshold to the average signal level) and $f_M = (v_m/c)f_c$ is the maximum Doppler shift at the given center frequency. It can be seen in Figure 4-1 that (given an RSS moving average) the curves fit well, as would be assumed. However, there is some deviation between the theoretical and measured plots as the receive power measurement of the WLAN devices is only accurate to within a few dB. Only the single tap Rayleigh channel case was examined as the theoretical

fade duration is derived for single tap Rayleigh fading channels. This comparison was made to ascertain the accuracy with which the channel was being emulated[§§].

4.5 Modeling Average Throughput

Throughput was measured and modeled as a function of power for four channels. The constant channel was included as a baseline to gauge what the ideal performance is. Statistical data was collected on the DLRs used for each sample, from which the theoretical maximum throughput values are derived. Additionally, actual throughput plots, which were found by taking the total data sent for a given sample divided by the duration of the sample, are shown. The former set of figures represents the theoretically achievable throughput given the DLR distribution for the given sample while the latter set of figures shows the actual throughput observed. Piecewise linear models, found by line-fitting to the throughput data, are presented as models describing the throughput/power relationship for the given channels. Figure 4-2 shows sample scatter plots of instantaneous throughput data for IEEE 802.11b and 802.11g WLANs to illustrate how the variable throughput was reduced to models.

(a)   (b)
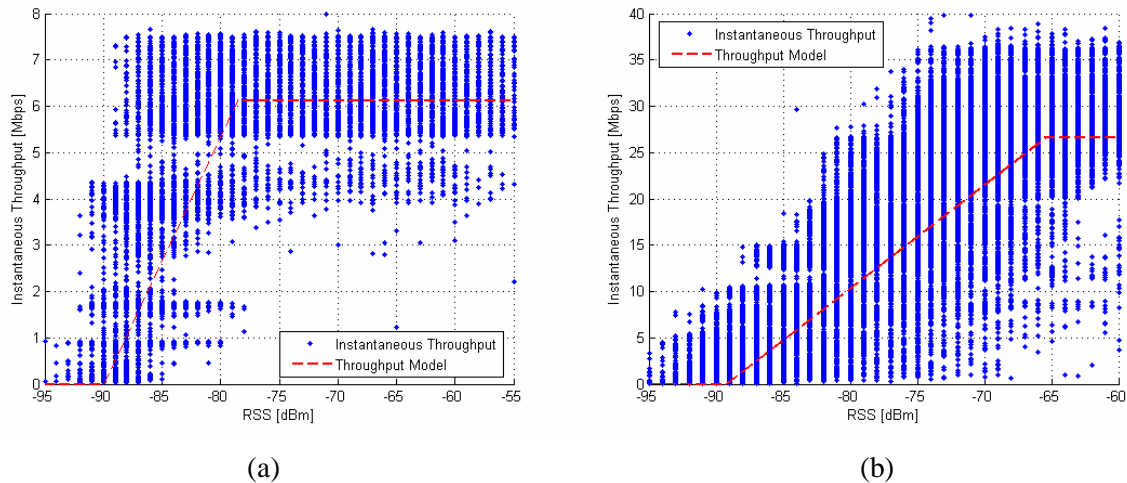
Figure 4-2 Sample of scatter plots of instantaneous throughput for IEEE 802.11b and 802.11g

---

[§§] A more accurate comparison of theoretical and measured fade duration and frequency would involve using a power meter or other calibrated, highly accurate test device to gather RSS data instead of relying on the RSS measurement reported by a WLAN device. Likewise, the comparison could be made by utilizing the channel emulators tap coefficients.

4.5.1 Data Collection and Analysis

The maximum achievable throughput was determined for multiple received powers by collecting packet information, such as RSS and DLR for 10,000 packets for 802.11b and 50,000 packets for 802.11g. The number of packets was such that for a constant channel with high RSS, the sample time was approximately 20 seconds[***]. Five times the number of 802.11b packets was collected for 802.11g as the maximum 802.11g PHY layer rate is approximately five times that of 802.11b. Packet lists were collected for decreasing received power at 1 dB increments. The 20 second sample time covers N_{τ_c} coherence times, as shown by (4.3).

$$N_{\tau_c} = 20\left(\frac{1}{\tau_c}\right) = 20(B_D) = 20(2f_M) = 40f_M \qquad \textbf{(4.3)}$$

Given the calculation shown in (4.3), packet statistics were collected for a period greater than approximately $40f_M$, or 324.93 channel coherence times at 2.437 GHz. This yields sufficient channel variation during the measurement sample time so that channel effects on performance can be examined.

Packet lists were collected for all measurement samples (attenuator settings). These were first parsed using C to generate one column numerical files easily loaded into MATLAB. Each packet list *.txt file was mapped to five *.out files, with each file containing the RSS, DLR, packet time delta, cumulative time, and associated flags. These files were loaded into MATLAB as desired and analyzed.

4.5.1.1 Throughput Data Generation

Several steps were involved in generating throughput data points. These were performed using MATLAB and are outlined below:

[***] For lower RSS and a time-varying channel, the frames would be transmitted at varying rates and possibly lost, resulting in the sample duration for a fixed number of packets to be longer.

1) Load desired parsed data files for given measurement sample (DLR, RSS, inter-frame durations, etc.)

2) Parse into different DLRs for the given sample

3) Calculate associated DLR probabilities from parsed DLR results

4) Calculate average RSS for the given sample

5) Utilize DLR probabilities along with theoretical throughputs per DLR for the given WLAN device and network configuration to find the throughput for the given measurement sample

6) Eliminate any throughput data points where the:

    a. Adjacent sample average RSSs are very close together (less than 0.1 dB) so that data points are not overlapping

    b. Average throughput was discontinuous (dropped down or jumped up significantly) and thus represented outliers

7) Plot average throughput data versus the average RSS per measurement sample, enabling modeling of average throughput versus average RSS

Generation of throughput samples from DLR probabilities involves knowing the theoretical maximum throughput for a given DLR. These can be calculated for many network and device scenarios; for our work, the per-DLR throughputs were calculated for a simple one AP, one STA infrastructure configuration with a long preamble for IEEE 802.11b. The vector product of the ith DLR probability vector and the calculated theoretical throughput vector yields the ith throughput, as given by (4.4).

$$S_i = \vec{P}_{DLR,i} \, \vec{S}_{DLR} \qquad\qquad \textbf{(4.4)}$$

where $\vec{P}_{DLR,i}$ is a vector containing the DLR probabilities for the ith measurement sample and $\vec{S}_{DLR}$ is a vector containing the per DLR calculated throughputs (maximum or otherwise). It is necessary to include the 0 Mbps throughput case and associated probability in this calculation. The medium time associated with a "0 Mbps" frame is referred to as medium *deadtime* – the medium time that is not being used for a frame exchange (e.g., from backoff due to retransmissions, frame loss, frames with

CRC errors, etc.). Medium deadtime, as it pertains to the calculation of maximum throughput data points is described in Section 4.5.1.3.

4.5.1.2   DLR Probability Histogram Samples

To illustrate the change in DLR probabilities that occurs as the RSS decreases, sample histograms are given for IEEE 802.11b and 802.11g WLANs operating in four different channels. Figure 4-3 through Figure 4-6 show sample DLR histograms at varying RSS values for a constant channel, and Channel Models A, B, and C respectively.

<center>(a)   (b)</center>
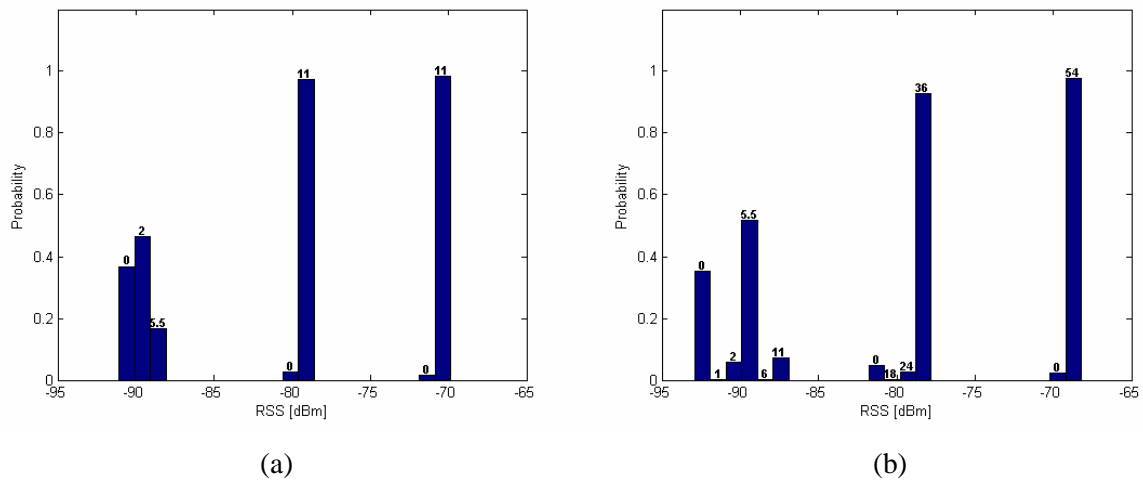
Figure 4-3 Sample DLR probability histograms for a constant channel at three sample average RSS values: (a) IEEE 802.11b and (b) IEEE 802.11g. Observe that the spread in data rates utilized increases as the RSS decreases. At high RSS, the fastest data rate is dominant, with some probability of the 0 Mbps case.

(a)

(b)
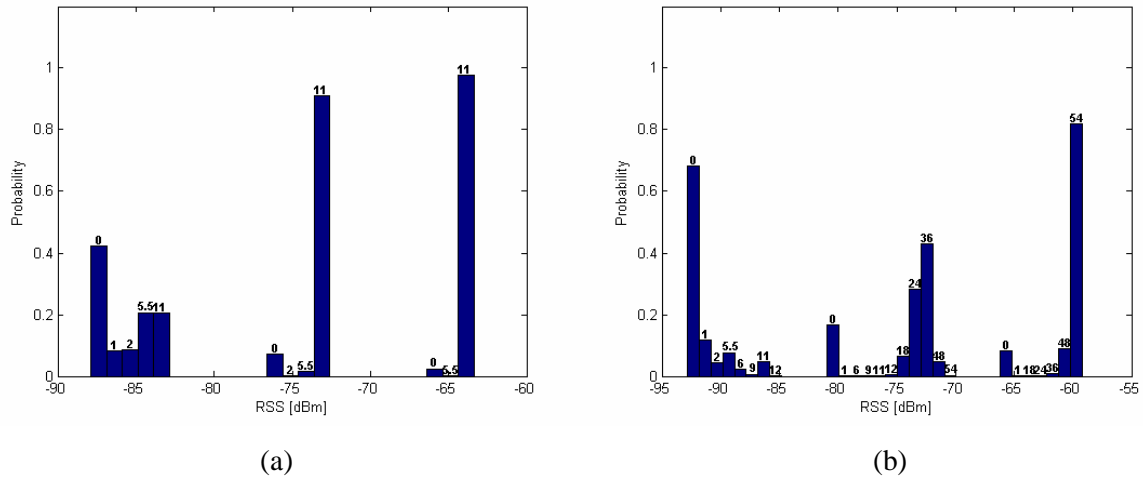
Figure 4-4 Sample DLR probability histograms for TGn Channel Model A at three sample average RSS values: (a) IEEE 802.11b and (b) IEEE 802.11g. Note that the number of different data rates utilized has increased even for high RSS.

(a)

(b)
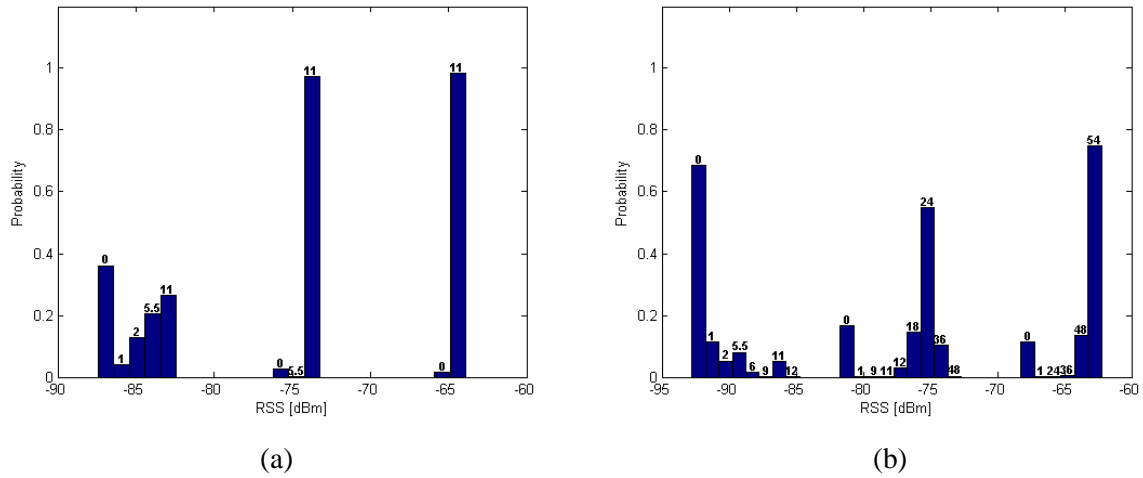
Figure 4-5 Sample DLR probability histograms for TGn Channel Model B at three sample average RSS values: (a) IEEE 802.11b and (b) IEEE 802.11g.

(a)   (b)
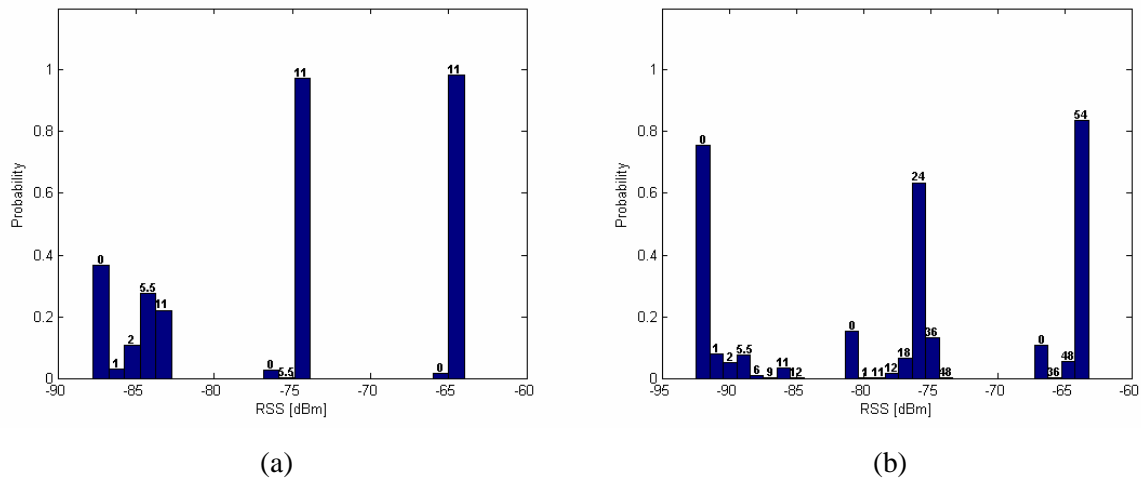
Figure 4-6 Sample DLR probability histograms for TGn Channel Model C at three sample average RSS values: (a) IEEE 802.11b and (b) IEEE 802.11g.

From the figures above, it can be seen the impact that a multipath fading channel has on the DLR probabilities. For a constant channel, the DLR is relatively constant at 11 and 54 Mbps for IEEE 802.11b and 802.11g, for high RSS. However, once fading is introduced, the DLR begins to fluctuate and causes the histogram to spread out. This is particularly noticeable for the 802.11g operational mode, where there are more PHY rates and their respective drop-offs are at higher RSSs.

4.5.1.3   Probability of Wireless Medium Deadtime

The concept of medium deadtime is used to describe medium time that is not actively being used for the ideal transmission of data frames[†††]. This includes backoff due to retransmission, frames that have an incorrect CRC, and frames dropped due to probability of outage when at the edge of an APs coverage area. This term is necessary when examining throughput using DLR probabilities, as the amount of time that the medium is ideal must be accounted for to get accurate throughput results. When considering deadtime in the context presented here, it is important to note that traffic must be streamed

---

[†††] Ideal frame transmission refers to a frame exchange that does not include any lost frames or retransmissions.

at 100 % of the possible traffic density. The metric will then describe the amount of airtime that is unused in relation to the maximum possible throughput[‡‡‡].

There are several assumptions that underlie calculation of deadtime in relation to its use in this thesis:

1) Management frames, such as beacons, are grouped into the deadtime metric. For WLANs operating in DCF mode, management frames occupy the medium a small percentage of the time when compared to data frames, especially when data is streamed to examine maximum achievable throughput.

2) For a given sample, the average frame exchange time for an ideal frame exchange is calculated as the vector product of the DLR probability vector and vector of frame exchange durations per DLR. The resulting frame exchange time represents the average time for an ideal (without retransmission) frame exchange for the current sample.

3) The deadtime is perceived from the reference frame of the WLAN sniffer. The testbed was implemented to as to balance (to the degree possible) the received power seen at the sniffer and AP, but variations may result is one receiving a frame correctly while another does not, especially when the RSS is very low.

The average frame exchange duration is calculated in a similar manner as that used to find the maximum attainable throughput for a given sample as shown in (4.4). Note that the DLR probability vector $\overrightarrow{P'}_{DLR,i}$ in this case does not include the 0 Mbps probability, as the objective is to determine the average frame exchange duration for actual frame exchanges with a valid FCS that have occurred.

$$T_{fxavg,i} = \overrightarrow{P'}_{DLR,i}\overrightarrow{T}_{DLR} \tag{4.5}$$

[‡‡‡] Medium deadtime, as all other performance metrics derived from measurements taken from actual WLAN equipment, is affected by the particular devices implementation. If the WLAN device can no sustain a constant stream of traffic, then the deadtime probability will increase.

Given the duration of a measurement sample T_{sample}, the probability of deadtime can be calculated through knowledge of the average duration of a frame exchange T_{fxavg}, as shown in (4.6).

$$P_{deadtime} = \frac{T_{sample} - T_{frames}}{T_{sample}} \tag{4.6}$$

where $T_{frames} = T_{fxavg}\left(N_{frames} - N_{CRC}\right)$, N_{frames} being the total number of filtered data frames and N_{CRC} being the number of filtered data frames having an invalid FCS (CRC errors). T_{frames} represents the duration of time ideal frame exchanges (for a given measurement sample) occupied the medium. This probability is the value in $\vec{P}_{DLR}$ that represents the probably of having a 0 Mbps DLR. The remaining DLR probability must be scaled so that the sum of the DLR probabilities (including the deadtime probability) will equal 1, as shown in (4.7).

$$\vec{P}_{DLR} = [\vec{P'}_{DLR} P_{active} \quad P_{deadtime}] = [\vec{P'}_{DLR}\left(1 - P_{deadtime}\right) \quad P_{deadtime}] \tag{4.7}$$

where P_{active} is the probability associated with active medium usage and is comprised of the individual scaled DLR probabilities for the various PHY rates.

4.5.2   One-Tap Constant Channel

The one-tap constant channel represents a maximum achieved throughput for the WLAN devices utilized. Throughput was measured with this ideal channel to obtain a baseline upon which to compare throughput measured with more realistic channels to. Figure 4-7 and Figure 4-8 show the average throughput and probability of deadtime versus received power for IEEE 802.11b and IEEE 802.11g WLANs, respectively. Average throughput models are shown with the throughput data.

(a)   (b)

Figure 4-7 Average throughput data versus average RSS with average throughput model and deadtime probability versus average RSS for an IEEE 802.11b WLAN (long preamble) operating in a constant channel: (a) average throughput data with model and (b) deadtime probability per sample.

The piecewise linear model describing the maximum achievable throughput for an IEEE 802.11b WLAN operating in a one tap constant channel is given by (4.8).

$$S_{avg}(p) = \begin{cases} 6.15 & , p > -84.73 \\ 0.94p + 86.04 & , -91.25 < p \le -84.73 \\ 0 & , p \le -91.25 \end{cases} \quad [\text{Mbps}] \qquad \textbf{(4.8)}$$

where p is the received power in dBm.

(a)   (b)

Figure 4-8 Average throughput data versus average RSS with average throughput model and deadtime probability versus average RSS for an IEEE 802.11g WLAN operating in a constant channel: (a) average throughput data with model and (b) deadtime probability per sample.

The piecewise linear model describing the maximum achievable throughput for an IEEE 802.11g WLAN operating in a one tap constant channel is given by (4.9).

$$S_{avg}(p) = \begin{cases} 29.15 & , p > -72.82 \\ 1.51p + 138.79 & , -92.18 < p \le -72.82 \\ 0 & , p \le -92.18 \end{cases} \quad \text{[Mbps]} \qquad \textbf{(4.9)}$$

where p is the received power in dBm.

4.5.3   One-Tap IEEE 802.11n Model A Channel

Channel Model A represents a one-tap Rayleigh fading channel. It is not a very realistic channel and rarely occurs in actual environments [IEE04], having only one propagation path. Figure 4-9 and Figure 4-10 show the Rayleigh fading channel throughput and probability of deadtime versus received power for IEEE 802.11b and IEEE 802.11g WLANs, respectively. Notice that the throughput falls off quicker than in the constant channel case and that the probability of deadtime being higher at lower received power. Additionally, the deadtime probability appears to exhibit less variation.

(a)   (b)

Figure 4-9 Average throughput data versus average RSS with average throughput model and deadtime probability versus average RSS for an IEEE 802.11b WLAN (long preamble) operating in TGn Channel Model A: (a) average throughput data with model and (b) deadtime probability per sample.

The piecewise linear model describing the maximum achievable throughput for an IEEE 802.11b WLAN operating in a one tap Rayleigh fading channel (Model A) is given by (4.10).

$$S_{avg}(p) = \begin{cases} 6.06 & , p > -76.42 \\ 0.38p + 35.37 & , -92.21 < p \leq -76.42 \\ 0 & , p \leq -92.21 \end{cases} \quad [\text{Mbps}] \qquad \textbf{(4.10)}$$

where p is the received power in dBm.

(a)   (b)

Figure 4-10 Average throughput data versus average RSS with average throughput model and deadtime probability versus average RSS for an IEEE 802.11g WLAN operating in TGn Channel Model A: (a) average throughput data with model and (b) deadtime probability per sample.

The piecewise linear model describing the maximum achievable throughput for an IEEE 802.11g WLAN operating in a one tap Rayleigh fading channel (Model A) is given by (4.11).

$$S_{avg}(p) = \begin{cases} 26.94 & , p > -65.84 \\ 1.13p + 101.30 & , -89.69 < p \leq -65.84 \quad \text{[Mbps]} \\ 0 & , p \leq -89.69 \end{cases} \qquad \textbf{(4.11)}$$

where p is the received power in dBm.

4.5.4   Multi-Tap IEEE 802.11n Model B Channel

A more realistic channel is modeled by Channel Model B, which is a multi-tap, two cluster multipath model representing an indoor residential area. Figure 4-11 and Figure 4-12 show the average throughput and deadtime probability versus received power for IEEE 802.11b and IEEE 802.11g WLANs, respectively. The throughput for IEEE 802.11b starts falling off at a lower received power in this case when compared to the Rayleigh fading channel throughput (see Figure 4-9a), with the deadtime probability being slightly lower between -70 and -80 dBm. However, for IEEE 802.11g, the throughput and deadtime probability appear to be very similar.

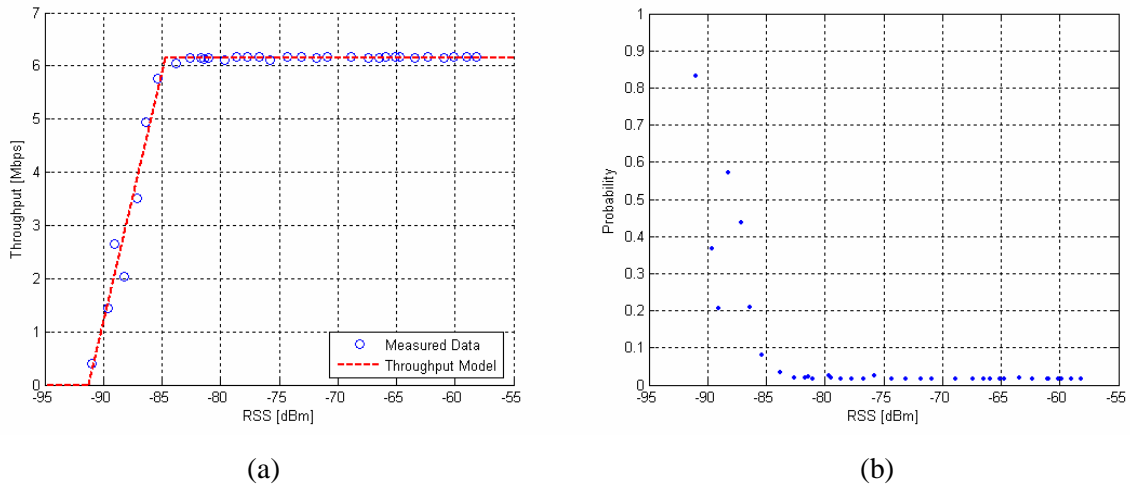(a)   (b)

Figure 4-11 Average throughput data versus average RSS with average throughput model and deadtime probability versus average RSS for an IEEE 802.11b WLAN (long preamble) operating in TGn Channel Model B: (a) average throughput data with model and (b) deadtime probability per sample.

The piecewise linear model describing the maximum achievable throughput for an IEEE 802.11b WLAN operating in the multi-tap IEEE Channel Model B fading channel is given by (4.12).

$$S_{avg}(p) = \begin{cases} 6.12 & , p > -78.55 \\ 0.54p + 48.16 & , -89.98 < p \leq -78.55 \\ 0 & , p \leq -89.98 \end{cases} \quad \text{[Mbps]} \qquad \textbf{(4.12)}$$

where p is the received power in dBm.

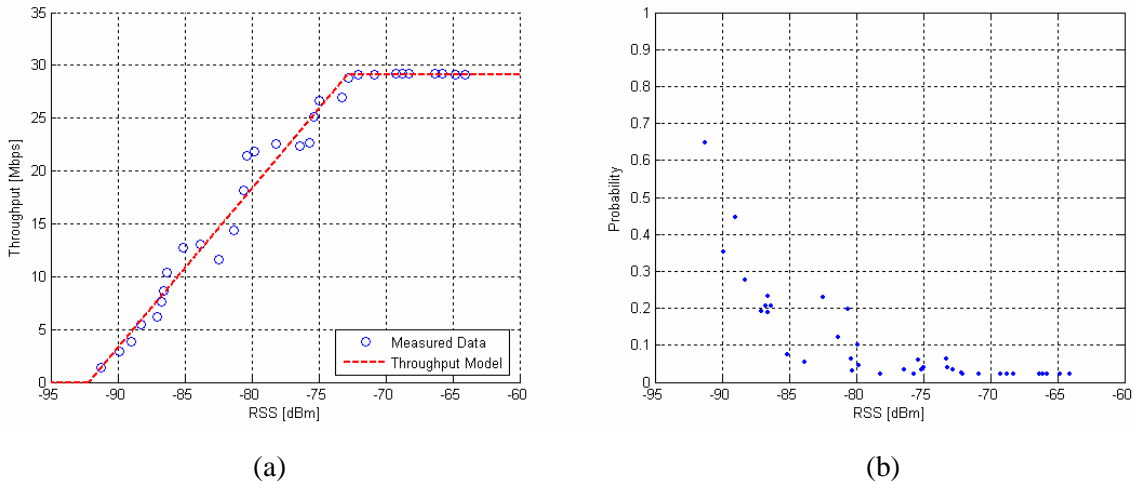(a)   (b)
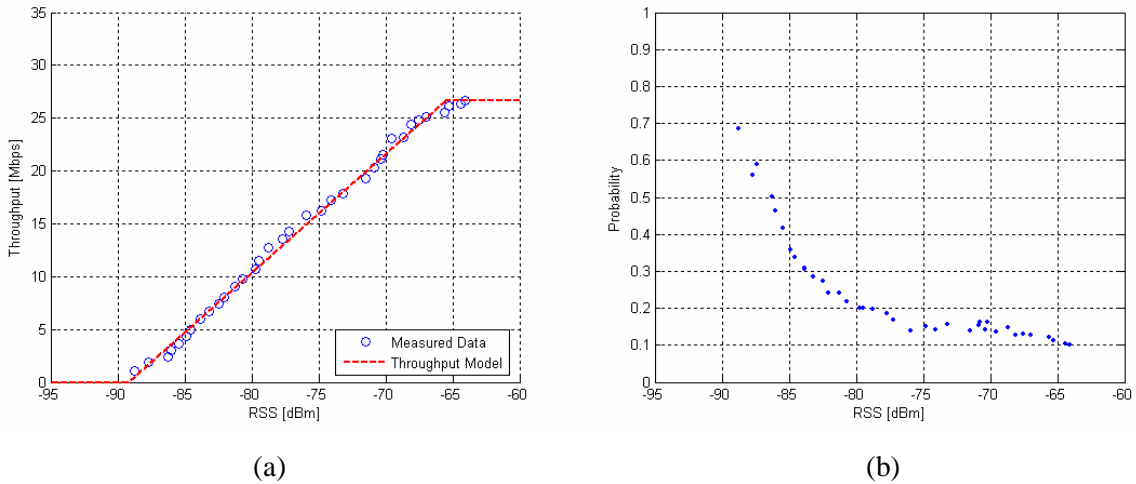
Figure 4-12 Average throughput data versus average RSS with average throughput model and deadtime probability versus average RSS for an IEEE 802.11g WLAN operating in TGn Channel Model B: (a) average throughput data with model and (b) deadtime probability per sample.

The piecewise linear model describing the maximum achievable throughput for an IEEE 802.11g WLAN operating in the multi-tap IEEE Channel Model B fading channel is given by (4.13).

$$S_{avg}(p) = \begin{cases} 26.61 & , p > -65.49 \\ 1.12p + 99.92 & , -89.27 < p \leq -65.49 \\ 0 & , p \leq -89.27 \end{cases} \quad \text{[Mbps]} \qquad \textbf{(4.13)}$$

where p is the received power in dBm.

4.5.5   Multi-Tap IEEE 802.11n Model C Channel

Channel Model C represents a slightly harsher channel than Channel Model B, having more taps and a greater RMS delay spread. However, when comparing the throughput and deadtime probability for these two channels, they appear to be relatively unchanged. Figure 4-13 and Figure 4-14 show the average throughput and deadtime probability versus received power for IEEE 802.11b and IEEE 802.11g, respectively.

(a)   (b)
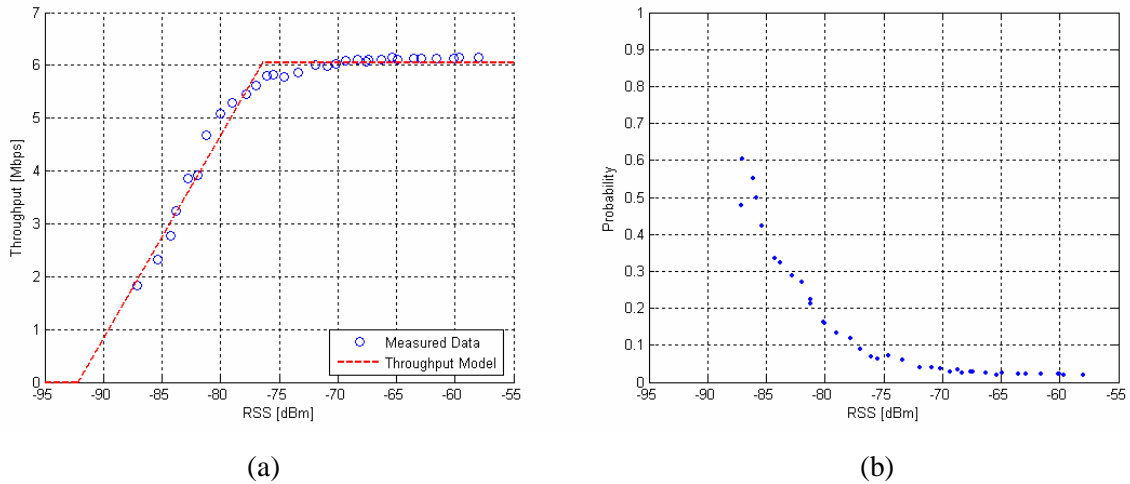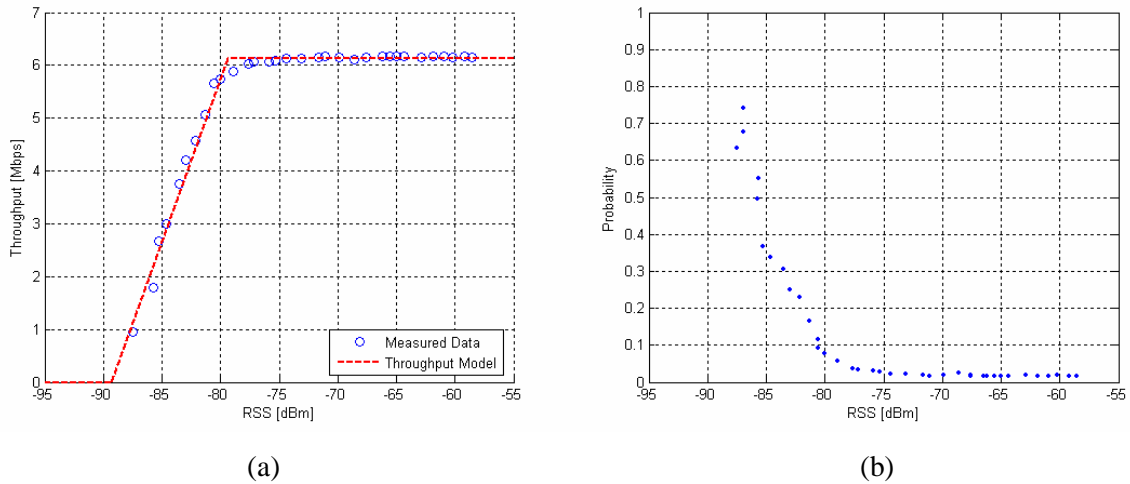
Figure 4-13 Average throughput data versus average RSS with average throughput model and deadtime probability versus average RSS for an IEEE 802.11b WLAN (long preamble) operating in TGn Channel Model C: (a) average throughput data with model and (b) deadtime probability per sample.

The piecewise linear model describing the maximum achievable throughput for an IEEE 802.11b WLAN operating in the multi-tap IEEE Channel Model C fading channel is given by (4.14).

$$S_{avg}(p) = \begin{cases} 6.14 & , p > -79.40 \\ 0.62p + 55.21 & , -89.33 < p \leq -79.40 \quad \text{[Mbps]} \\ 0 & , p \leq -89.33 \end{cases} \qquad \textbf{(4.14)}$$

where p is the received power in dBm.

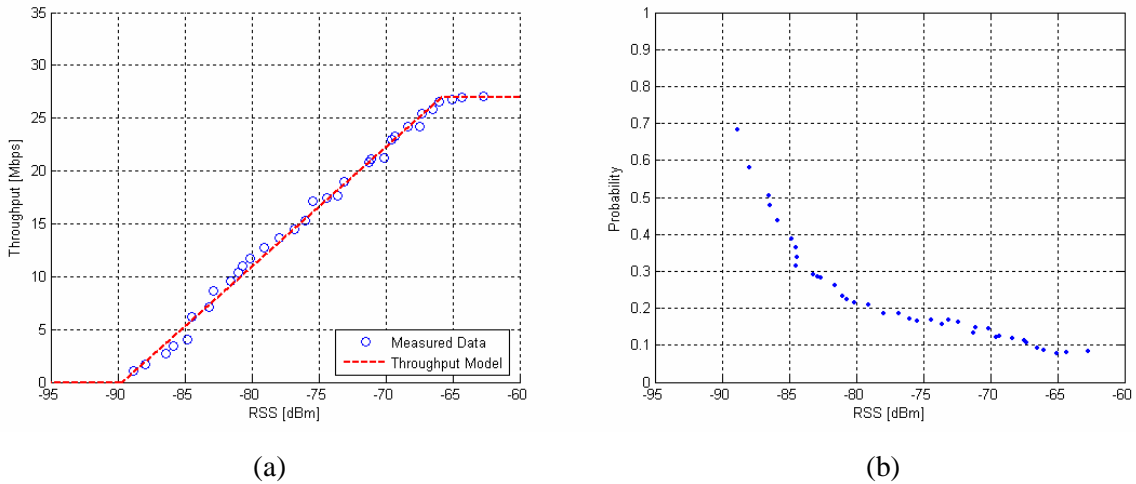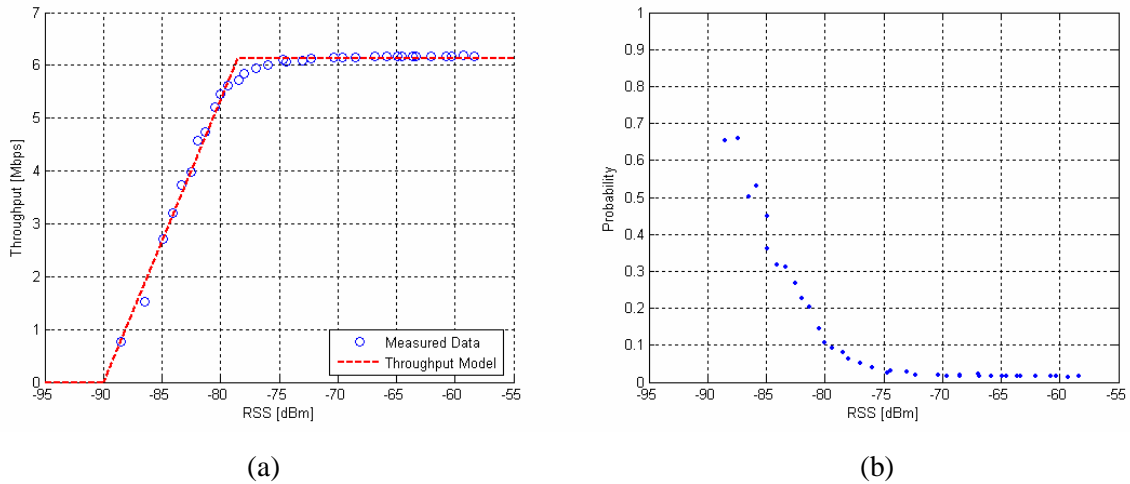(a)   (b)
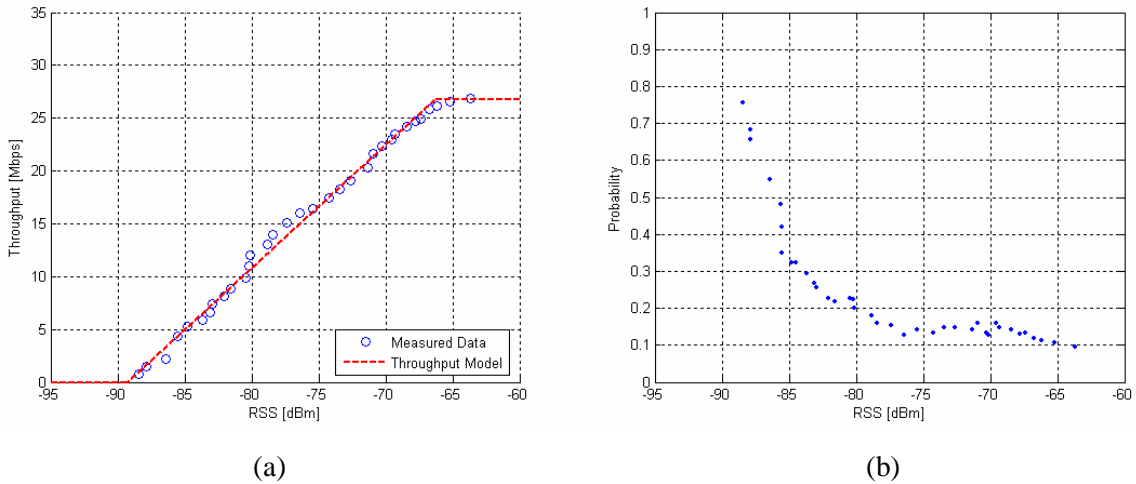
Figure 4-14 Average throughput data versus average RSS with average throughput model and deadtime probability versus average RSS for an IEEE 802.11g WLAN operating in TGn Channel Model C: (a) average throughput data with model and (b) deadtime probability per sample.

The piecewise linear model describing the maximum achievable throughput for an IEEE 802.11g WLAN operating in the multi-tap IEEE Channel Model C fading channel is given by (4.15).

$$S_{avg}(p) = \begin{cases} 26.71 & , p > -66.33 \\ 1.16p + 103.79 & , -89.32 < p \leq -66.33 \\ 0 & , p \leq -89.32 \end{cases} \quad \text{[Mbps]} \qquad \textbf{(4.15)}$$

where p is the received power in dBm.

4.5.6   Comments on Average Throughput Models

The average throughput was observed to have a piecewise linear relationship to average received power, as shown in Sections 4.5.2-4.5.5. However, this relationship is more pronounced in the case of multipath fading channels (TGn Channel Models B and C). Channel Model A (single-tap Rayleigh fading channel) also shows a piecewise linear relationship, although it is not as pronounced for IEEE 802.11b WLAN case. For the constant channel, which is included as a baseline reference, the piecewise linear relationship does not hold up well as the throughput-power relationship is reminiscent

of a step function, which aligns with the multi-rate WLAN device specifications. A piecewise linear model is proposed for simplicity, although a more accurate model would be a step function[§§§].

4.5.7   Comparison of Average Throughputs

A comparison between the throughput plots for the constant channel, Channel Model A, Channel Model B, and Channel Model is made to examine the impact of the wireless channel on SISO WLANs. The constant channel acts as a baseline upon which to compare the Channel Model B and C throughput-power results. Channel Models B and C are compared to each other and to the constant channel baseline as they represent PDPs of realistic WLAN operating environments; Channel Model A (single-tap Rayleigh) is compared to the constant channel. The single-tap Rayleigh fading channel, in comparison to the constant channel, shows the impact of received power fluctuations on performance absent of the impact of multipath. Figure 4-15 shows the throughput versus power plots for the constant channel and single-tap Rayleigh fading channel for IEEE 802.11b and 802.11g.

(a)   (b)
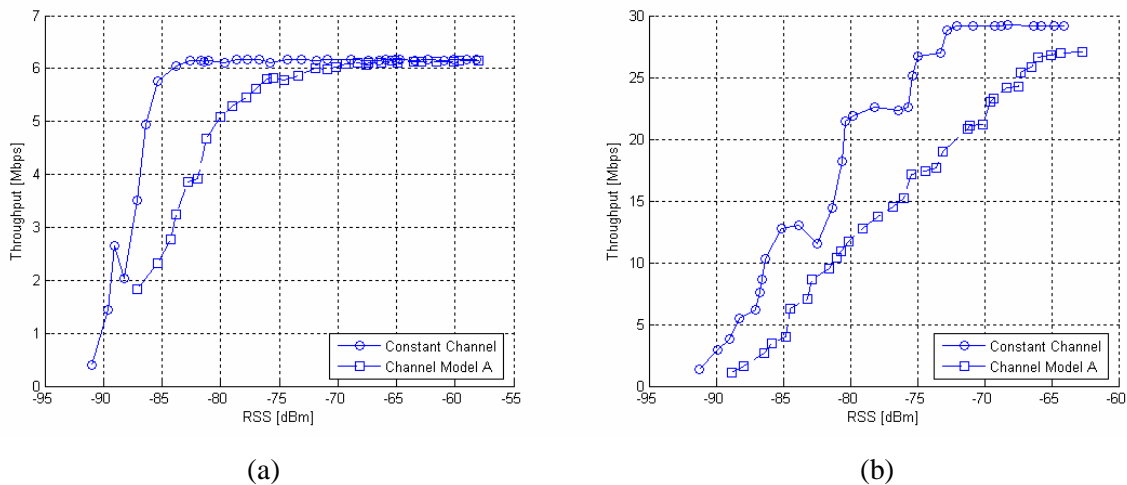
Figure 4-15 Comparison of average throughputs versus average RSS for WLANs operating in a constant channel and TGn Channel Model A: (a) IEEE 802.11b and (b) IEEE 802.11g.

Observe that in Figure 4-15a, the drop-off in throughput occurs at a lower RSS than in Figure 4-15b. Also, for both IEEE 802.11b and 802.11g cases, the throughput achieved with the Rayleigh fading

---

[§§§] It was observed that the manufacturer specified RSS cutoffs, which can be used to generate the ideal step function of throughput versus RSS, overestimates the actual performance that can be achieved.

channel is lower than that achieved with the constant channel, as would be expected. It can be seen in Figure 4-15b that the Rayleigh fading throughput displays a piecewise linear relationship with the maximum throughput not being achieved whereas the constant channel throughput is a step function. In Figure 4-16 a comparison is made between the throughput-power plots with a constant channel, Channel Model B, and Channel Model C for IEEE 802.11b and 802.11g.

(a)   (b)
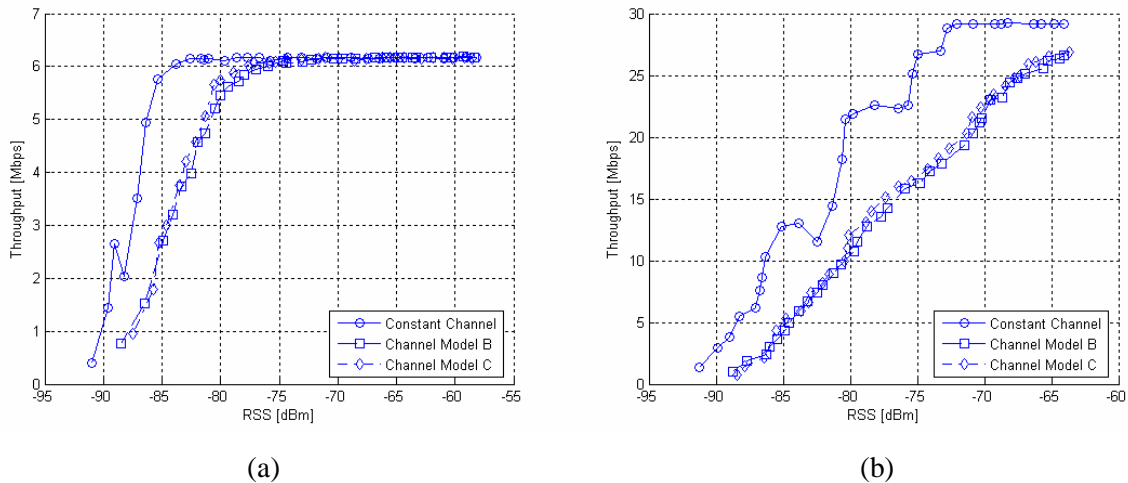
Figure 4-16 Comparison of average throughputs versus average RSS for WLANs operating in a constant channel, TGn Channel Model B, and TGn Channel Model C: (a) IEEE 802.11b and (b) IEEE 802.11g.

The key point that needs to be made regarding Figure 4-16a and Figure 4-16b is that the average throughput versus power achieved with Channel Model B and Channel Model C is effectively the same. This is not surprising considering that the two channel models do not differ significantly in delay spread and number of taps. Again, the throughput in a fading channel is lower than for the constant channel; note that for the 802.11b case, the achieved average throughput with the multipath fading Channel Models B and C appears to be slightly higher than for the single-tap Rayleigh fading channel.

4.6   Throughput Variations

Understanding throughput variations is critical to gaining insight into the nature of how certain channels degrade the achievable throughput. The average throughput gives you an idea of the long term throughput expectations given certain channel conditions. On the other hand, throughput variations show you how much the throughput varies given a fixed location and average power. An unambiguous method for showing throughput variations is to plot the CDF of the throughput samples (either instantaneous or with a specified averaging period). For constant channels, the CDF will fall off

sharply; as the channel becomes harsher, the CDF spreads out as there are times when the throughput is momentarily very low. Modeling these variations allows for augmentation of the average throughput models described in Section 4.5 and more accurate implementation of throughput modeling.

4.6.1　Understanding Throughput Variations

Throughput variation, either instantaneous or over the long term, can cause the performance of a WLAN to degrade. In the ideal case, there would be minimal throughput variation, especially when considering streaming media, where a steady throughput is desirable.   In the case of WLANS, throughput variations have three main causes:

  1) Medium contention due to the DCF access mechanism

  2) Variations in DLR due to channel fluctuations

  3) Packet loss (due to collisions or channel fluctuation) that results in retransmission

When examining per packet throughput, the variability of the time between frames (jitter) causes such throughput variations. A constant channel exhibits relatively little throughput variation from the mean throughput for a given sample whereas a multipath channel such as Channel Model B shows considerable throughput spread, especially at lower RSS values. When the RSS is relatively high and the DLR is not varying as a result of high SNR, it should be noted that there is still throughput variation occurring even in a single AP, single client network configuration. This is a result of the DCF backoff mechanism results in the inter-frame delay to vary, causing the instantaneous throughput to change. A good example of throughput variation that remains steady as the power varies (with the rate also remaining steady) can be seen in Figure 4-17, which shows the CDFs for different RSSs for IEEE 802.11b operating in a constant channel.

When examining throughput variation, an averaging can be performed on the data to smooth the results. This is relevant when probing throughput variation with respect to a given application such as video streaming. Certain applications have certain throughput requirements over a given window of time as buffering is incorporated to compensate for variations in throughput. If throughput is averaged over this window, the throughput variation with respect to the application is determined. This would prove helpful in determining the probability that any given application would perform acceptably under certain propagation conditions.

4.6.2   Data Collection and Analysis

Data collection for throughput variation analysis was performed as in the throughput versus power case except that packets were captured for a fixed duration of 1 minute. Having a 1 minute sample duration encompasses the specified PROPSim™ channel emulation time of 60 seconds while providing for a sufficiently long sample period to be able to analyze how the variations in the channel affect the throughput for a fixed average received power. Three different frame lengths were utilized (128, 512, and 1536 bytes) to examine the effects of packet length on throughput variation. As before, multiple channel models were used for both IEEE 802.11b and 802.11g operational modes. Packet lists were collected for decreasing received powers, with attenuation increasing in 5 dB increments.

Instantaneous throughput data were calculated by taking the data segment length of the captured data packet and dividing by the per-packet inter-frame duration. This yielded the throughput achieved for the transmission of a given frame. Outliers were removed, as the inter-frame durations were not always reported correctly by Airopeek, resulting in negative instantaneous throughputs or instantaneous throughputs that are practically not possible. CDFs of the instantaneous throughput data were generated and used for modeling of instantaneous throughput variations.

4.6.3   Throughput Variations per Channel

Instantaneous throughput was calculated for the constant channel and Channel Models A, B, and C for 8 different measurement samples with different average RSSs. CDFs showing the throughput variation for the various channels as the RSS decreased were generated using the instantaneous throughput data. Throughput outliers, i.e. data below 0 Mbps (error in inter-frame duration such as a negative value) and throughput values that are theoretically too high (inter-frame duration too small thus giving the impression of very high throughput) were removed. Each CDF for the decreasing RSSs (for IEEE 802.11b and 802.11g modes) was plotted on a 3D plot versus RSS, with the RSS being the average over the given sample period.

Figure 4-17 through Figure 4-24 show the CDFs of instantaneous throughput variation versus RSS for the four channels. The frame size for the data collected to generate these figures was 1536 bytes. The instantaneous throughput data was mapped to a CDF using 500 histogram bins. For IEEE 802.11b, the

maximum instantaneous throughput considered for the CDF was 9 Mbps whereas for 802.11g, the maximum instantaneous throughput considered was 45 Mbps[****].

Figure 4-17 CDFs depicting the measured instantaneous throughput variation at eight average RSS values for an IEEE 802.11b (long preamble) WLAN operating in a constant channel. Observe that the CDF changes at the average RSS is decreased.

[****] There were outliers in the data that resulted in unrealistically high instantaneous throughputs. By capping the throughputs utilized in the CDFs, a more accurate CDF was generated; one that eliminated outliers.
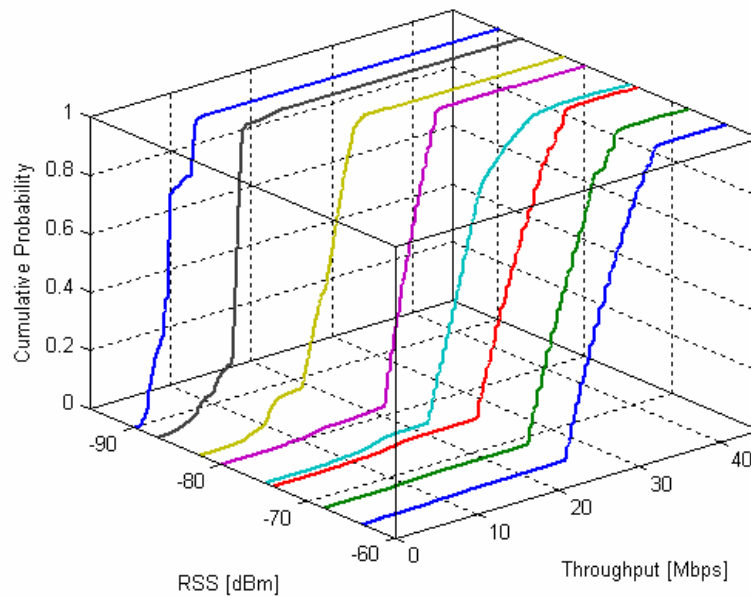
Figure 4-18 CDFs depicting the measured instantaneous throughput variation at eight average RSS values for an IEEE 802.11g WLAN operating in a constant channel. Observe that the CDF changes at the average RSS is decreased.
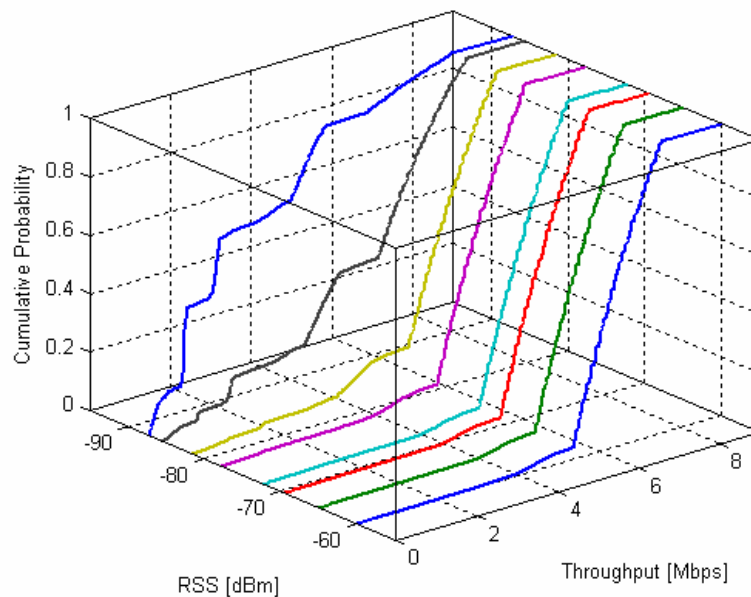
Figure 4-19 CDFs depicting the measured instantaneous throughput variation at eight average RSS values for an IEEE 802.11b (long preamble) WLAN operating in TGn Channel Model A. Observe that the CDF changes at the average RSS is decreased.
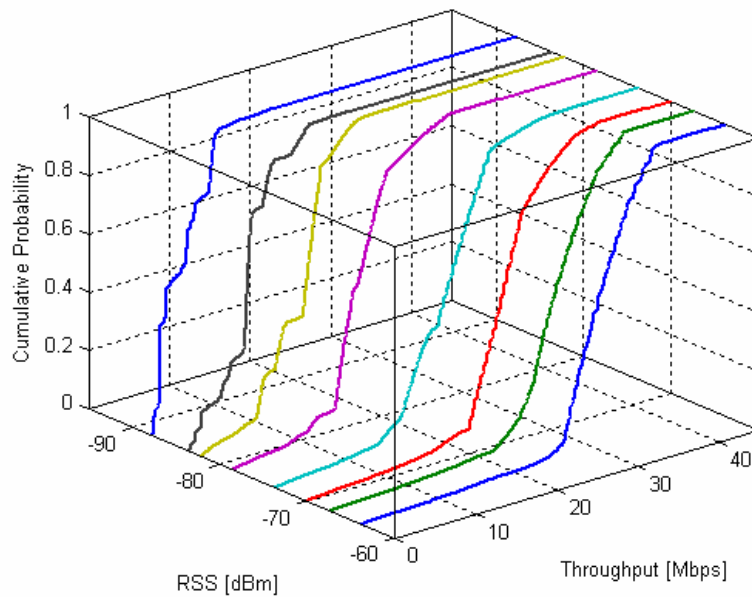
Figure 4-20 CDFs depicting the measured instantaneous throughput variation at eight average RSS values for an IEEE 802.11g WLAN operating in TGn Channel Model A. Observe that the CDF changes at the average RSS is decreased.
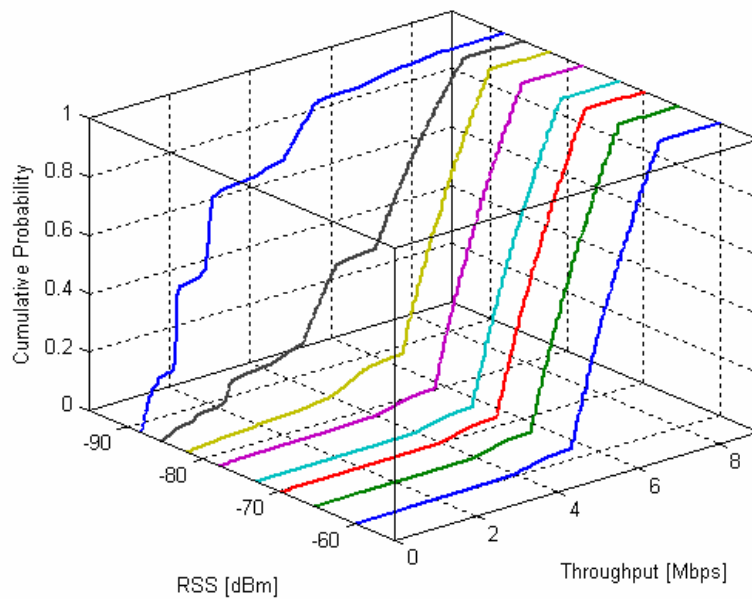
Figure 4-21 CDFs depicting the measured instantaneous throughput variation at eight average RSS values for an IEEE 802.11b (long preamble) WLAN operating in TGn Channel Model B. Observe that the CDF changes at the average RSS is decreased.
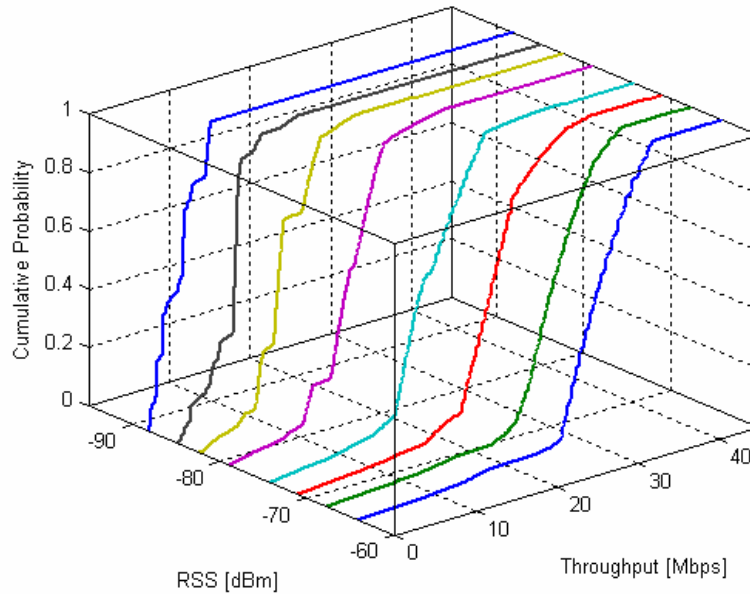
Figure 4-22 CDFs depicting the measured instantaneous throughput variation at eight average RSS values for an IEEE 802.11g WLAN operating in TGn Channel Model B. Observe that the CDF changes at the average RSS is decreased.
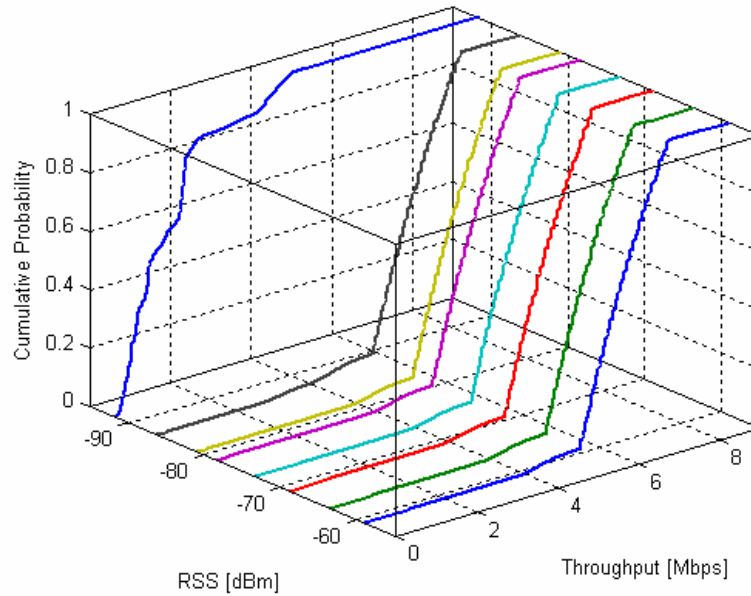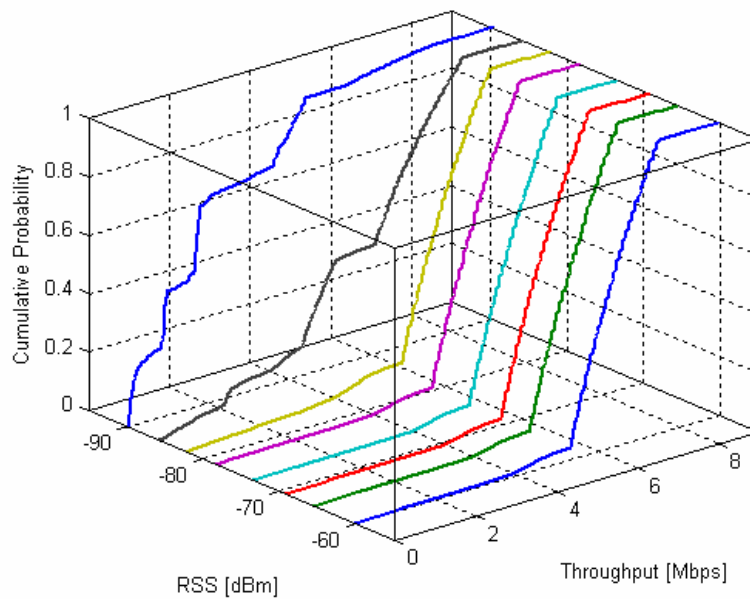

Figure 4-23 CDFs depicting the measured instantaneous throughput variation at eight average RSS values for an IEEE 802.11b (long preamble) WLAN operating in TGn Channel Model C. Observe that the CDF changes at the average RSS is decreased.
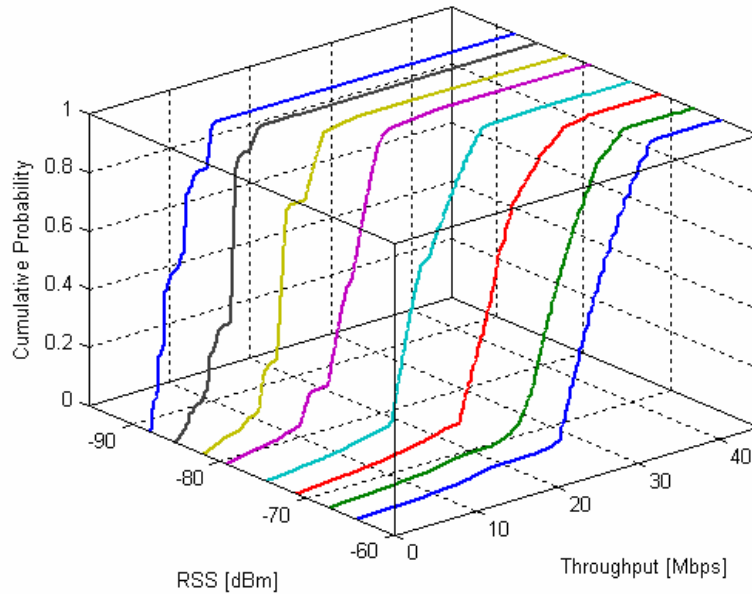
Figure 4-24 CDFs depicting the measured instantaneous throughput variation at eight average RSS values for an IEEE 802.11g WLAN operating in TGn Channel Model C. Observe that the CDF changes at the average RSS is decreased.

4.6.4   Modeling Throughput Variations Using Weibull

From the CDFs shown in Figure 4-17 through Figure 4-24, it can be seen that the shape and mean of the throughput variation CDF for a given channel changes as the average RSS (for a given sample) decreases. For IEEE 802.11b operating in a constant channel, this change does not happen until the RSS has is in the -85 to -90 dBm range. For an IEEE 802.11g WLAN also operating in a constant channel, this change in the CDF begins to occur at a higher average RSS. For harsher channels, such as Channel Models B and C, there is a more gradual change in the CDF. It was observed that this change in the CDF appeared to be related to the change in average throughput as a function of the received power, which we have modeled as a piecewise linear function. In Figure 4-17, there is an apparent breakpoint visible where the 802.11b constant channel CDF suddenly changes.
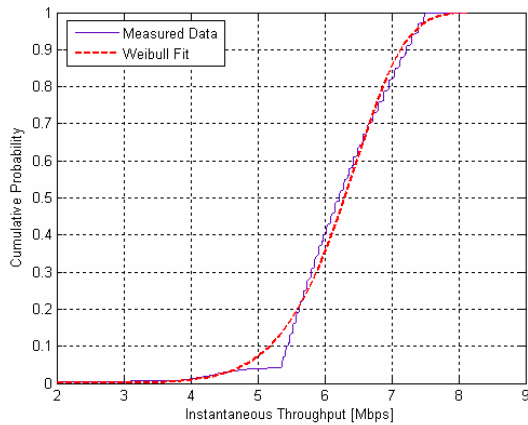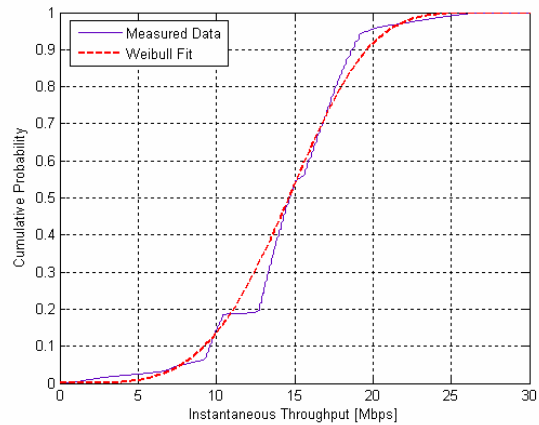
(IEEE 802.11b, Model B)   (IEEE 802.11g, Model B)

Figure 4-25 Sample measured instantaneous throughput variation CDFs with Weibull distribution fit for IEEE 802.11b and 802.11g WLANs.

Probability distribution function fitting to the throughput variation CDFs resulted in the Weibull distribution being a generally good fit for the channels and operational modes examined (see Figure 4-25 for Weibull fit examples), although it should be noted that the instantaneous throughput CDFs are not smooth functions and sometimes show significant deviation from the Weibull distribution. The Weibull distribution has two parameters, the *scale* and *shape* parameters that define the shape of the distribution, the PDF of which is given by (4.16)[††††].

$$f_X(x; k, \lambda) = \frac{k}{\lambda}\left(\frac{x}{\lambda}\right)^{k-1} e^{(x/\lambda)^k} \tag{4.16}$$

where k is the shape parameter and λ is the scale parameter. The scale and shape parameters for a given channel, operational mode, and sample were plotted versus the average throughput calculated from the throughput models in Section 4.5 using the average RSS of the measurement sample, and are given in Figure 4-26 through Figure 4-33. The parameters were drawn from Weibull distribution fits to the

---

[††††] See < http://en.wikipedia.org/wiki/Weibull_distribution >.

CDFs in Section 4.6.3. It can be seen that the Weibull parameters are linear functions of the average throughput and a best-fit line for each case is overlaid on the figures[‡‡‡‡].

Figure 4-26 Weibull parameters plotted versus the average throughput calculated using average the throughput models at the given measurement sample average RSS for an IEEE 802.11b WLAN (long preamble) operating in a constant channel: (a) scale parameter and (b) shape parameter.

Note that in Figure 4-26 there are a few data points overlapping around 6 Mbps average throughput. This is the result of the constant channel throughput for IEEE 802.11b dropping off at a low RSS.

[‡‡‡‡] The shape parameter with IEEE 802.11g operating in a constant channel showed greater variation than the other channels and modes. There was variation from the model with the average throughput as well. This could be attributed to the linear fit being assumed, although the actual throughput versus power was more stepwise.

Figure 4-27 Weibull parameters plotted versus the average throughput calculated using average the throughput models at the given measurement sample average RSS for an IEEE 802.11g WLAN operating in a constant channel: (a) scale parameter and (b) shape parameter.

In Figure 4-27b, the fit is not as good as in the other cases, which is likely due to the linear dropoff approximation made to a stepwise average throughput function. However, there isn't a significant deviation from the fit, which is at most about 4. It should be noted that the constant channel cases are included for comparison only and do not play much of a role in throughput modeling and simulation as the constant channel is an ideal channel and never exists in actual installation environments.

Figure 4-28 Weibull parameters plotted versus the average throughput calculated using average the throughput models at the given measurement sample average RSS for an IEEE 802.11b WLAN (long preamble) operating in TGn Channel Model A: (a) scale parameter and (b) shape parameter.
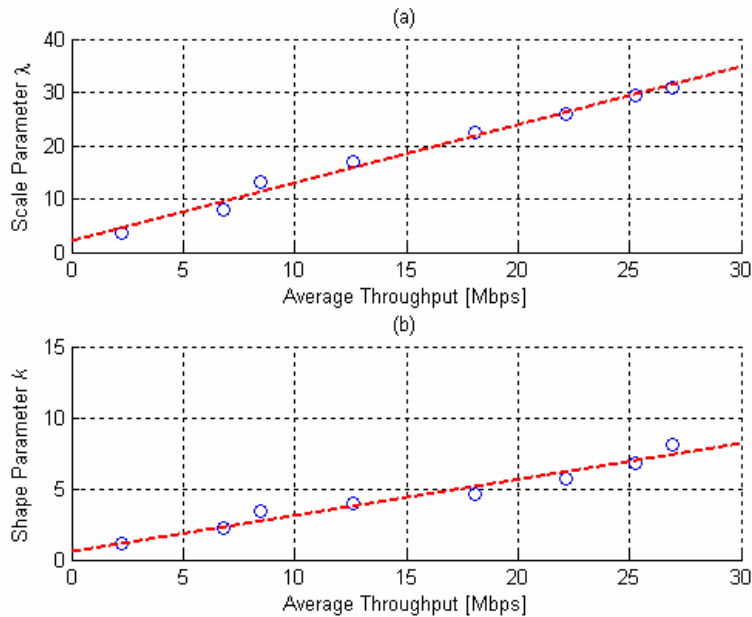
Figure 4-29 Weibull parameters plotted versus the average throughput calculated using average the throughput models at the given measurement sample average RSS for an IEEE 802.11g WLAN operating in TGn Channel Model A: (a) scale parameter and (b) shape parameter.
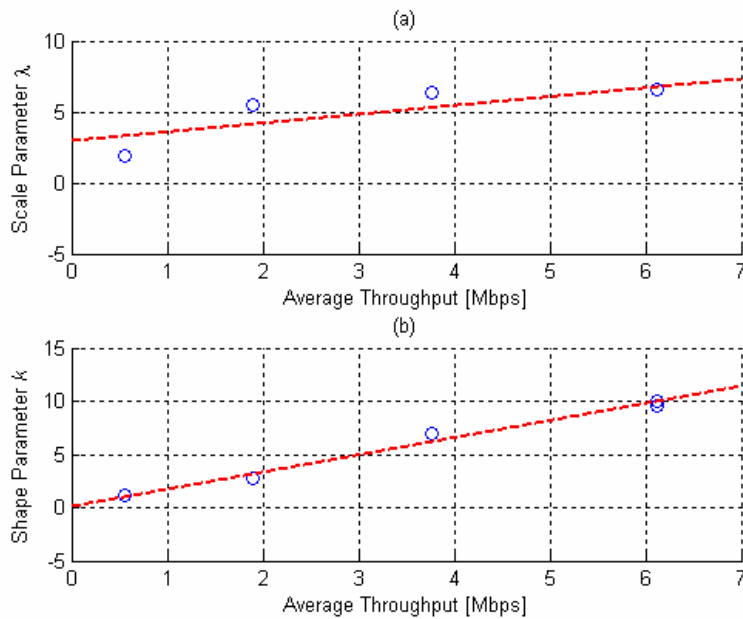
Figure 4-30 Weibull parameters plotted versus the average throughput calculated using average the throughput models at the given measurement sample average RSS for an IEEE 802.11b WLAN (long preamble) operating in TGn Channel Model B: (a) scale parameter and (b) shape parameter.
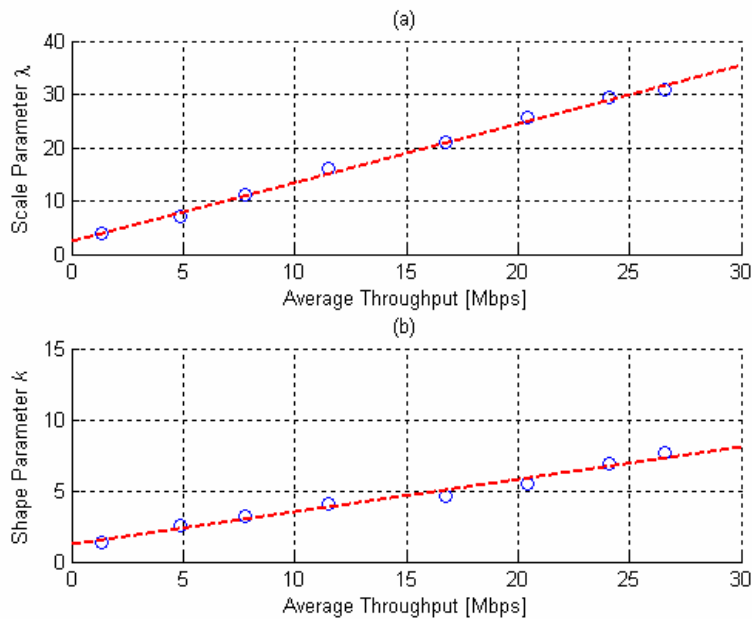
Figure 4-31 Weibull parameters plotted versus the average throughput calculated using average the throughput models at the given measurement sample average RSS for an IEEE 802.11g WLAN operating in TGn Channel Model B: (a) scale parameter and (b) shape parameter.
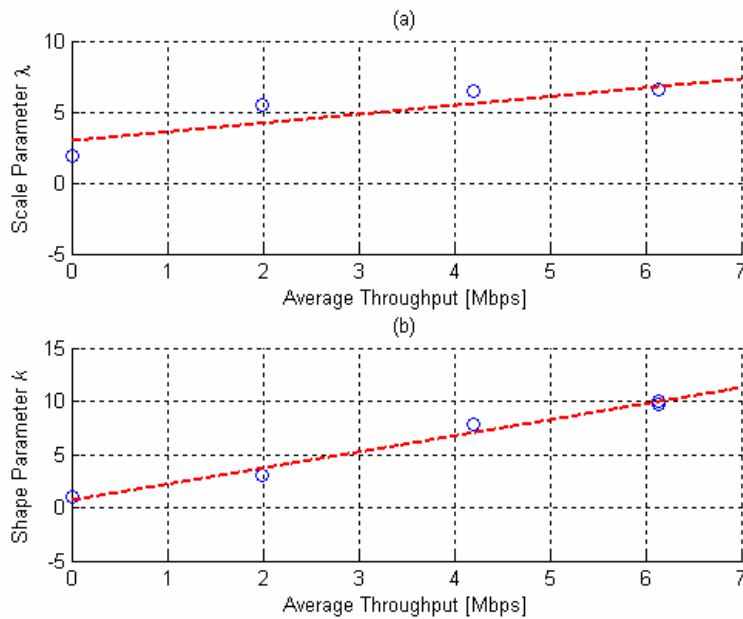
Figure 4-32 Weibull parameters plotted versus the average throughput calculated using average the throughput models at the given measurement sample average RSS for an IEEE 802.11b WLAN (long preamble) operating in TGn Channel Model C: (a) scale parameter and (b) shape parameter.
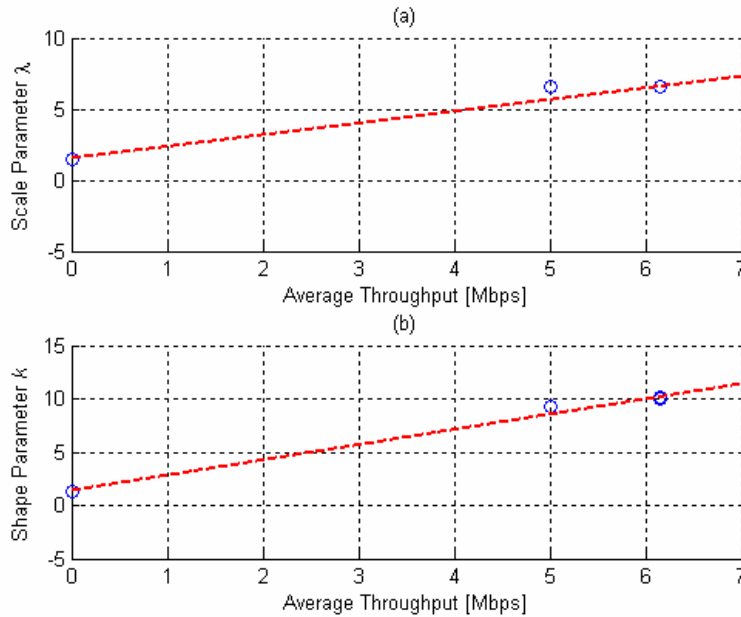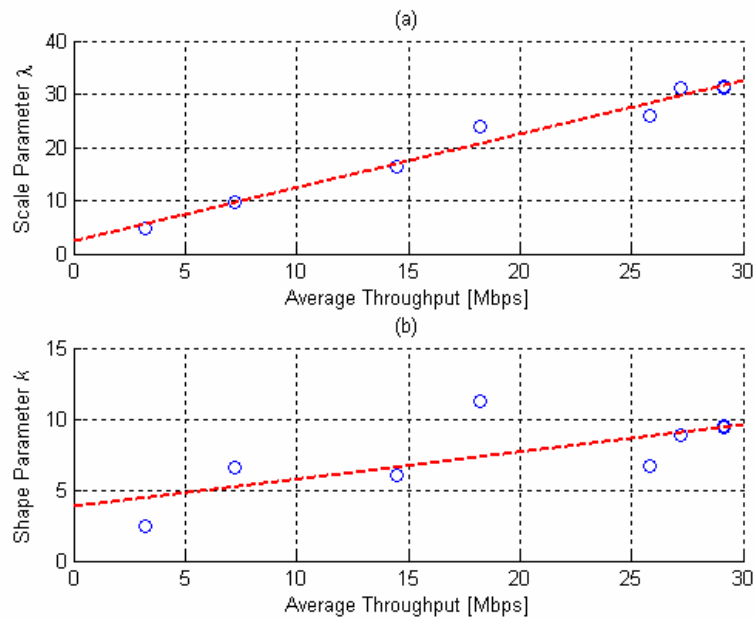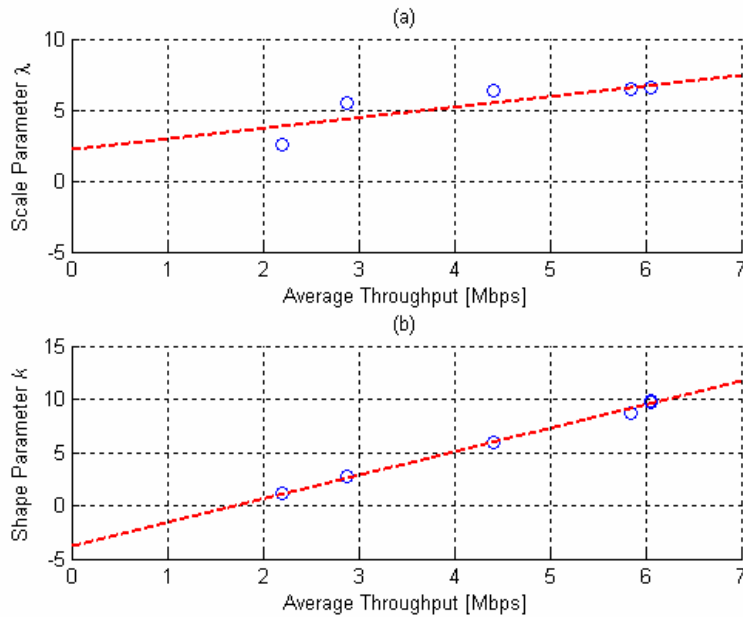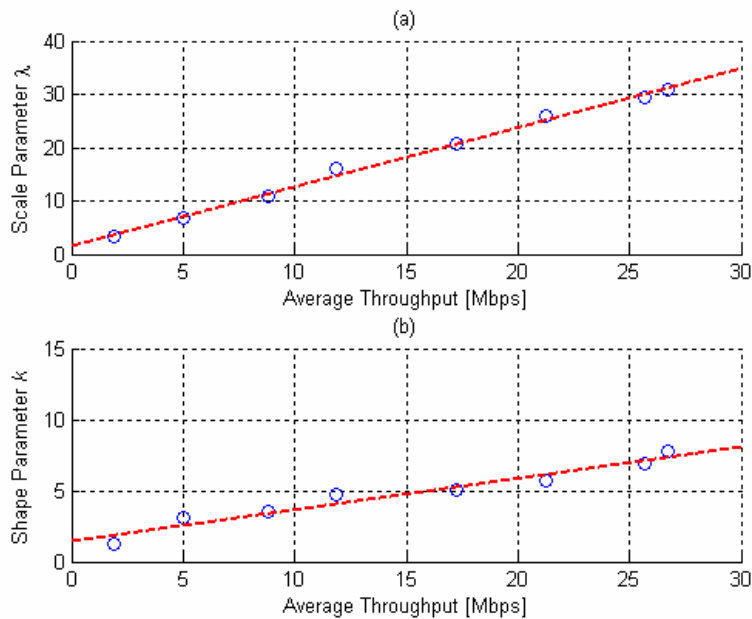

Figure 4-33 Weibull parameters plotted versus the average throughput calculated using average the throughput models at the given measurement sample average RSS for an IEEE 802.11g WLAN operating in TGn Channel Model C: (a) scale parameter and (b) shape parameter.

The functions presented above relating the average throughput (found using the average throughput models) for a given RSS to the Weibull scale and shape parameters relate the average throughput to the distribution of throughput that is seen at the given received power. These functions vary for different operational modes (802.11b and 802.11g in this thesis) and channels[§§§§]. By utilizing these functions, a comprehensive throughput model has been developed that describes not only the average throughput for a given RSS but also the distribution of the throughput variation (see Section 4.7). Although only IEEE 802.11b and 802.11g operating in four different channels was explored here, this method can be applied to other channels (D-F and arbitrary channels) and WLAN operational modes.

For all the channels examined, the relationship between the Weibull scale and shape parameters to the average throughput is given by (4.17) and (4.18) for scale and shape parameters, respectively.

$$\lambda\big(S_{avg}(p)\big)=m_{\lambda}S_{avg}(p)+b_{\lambda} \tag{4.17}$$

$$k\big(S_{avg}(p)\big)=m_{k}S_{avg}(p)+b_{k} \tag{4.18}$$

where $S_{avg}(p)$ is the average throughput given a received power p, $m_{\lambda,k}$ is the slope of the function, and $b_{\lambda,k}$ is the y-intercept of the function, for the respective parameters. Table 4-2 gives the function parameters for the best-fit lines given Figure 4-26 through Figure 4-33.

Table 4-2 Scale and Shape Function Parameters for Weibull Modeling

Channel Model	IEEE 802.11b		IEEE 802.11g	
	m_{λ}, b_{λ}	m_k, b_k	m_{λ}, b_{λ}	m_k, b_k
Constant	0.83, 1.58	1.43, 1.42	1.01, 2.39	0.19, 3.91
Model A	0.75, 2.18	2.22, -3.72	1.09, 2.10	0.25, 0.65
Model B	0.61, 3.00	1.60, 0.19	1.10, 2.49	0.23, 1.21
Model C	0.61, 3.00	1.52, 0.69	1.11, 1.63	0.22, 1.48

[§§§§] And for different packet lengths, as illustrated in Section 4.6.6.

4.6.5   Modeling Throughput Variations with Gaussian Assumption

An alternative approach to modeling throughput variations is to assume that the distribution of the throughput variations around the average throughput will have a Gaussian distribution. This has the advantage of being simpler to simulate as well as enabling a simpler comprehensive throughput model format, as described in Section 4.7. However, the approach to Gaussian modeling taken here does not take into consideration the changes to the throughput variation CDF that occurs as the RSS (and consequently average throughput) decreases. This is an area for further exploration – the modeling of changes to the standard deviation (when using the Gaussian modeling approach) of the throughput variation CDFs as a function of RSS or average throughput.

For a given channel and WLAN operational mode, the mean of the instantaneous throughputs was subtracted from each instantaneous throughput sample for each measurement sample (attenuation setting). This yielded only the throughput variation from the mean. A CDF of the histogram of *all* of the throughput samples for all of the measurement samples was taken and fitted with a Gaussian, as shown in Figure 4-38 through Figure 4-41 for IEEE 802.11b and 802.11g for all the channels examined.

Figure 4-34 CDF depicting the measured instantaneous throughput variations for all the measurement samples with the Gaussian distribution fit overlaid for an IEEE 802.11b WLAN (long preamble) operating in a constant channel.

Figure 4-35 CDF depicting the measured instantaneous throughput variations for all the measurement samples with the Gaussian distribution fit overlaid for an IEEE 802.11g WLAN operating in a constant channel. Note that the spread of the CDF is greater than in the IEEE 802.11b case, which is a result of the frame durations being shorter (due to higher rate DLRs) and thus the impact of the random backoff on the frame exchange duration is more pronounced, causing the instantaneous throughput to vary more.
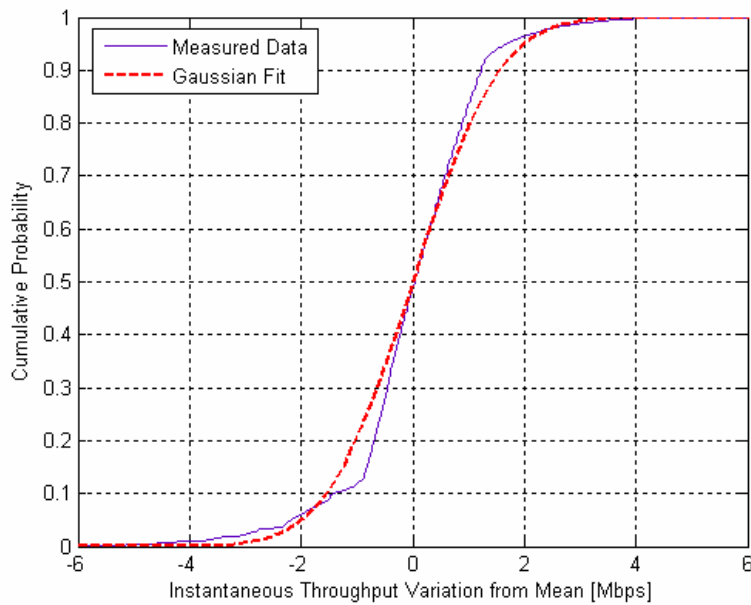
Figure 4-36 CDF depicting the measured instantaneous throughput variations for all the measurement samples with the Gaussian distribution fit overlaid for an IEEE 802.11b WLAN (long preamble) operating in TGn Channel Model A.
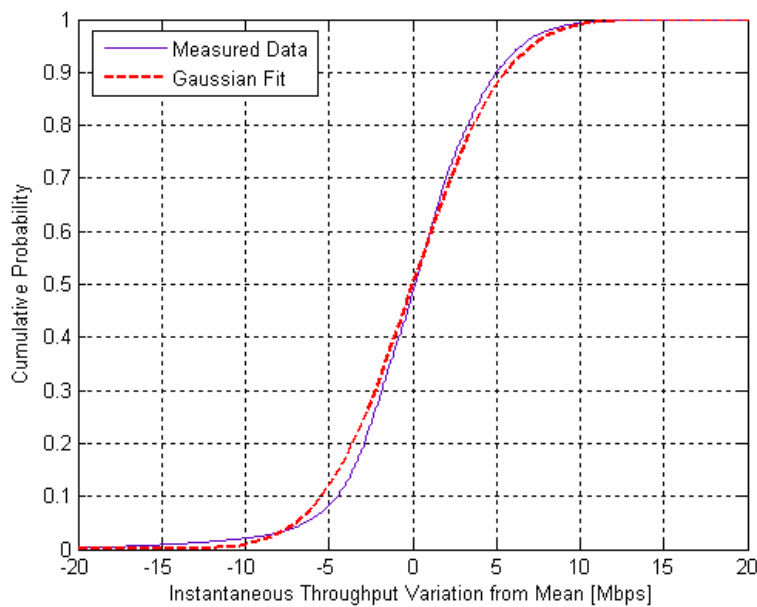
Figure 4-37 CDF depicting the measured instantaneous throughput variations for all the measurement samples with the Gaussian distribution fit overlaid for an IEEE 802.11g WLAN operating in TGn Channel Model A.
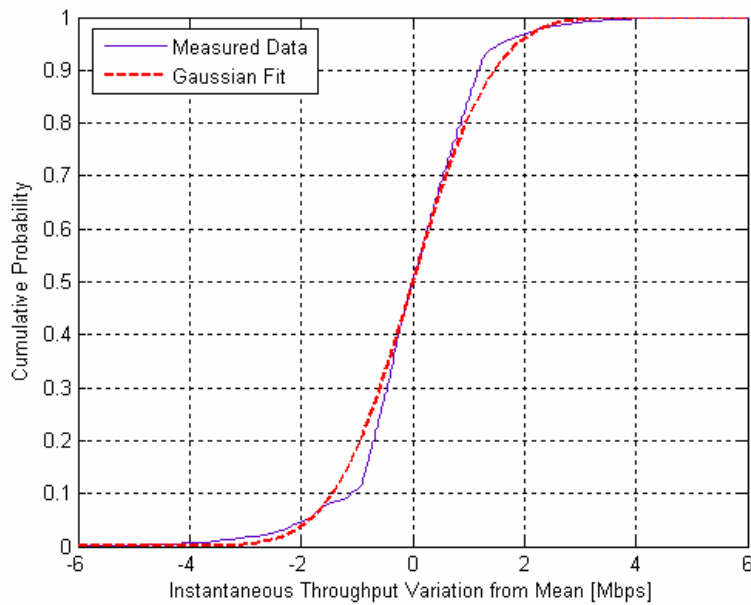
Figure 4-38 CDF depicting the measured instantaneous throughput variations for all the measurement samples with the Gaussian distribution fit overlaid for an IEEE 802.11b WLAN (long preamble) operating in TGn Channel Model B.
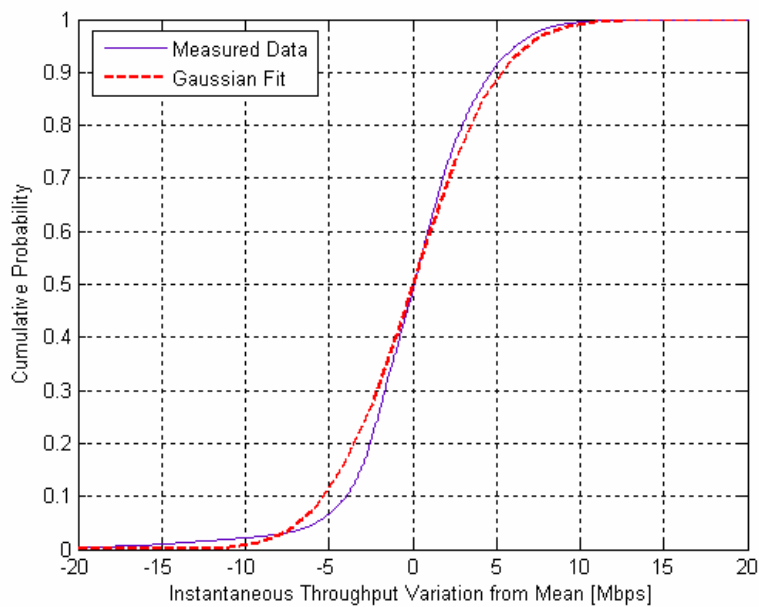
Figure 4-39 CDF depicting the measured instantaneous throughput variations for all the measurement samples with the Gaussian distribution fit overlaid for an IEEE 802.11g WLAN operating in TGn Channel Model B.
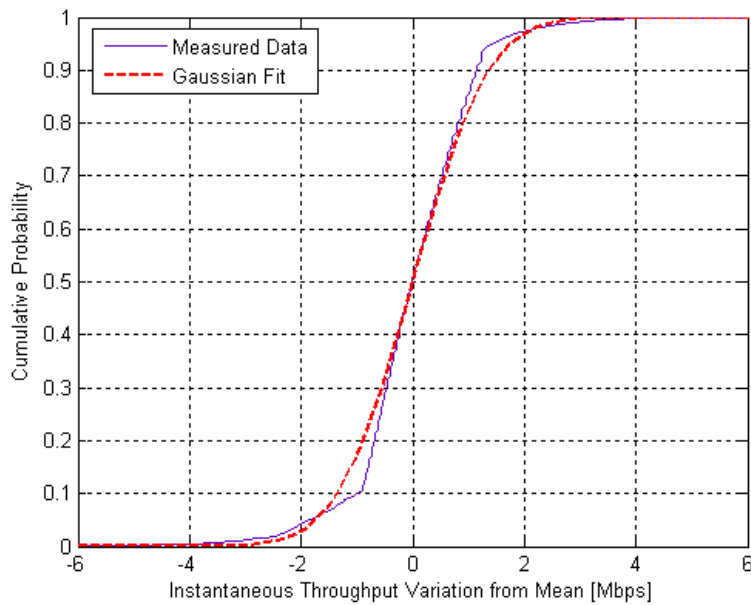
Figure 4-40 CDF depicting the measured instantaneous throughput variations for all the measurement samples with the Gaussian distribution fit overlaid for an IEEE 802.11b WLAN (long preamble) operating in TGn Channel Model C.
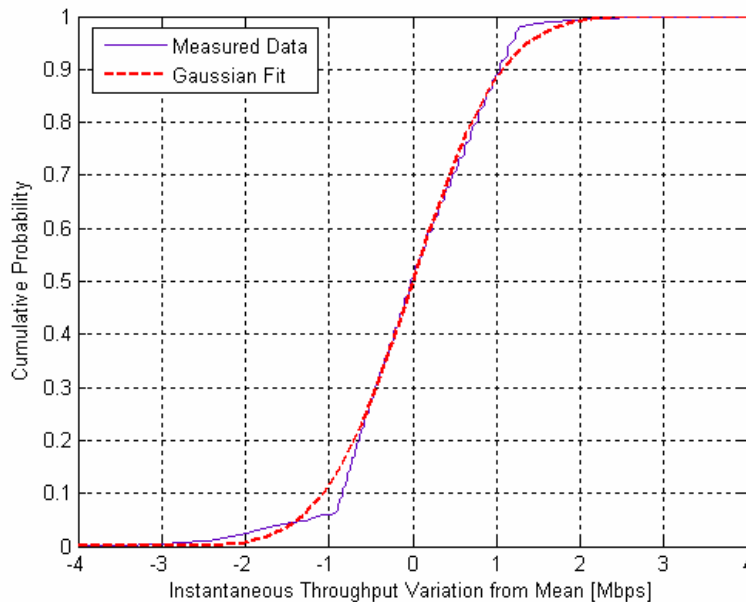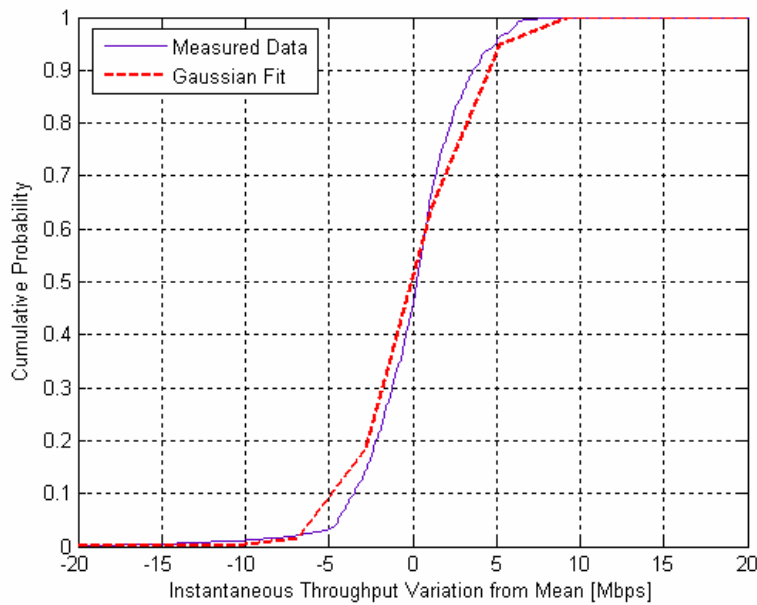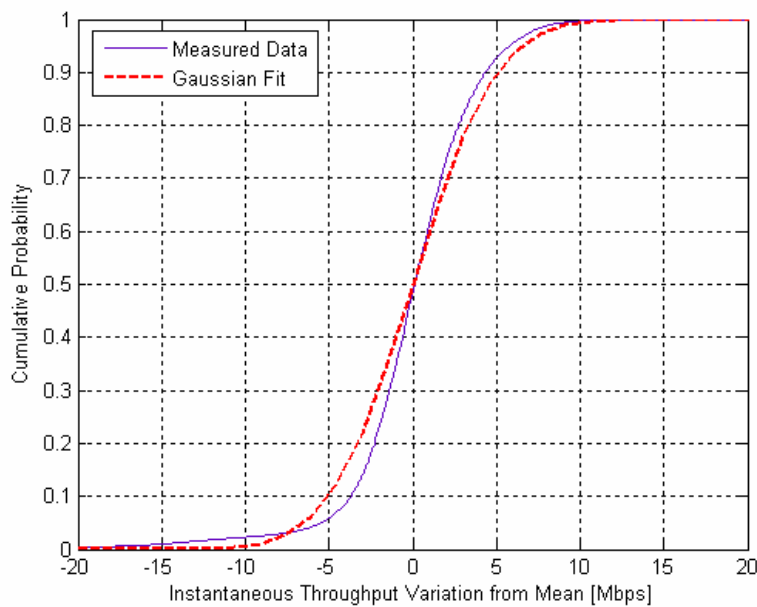

Figure 4-41 CDF depicting the measured instantaneous throughput variations for all the measurement samples with the Gaussian distribution fit overlaid for an IEEE 802.11g WLAN operating in TGn Channel Model C.

The average throughput per measurement sample was calculated as the mean of all the instantaneous throughput samples in the given measurement sample. This is different from the approach taken to find the average throughput samples for average throughput modeling performed in Section 4.5, where the DLR probabilities were determined for a measurement sample and the maximum achievable throughput was calculated using per-DLR theoretical throughputs. As a result, the throughput models in Section 4.5 give a pseudo-theoretical bound on throughput performance and if utilized here, would not yield a zero mean CDF. However, the average throughput models can still be utilized to find the average throughput for a given RSS, and the Gaussian model used to determine the throughput deviation around that average throughput. By utilizing the mean of the instantaneous throughputs, an effectively zero mean distribution was guarantied.

Table 4-3 gives the standard deviations for modeling the throughput variation per channel per mode with the Gaussian fit assumption for the throughput variations.

Table 4-3 Gaussian Model Standard Deviations per Channel per Operational Mode

Channel Model	Gaussian Model Standard Deviation [Mbps]	
	IEEE 802.11b	IEEE 802.11g
Constant	0.8376	3.1854
Model A	1.2162	4.2839
Model B	1.1312	4.0961
Model C	1.0660	3.9394

It should be noted that the standard deviations in Table 4-3 are for the specific RSS range that the throughput variations were measured over. Since all throughput variations for all measurement samples are collected into a single distribution, the range would have an effect on the overall distribution as there are variations in the distribution for different RSSs. These distribution variations are what the Weibull distribution modeling approach addresses. Figure 4-42 shows a sample comparison between the measured instantaneous throughput data CDF, the Weibull model CDF, and Gaussian model CDF.
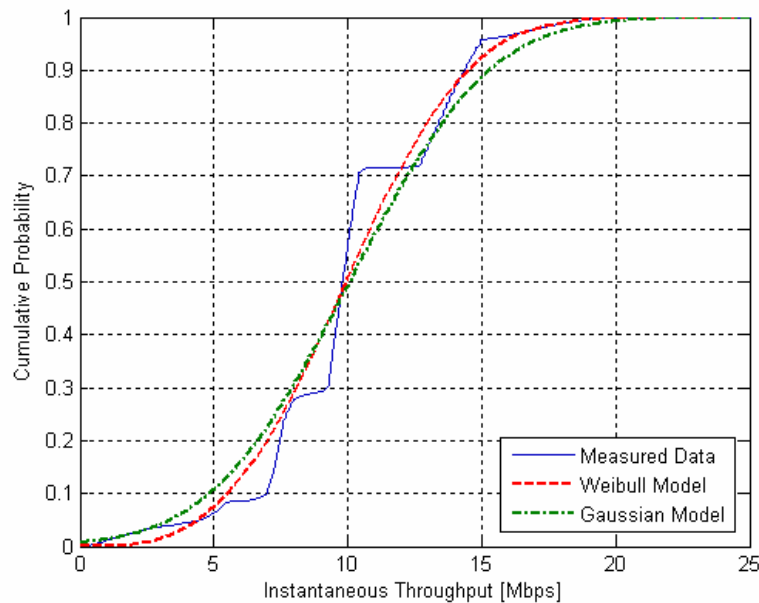
Figure 4-42 Example comparison of measured instantaneous throughput data CDF for IEEE 802.11g operating in TGn Channel Model B with Weibull and Gaussian Models.

4.6.6 Effects of Packet Length on Throughput Variation

It is understood that a shorter packet length reduces the overall maximum achievable throughput. The effects from different channels on different packet lengths would vary, but in general, the throughput would decrease as the packet length was shortened. Models were not presented in Section 4.5 for different packet lengths as the aim was to model the maximum achievable throughput for a given channel as a function of the received power, with thee results effectively presenting a channel-wise upper bound on throughput performance.

However, throughput variations may exhibit different behavior for different channels given different packets lengths. The data collection campaign included gathering data to analyze throughput variations for three different frame lengths: 128, 512, and 1536 bytes. Figure 4-43 and Figure 4-44 compare the instantaneous throughput CDFs for different average RSSs and different frame lengths for IEEE 802.11b and 802.11g WLANs.
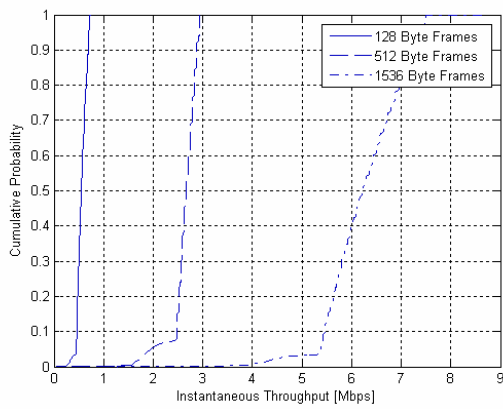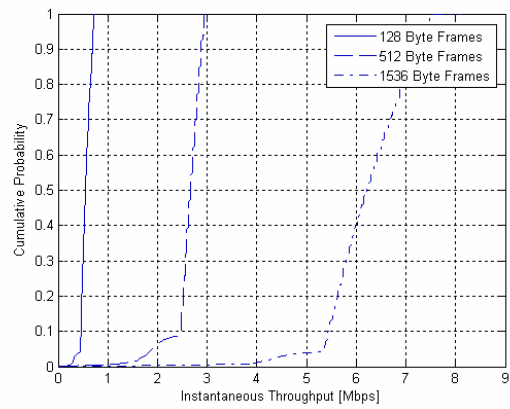
(a)   (b)
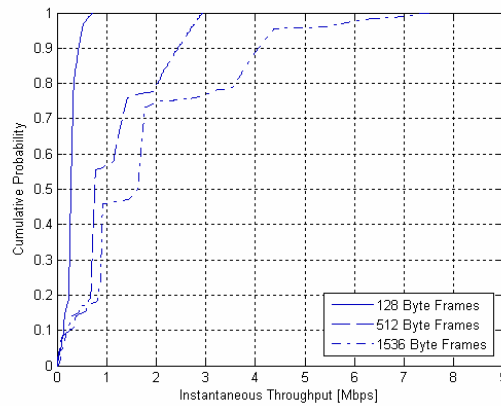
(c)

Figure 4-43 Comparison of instantaneous throughput CDFs for IEEE 802.11b with different frame lengths at three sample average RSS values: (a) ~-61 dBm, (b) ~-78 dBm, and (c) ~-89 dBm. Notice that the slope of the CDFs is sharper for the shorter frame length and, as would be expected, the mean is less for the shorter frames.

(a)

(b)

(c)
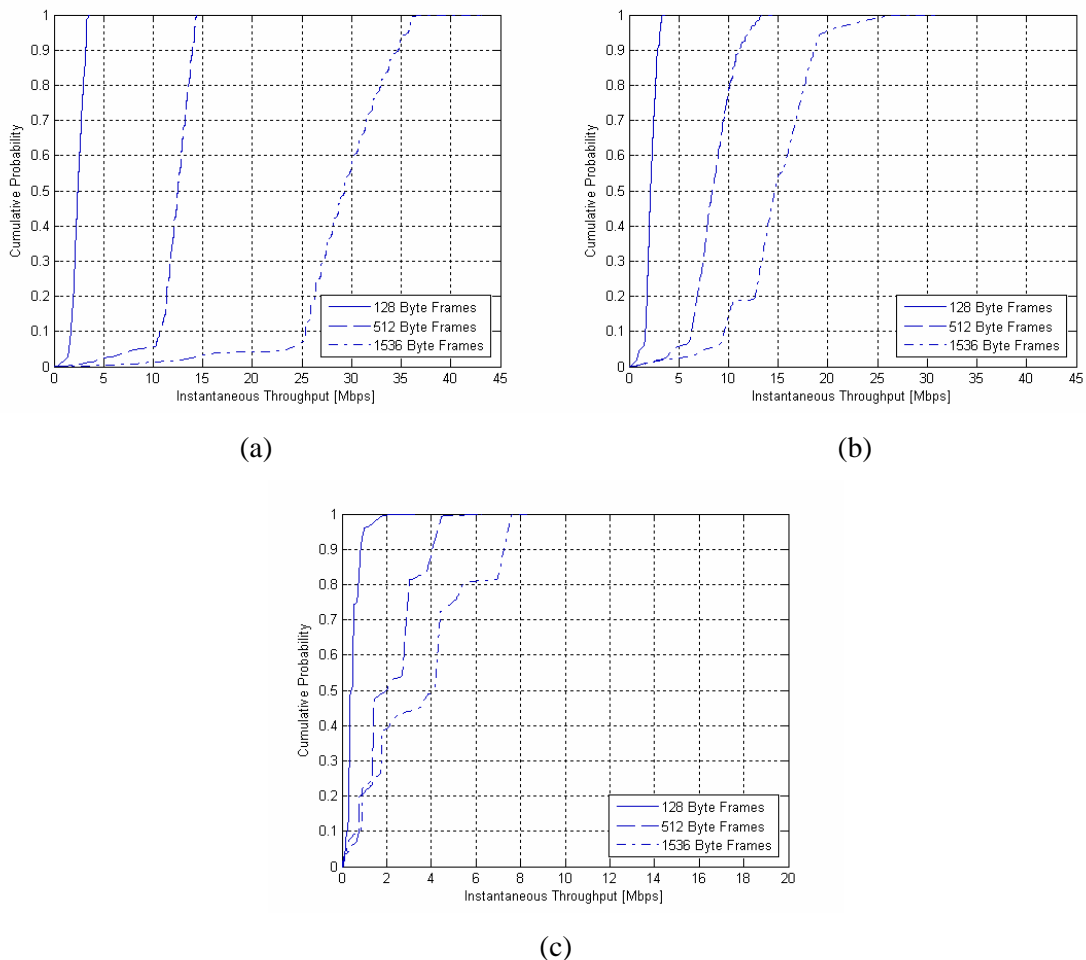
Figure 4-44 Comparison of instantaneous throughput CDFs for IEEE 802.11g with different frame lengths at three sample average RSS values: (a) ~-64 dBm, (b) ~-79 dBm, and (c) ~-88 dBm.

The comparison of instantaneous throughput variation CDFs for different packet lengths at different average RSSs above shows that the mean is less for shorter frames (as would be expected) and that there is a different in the slope of the CDF for different frame lengths. It appears that the throughput variation with shorter frames is less pronounced.

4.7   Comprehensive Throughput-Power Models

In Section 4.5, the average throughput was modeled as a function of power for four different channels. The models presented give insight into the expected average throughput for a given RSS, but does not express the variation in throughput that would be expected, given the variability of the WM and variation in instantaneous throughput experience due to the 802.11 MAC even for a fixed DLR. The variation in throughput was examined in Section 4.6 and the Weibull and Gaussian distributions

103

proposed as models for describing throughput variations. For the Weibull fit, it was shown that the *scale* and *shape* parameters of the Weibull distribution are linear functions of the average throughput for the four channels analyzed. The Gaussian assumption was also a good fit to throughput variations.

Combining the average throughput models and throughput variation models into a comprehensive throughput model provides a throughput model describing both the average throughput per channel and the variation in instantaneous throughput for that channel. The throughput variation modeling approach using the Weibull distribution performed in Section 4.6.4 inherently yields a comprehensive throughput model. Let the comprehensive throughput model, given by (4.19) be a Weibull distribution that is a function of the average throughput, which is likewise a function of the average RSS for a given measurement sample.

$$S(p) = \eta\big(S_{avg}(p)\big) \quad \text{[Mbps]} \tag{4.19}$$

where $S_{avg}(p)$ is found for a given power (in dBm) from the throughput models presented in Section 4.5 and $\eta\big(S_{avg}(p)\big)$ is a random variable with a Weibull distribution having scale and shape parameters that are linear functions of $S_{avg}(p)$, as given in Section 4.6. The RVs drawn from the Weibull distribution describe both the average throughput and throughput variation. Note that since the distribution extends to infinity, values greater than the theoretically possible maximum throughput must be cropped when generating throughput samples.

However, if using the Gaussian assumption of throughput variations, the form of the comprehensive throughput model changes to a sum of the average throughput and a random variable. This form is reminiscent of the approach taken to path-loss modeling, where the deterministic path-loss is varied using a lognormally distributed RV. For the Gaussian assumption of throughput variations, let the comprehensive throughput model be given by (4.20).

$$S(p) = S_{avg}(p) + \eta \quad \text{[Mbps]} \tag{4.20}$$

where η is an RV drawn from a zero mean Gaussian distribution with standard deviation determined by the channel and WLAN operational mode, as given in Table 4-3. Note that throughput deviations greater than the maximum theoretical throughput minus the average throughput and less than the negative of the average throughput need to be cropped for throughput sample generation. This comprehensive throughput modeling approach is simpler from two perspectives:

1. The number of calculations required to simulate throughput variations is less because there is no necessity to calculate scale and shape parameters, as in the Weibull modeling approach

2. Generation of throughput samples is more straightforward due to Gaussian distribution

However, a downside of the current form of the Gaussian modeling approach is that the model does not take into consideration variations in the distribution for different RSS values, instead modeling all throughput variations for numerous average RSSs as one distribution. Figure 4-45 shows a sample comparison between measured and simulated instantaneous throughput samples (1000 samples) for IEEE 802.11g operating in TGn Channel Model B.
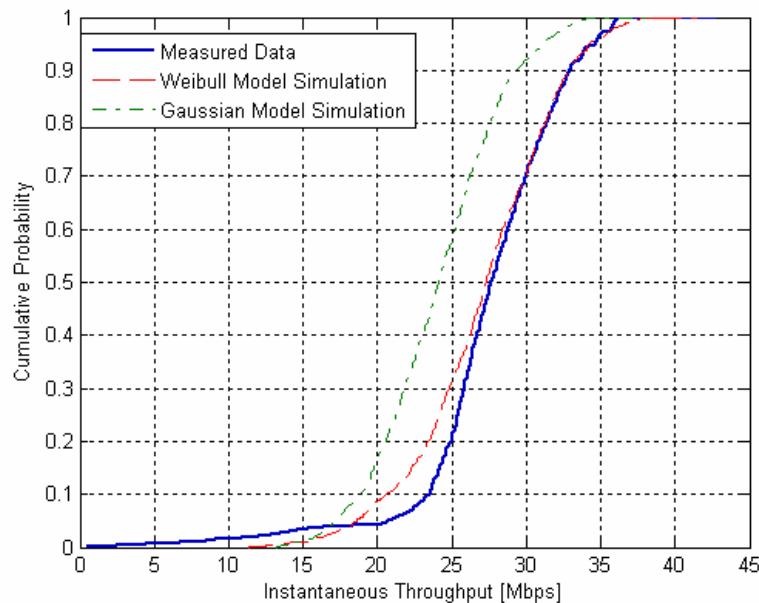
Figure 4-45 Example comparison between measured and simulated (1000 samples using Weibull and Gaussian models) instantaneous throughput for IEEE 802.11g operating in TGn Channel Model B. Note that there is an offset betwen the Gaussian samples and the measured data CDFs. This is because the mean of the measured instantaneous throughput samples is slightly different than the average throughput data utilized for the average throughput models for a given average RSS.

4.8   Simulation of WLAN Throughput

The comprehensive WLAN throughput models developed in this thesis and described in Section 4.7 allow for simulation of WLAN throughput for a given channel, average RSS, and operational mode. Generation of throughput samples can be easily performed using MATLAB. For Gaussian throughput variation modeling, invoking the `normrnd(`μ`,`σ`)` command with mean zero and standard deviation as given in Table 4-3 will generate the *throughput variations* about the average throughput, which then need to be added to the average throughput for a given average RSS as given by the models presented in Section 4.5. Gaussian RVs are also readily available by other means due to their universal nature.

For Weibull throughput variation modeling, the MATLAB function `wblfit(`λ`,`k`)` can be invoked to generate the *throughput* samples, where λ is the scale parameter and k the shape parameter, calculated using the equations given in Section 4.6.4 for a given average throughput, which in turn was calculated using the models in Section 4.5 for a given RSS. Although generation of throughput samples using MATLAB procedures is straightforward, even for the Weibull throughput variation model, doing so with other software or in hardware may be less so. The equation given by (4.21) yields RVs with a Weibull distribution[*****].

$$X = \lambda\left(-\ln(U)\right)^{1/k} \tag{4.21}$$

where λ is the Weibull scale parameter, k is the Weibull shape parameter, U is a uniformly distributed RV on the range (0,1], and X is an RV with a Weibull distribution defined by λ and k. The MATLAB functions for Gaussian and Weibull RV generation brought up in the previous two paragraphs were utilized for simulation of the throughput samples as given in the example shown in Figure 4-45.

4.9   Metric for Comparatively Analyzing Throughputs

A metric is proposed that will allow for relative comparison between the channel performance of different WLAN devices. This metric yields the normalized throughput for a give device in a given channel. An RF-isolated test platform, such as that developed and used for this thesis, is necessary for

---

[*****] See < http://en.wikipedia.org/wiki/Weibull_distribution >.

this metric so as to effectively compare devices. The control of the channel enabled through use of a multipath testbed allows for the necessary control required for comparative evaluation.

Calculation of the metric for comparative analysis of throughput involves three broad steps:

1) Find the area under the ideal throughput function (as a function of RSS) for a given device, in a given mode, in a given channel with the DLR cutoffs as specified by the manufacturer. Ensure that a specific configuration is utilized for calculation of the maximum achievable throughputs.

2) Collect data and calculated the maximum achievable throughput versus RSS, as described in Section 4.5.1 for the given device, in a given mode, in a given channel. Find the area under this function.

3) Divide the integrated measured throughput with the summation of the ideal throughput. The resulting value represents the fraction of the throughput given ideal circumstances and performance for a given device, in a given mode, for a given channel.

The metric should typically be less than 1, with more hostile channels yielding smaller values. When comparing the performance of two devices in the same channel, it can be noted which has superior performance simply by comparing the resulting metric. It should be noted that both devices should have similar performance specifications, such as DLRs supported. If a device does not support a higher rate, the rate could be included in the calculation of the ideal throughput for device comparison purposes. This metric effectively provides a relationship between the claimed performance of a given device and the channel that it is operating in. The equation describing the throughput comparison metric is given by (4.22). Note that the maximum power p_1 must be selected and kept the same for all devices being comparatively analyzed. A value of -40 dBm is suggested as this RSS represents a value at which all WLAN devices should be at optimum performance.

$$\Gamma = \frac{\int_{p_{\min}}^{-40} S_{avg}(p)dp}{\sum_{i=2}^{N} S_{i-1}(p_{i-1} - p_i)} \tag{4.22}$$

where $S_{avg}(p)$ is the measured average throughput versus average RSS function (in an RF-isolated testbed using an emulated channel), p_{min} is the RSS where the measured throughput goes to zero, S_i the theoretical per-DLR throughputs for the given WLAN operational mode, p_i the manufacturer specified DLR cutoffs, and N the number of DLRs plus one. For devices that have multiple DLRs with the same RSS cutoff, it is suggested to examine which DLR is utilized the most and use the theoretical throughput for that DLR or to calculated the weighted average of the multiple throughputs.
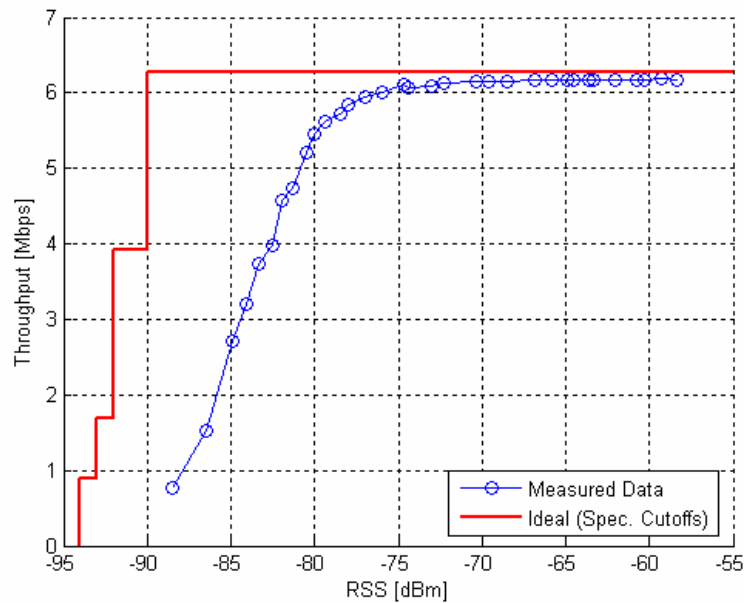
Figure 4-46 Average throughput data and versus average RSS with manufacturer specified upper bound on performance (calculated per-DLR throughputs with RSS cutoffs) for an IEEE 802.11b WLAN (long preamble) operating in TGn Channel Model B. The area under the measured data curve divided by the area under the manufacturer specified performance step function yields the comparative performance metric.

As an example, let us examine the proposed throughput performance metric for an IEEE 802.11b WLAN operating in Channel Model B. Figure 4-46 shows the measured throughput versus power data with the ideal throughput (calculated) overlaid at the cutoffs specified by the WLAN device manufacturer (Cisco). The area underneath the ideal throughput function (shown in red) represents the normalization factor in the metric whereas the area underneath the measured throughput function (shown in blue with circles at the data points) represents the total achieved throughput.

A numerical approximation to the integral of the measured data, from -40 dBm to -90 dBm (the projected RSS where the average throughput goes to 0 Mbps, as determined using the throughput model for the same operational mode and channel) yielded a throughput area of **2.7135x10^8 bps·dB**. The normalizing factor is **3.2384x10^8 bps·dB**. The ratio of the areas yields the performance metric Γ of **0.8379**, which can be interpreted as the WLAN device obtaining 83.79% of the ideal performance in the given channel (TGn Channel Model B) with the given operational mode (IEEE 802.11b).

Chapter 5:   Conclusions and Future Work

A multipath RF-isolated real-time multipath testbed was designed and implemented that enabled performance evaluation of WLANs in a controlled test environment for exploring the effects of the channel on performance, namely the average throughput versus average RSS and instantaneous throughput variation. A measurement database of IEEE 802.11b and 802.11g WLAN performance data in four channels emulated was compiled for analysis and modeling of throughput using the multipath testbed. The performance data was utilized to develop models describing the average throughput as a function of average RSS and instantaneous throughput variation.

WLAN throughput data showed that the wireless channel has a significant impact on the achievable throughput. A highly piecewise linear relationship between average throughput and average RSS was observed for fading channels; this relationship was less correlated for the constant (ideal) channel because WLAN devices have a stepwise throughput-power relationship when operated in an ideal environment. The stepwise throughput-power relationship is a result of the multi-rate IEEE 802.11 PHY layer. Nonetheless, the piecewise linear model was adopted for the constant channel due to its simplicity and also because the constant channel is analyzed merely as a reference (it does not represent a realistic environment).

Analysis of the instantaneous throughput variations showed that fading channels increase the spread in throughput variation and that the spread in variation changes as the average RSS decreases, which is shown and modeled using CDFs for the four different channels analyzed. Models were designed to describe the instantaneous throughput variations for the constant channel, and TGn Channel Models A, B, and C using the Weibull and Gaussian distributions. For Weibull modeling, the Weibull scale and shape parameters were modeled as functions of the average throughput, which can be calculated if given an average RSS, the channel that the WLAN is operating in, and the WLAN operational mode using the average throughput models developed in this thesis. This has the advantage of varying the shape of the CDF with respect to changes in average throughput, which was the behavior observed. Gaussian modeling combined all throughput variations into a single zero-mean distribution that globally describes the throughput variations for a given channel and WLAN operational mode.

The average throughput models and throughput variation models are combined to form comprehensive throughput models that describe both the average throughput and throughput variation.   The comprehensive throughput models proposed use both the Weibull and Gaussian throughput variation

models, yielding slightly different comprehensive throughput models for each case. These models can be used to describe throughput behavior and realistically simulate throughput samples. The models are applicable to researchers working in the higher layers, allowing them to incorporate the expected average throughput and throughput variation for a given average RSS into their research, thereby enabling more applicable results.

The repeatable average throughput versus average RSS data collected using the multipath testbed can be utilized for comparative performance analysis because of channel controllability in the testbed. A metric is proposed for comparative performance evaluation of WLAN devices that relates the achieved throughput performance to the manufacturer specified performance bound. The metric describes the relative performance of a WLAN device under certain set conditions, disregarding the maximum achievable performance, which is normalized out. A sample calculation with the Cisco Aironet WLAN client connected to the Linksys AP in IEEE 802.11b mode and operating in TGn Channel Model B showed that the WLAN client achieved 0.8379 (83.79%) of the possible performance. In stable channels, the metric will be closer to one and become smaller for more hostile channels.

Future work in this area would include expansion of the multipath testbed for performance evaluation of MIMO WLANs, measurements and modeling of throughput performance of MIMO WLANs, analysis of the effects of the wireless channel on packet loss and jitter, and further analysis into the impact of packet length on performance. Performance analysis and modeling of VoIP and video streaming applications could be performed using the multipath testbed to understand how streaming applications are impacted by the variability of the wireless channel. Additionally, WLAN performance could be analyzed and modeled for multi-client/multi-AP WLAN network configurations. Automation of the data collection procedure would facilitate a broader, more comprehensive data collection and performance modeling campaign.

Appendix A: IEEE 802.11n Channel Model PDPs

The tap delay and average power are given in Table A-1 and Table A-2 for IEEE 802.11n channel models B and C. The PDP parameters for Channel Model A and the constant channel are not given as there is only one tap in these cases, with a delay of 0 ns and an average power of 0 dB. For more information on these channel models see [IEE04].

Table A-1 Tap Delay and Average Power Specifications for Channel Model B

Tap Delay [ns]	*Average Tap Power [dB]*	
	Cluster 1	*Cluster 2*
0	0	–
10	-5.4	–
20	-10.8	-3.2
30	-16.2	-6.3
40	-21.7	-9.4
50	–	-12.5
60	–	-15.6
70	–	-.18.7
80	–	-21.8

Table A-2 Tap Delay and Average Power Specifications for Channel Model C

Tap Delay [ns]	Average Tap Power [dB]	
	Cluster 1	Cluster 2
0	0	–
10	-2.1	–
20	-4.3	–
30	-6.5	–
40	-8.6	–
50	-10.8	–
60	-13.0	-5.0
70	-15.2	-7.2
80	-17.3	-9.3
90	-19.5	-11.5
110	–	-13.7
140	–	-15.8
170	–	-18.0
200	–	-20.2

Appendix B: Azimuth™ Systems 801W Tutorial

A brief tutorial on setting up a WLAN client and AP within the Azimuth™ Systems 801W test platform is presented here.   For more details on setting up the Azimuth™ test system and details on its implementation, the reader is referred to [AZI04a, AZI04b, AZI05] and other documentation available from Azimuth™ Systems.   The tutorial aims to help in setting up a simple one client, one AP infrastructure network through the Azimuth™ test platform.   A simple traffic generation and capture is performed.   An extension of this tutorial is to use the network that is setup here and run the Azimuth™ Rate vs. Range script to get throughput versus path-loss results.

This tutorial assumes that an Azimuth™ Systems 801W with an RFM, STM, and WLA has been setup and is functional.   Additionally, there should be an accompanying MTH RF isolation chamber for the WLAN AP.   The RF connectors of the WLAN client and AP should be exposed (which required removal of device casing).   Azimuth™ recommends removal of the antennas on the WLAN devices; this can or cannot be done.   There will be degradation in performance (higher attenuation) due to there being a mismatch if antennas are left attached.

Step 1

Install any necessary drivers for the WLAN client.   The Azimuth™ DIRECTOR™ computer has a shared folder on the D: drive.   Place any drivers into the shared folder and these can be accessed from the STM PC by opening an Explorer window and connecting to the DIRECTOR™ PC using FTP (type **ftp:\\192.168.2.1** for the URL with username **console** and password **azimuth**).   The STM PC can be accessed via Remote Desktop from the DIRECTOR™ software by right clicking in the leftmost column on the STM icon.   For the purposes of this tutorial, we will leave the default settings for the WLAN client

Concerning the WLAN AP, it may be necessary to change the IP address from the default address as there may be an IP conflict.   Make sure the IP address is of the form **192.168.xx.1**.   Check that DHCP is enabled.   Leave all other settings at their default values.

Step 2

Insert the WLAN client into the Carrier Card that will be inserted into the STM.   Connect the RF cables with the correct RF connector to the ports of the WLAN card (there are typically two for a SISO

WLAN). If there is a splitter, connect both cables to the splitter; if not, terminate one end and connect the other end to the RF port of the Carrier Card. Insert the Carrier Card into the STM and securely close the door. This isolates the WLAN client from outside interference.

Likewise, connect the primary antenna of the WLAN AP to the RF port at the back of the MTH. There is typically a second antenna port on the AP – this should be terminated. The power connection and Ethernet connection (to the Azimuth™ Test-Net) must be connected through the filtered ports at the back of the MTH. Securely close the MTH cover so that the AP is isolated from outside interference.

Step 3

Connect the RF port of the MTH (that is connected to the AP internally) to RF Port 1A of the RFM. This is internally connected via the RF backplane of the 801W chassis to the WLAN client inside the STM. There are three attenuators in this propagation path; it is recommended to set one of the attenuators to 20 dB to ensure that the WLAN STAs are not saturating. However, it is recommended to change the attenuation of the signal path once the network is setup to see how the data rate changes as the path attenuation is increased, etc.

Check that the STM and WLA are set so that the RF signal is routed to the RF chassis common. This is done by right clicking on the respective module in the Director window left pane and clicking on RF Configuration, which brings up a window allowing the user to change the RF switch setting and attenuation of the attenuators in the modules. The WLAN client should not be able to associate to the WLAN AP.

Step 4

Set up the Azimuth™ traffic generator, which is accessible from the DIRECTOR™ window left pane by right clicking on the WLAN client and clicking on Traffic Generator. Add the MAC address of the WLAN AP as the destination and click the *enable traffic* checkbox. The other parameters, such as the traffic density and frame length can be adjusted as desired. The traffic can now be started and stopped from the DIRECTOR™ window toolbar.

Remote Desktop into the WLA by right clicking on the WLA in the DIRECTOR™ left pane. Start a packet capture (make sure to choose the correct channel, WLAN analyzer, etc.) and the packets traveling between the client and AP will be shown.

Appendix C: Elektrobit PROPSim™ C8 Tutorial

A brief tutorial describing the setup of a simple multipath fading channel using the PROPSim™ C8 is presented here. For the purposes of this tutorial, it will be assumed that channel 1 and 2 of the PROPSim™ are being used and that a setup similar to that used for data collection in this thesis, with a single WLAN client and WLAN AP infrastructure network that is already setup with uplink and downlink signal routed to the unidirectional PROPSim™ channels is being used. In order to utilize the channel setup here with the Azimuth™ system, a different Azimuth™ configuration than that which is described in Appendix B will need to be utilized.

An external RF local oscillator is needed to use the PROPSim™ RF input/output ports. This should be set to generate a continuous wave signal with the power at each PROPSim™ RF local oscillator input at 0 dBm. The frequency of the local oscillator needs to be 300 MHz above the center frequency if the center frequency being used is less than or equal to 3 GHz or 300 MHz below the center frequency if the center frequency being used is greater than 3 GHz.

Step 1

Set up the channel correlation matrix for the uplink and downlink PROPSim™ channels. For simplicity, this should be set to 1, which defines a reciprocal channel. Setup of the channel correlation matrix is done by running the PROPSim™ Correlation Editor program.

Step 2

Define the desired channel model by specifying the channel PDP using the PROPSim™ Channel Model Editor program. Since correlated uplink and downlink channels are being used, a single PDP must to be defined. When starting the Channel Model Editor program, specify that there are two channels and that a correlative channel model will be defined in the popup window that comes up. The center frequency, channel model accuracy, tap delays, tap powers, fading, Doppler, etc. need to be specified here for the channel that will be emulated.

Step 3

Specify the PROPSim™ channel(s) to be utilized, the signal routing, input power levels (can be changed later), output gain (can be changed later), etc. using the PROPSim™ Simulation Editor

program. Once the desired test configuration has been entered, the simulation setup should be saved followed by generation of the simulation file.

Step 4

Open the simulation that was generated using the PROPSim™ Simulation Editor using the PROPSim™ Simulator Control program. The WLAN clients connected should now be able to associate. Adjust the input power level setting at the PROPSim™ for the two channels being used so that there is not signal clipping, which will be indicated in the lower pane of the Simulator Control program when the simulation is running. The output attenuation (gain) can be changed to lower the RSS at the receiving STA. The Doppler can be varied by adjusting mobile velocity if desired. There is a run button in the Simulator Control window toolbar that is used to start the simulation. Note that some parameters can be changed during emulation while others can only be changed when the simulation is stopped (make sure to click the "apply" button or else the changes will not be reflected in the channel emulation). Variations in the RSS or SNR should now be observable if simulating a fading channel, using WLAN client software or a WLAN protocol analyzer.

Appendix D: Results Presented at CISS 2006

The results included in this Appendix were presented at the Conference on Information Sciences and Systems (CISS) in March 2006 at Princeton University, Princeton, NJ, USA. They represent preliminary results, as modifications to the testbed were made following submission of the paper. However, they do provide insight into the nature of throughput for IEEE 802.11b/g WLANs and how throughput can be modeled as a function of received power. Please see [MET06] for the complete final paper, which includes throughput-power models for IEEE 802.11b/g WLANs.

In the paper, the multipath testbed was described and data collection methodology presented. We then proceeded to show how maximum throughput is a function of the received power and propagation environment. Throughput versus power models were proposed using line fitting for four channels: single tap constant, single tap lognormal, single tap Rayleigh, and multi-tap IEEE 802.11n Channel Model B[†††††]. It should be noted that the uplink and downlink channels for these measurements were uncorrelated; this was a testbed modification made later. There were some other minor testbed modifications as well, such as the AP being changed and the AP signal being routed through the Azimuth™ RFM.

Another change was in the generation of throughput data points. The same methodology was implemented (taking the vector product of the DLR probabilities and calculate per DLR throughputs) to find the maximum throughput for a given measurement sample. However, the probability of having a "0 Mbps" frame was modified to be more accurate. In its place, a deadtime probability metric is utilised, which states the probability that the WM is not actively being used for an ideal frame transmission (one without any retransmissions). The previous method utilized the total number of frames that Airopeek received in relation to the total number of data frames that were filtered. See Section 4.5.1.3 for details on the calculation of deadtime probability.

[†††††] The Doppler spectrum for the IEEE 802.11n channel model B and other channels was flat. The channel model document specifies a flat spectrum for channel model A (single tap Rayleigh), but a bell-shaped spectrum for the other channels.

The objective of the paper was to present the multipath testbed that we had developed for examining the nature of channel effects on WLAN performance and provide channel dependent average throughput versus power models that could be used as a starting point for determining what throughput could be expected for a given received power in a given physical environment. We showed how power variations cause DLR variations, which we depicted as DLR histograms that ultimately lower maximum achievable throughput. The DLR probability distribution for a given received power can be used, along with calculated throughput per-DLR for a given transmission protocol, to determine what the maximum possible throughput for that given power level and channel is. Figure D-1 through Figure D-4 show the average throughput data with throughput models overlaid and sample DLR histograms for four different channels (constant, lognormal, Rayleigh, and TGn Channel Model B). The WLAN mode was IEEE 802.11b/g for the figures presented.

(a)   (b)

Figure D-1 Average throughput data versus average RSS with throughput model and sample DLR probability histograms for an IEEE 802.11b/g WLAN operating in a single-tap constant channel: (a) average throughput and (b) sample DLR histograms.

(a)   (b)

Figure D-2 Average throughput data versus average RSS with throughput model and sample DLR probability histograms for an IEEE 802.11b/g WLAN operating in a single-tap lognormal fading channel: (a) average throughput and (b) sample DLR histograms.

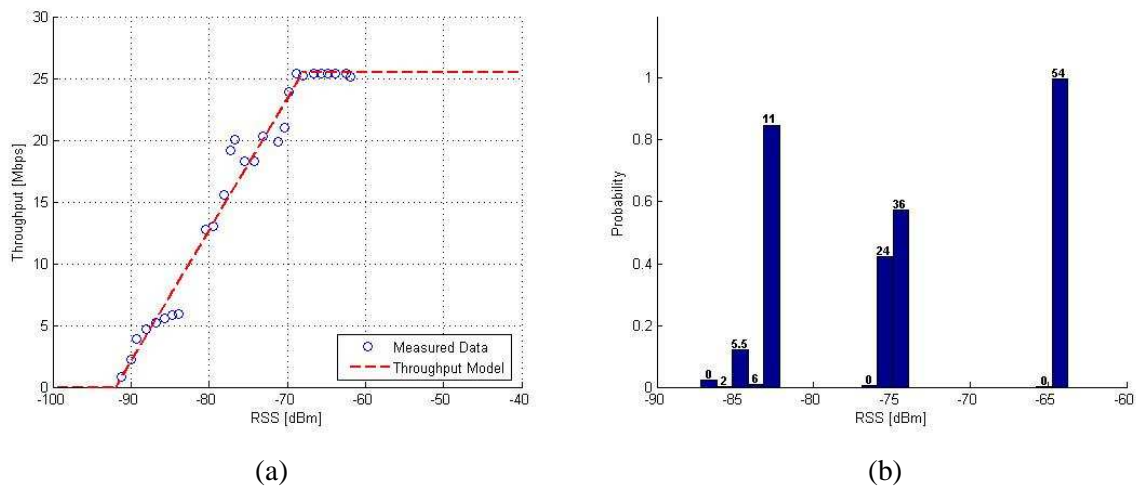(a)   (b)

Figure D-3 Average throughput data versus average RSS with throughput model and sample DLR probability histograms for an IEEE 802.11b/g WLAN operating in a single-tap Rayleigh fading channel: (a) average throughput and (b) sample DLR histograms.

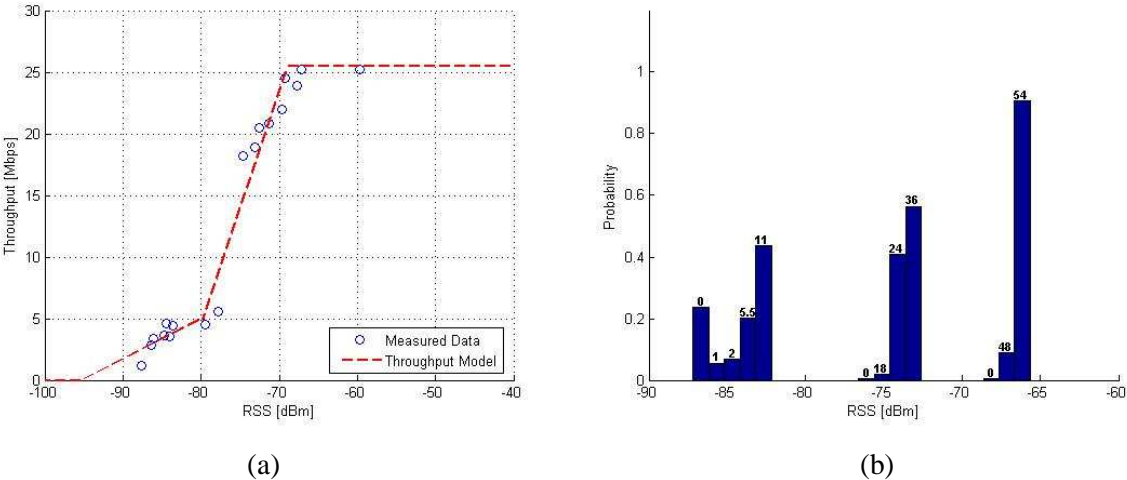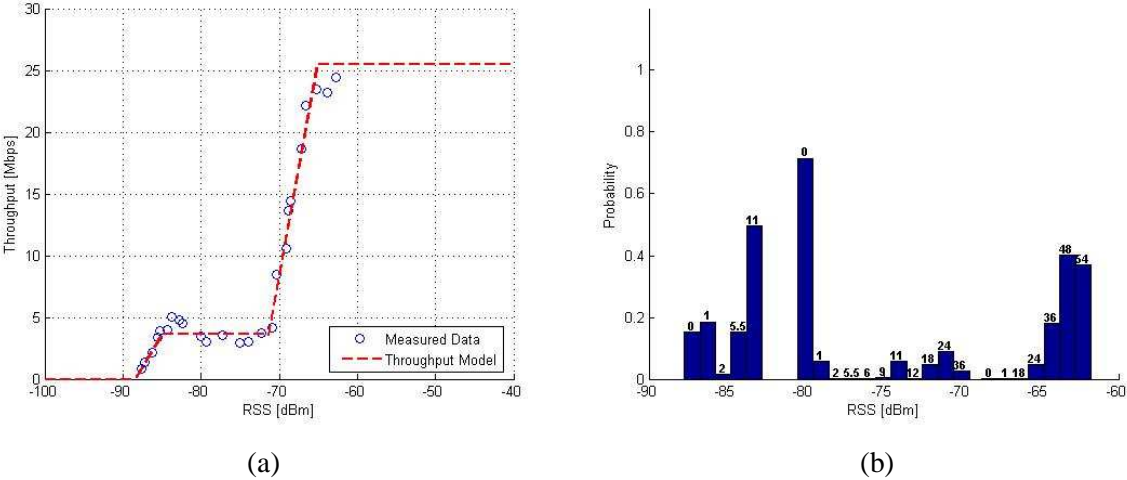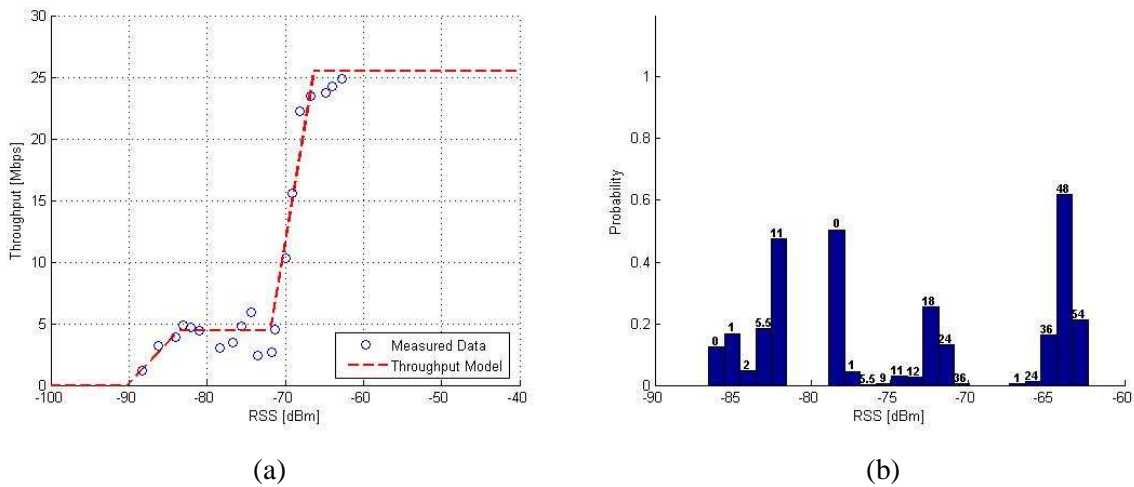(a)   (b)

Figure D-4 Average throughput data versus average RSS with throughput model and sample DLR probability histograms for an IEEE 802.11b/g WLAN operating in TGn Channel Model B: (a) average throughput and (b) sample DLR histograms.

Our results for an IEEE 802.11b/g WLAN showed that there is a significant decrease in throughput when comparing the multipath, fading IEEE 802.11n channel model B throughput versus power plot with that of a constant channel. Our throughput plots indicated that there was an approximately 15 Mbps drops in throughput between -70 dBm and -80 dBm between the ideal constant channel and more realistic channel model B. Additionally, the results for a single tap Rayleigh channel were similar to that of channel model B. The lognormal channel was slightly better, showing a slower drop in throughput than the fast fading channels. The models that were presented were piecewise linear, with the average RSS (in dBm) being the independent variable.

References

[AZI04a]   *Azimuth™ Mini RF Test Head User Guide*, Pub. No. 14219, Rev. v1.0.2, December 2004.

[AZI04b]   *Azimuth™ RF Port Module Hardware Installation and Description Guide*, Pub. No. 13749, Rev. v1.0.2, December 2004.

[AZI05]   *Azimuth™ Wireless LAN Analysis Platform Operations Guide and Azimuth™ DIRECTOR™ User Guide: Release 4.0*, Pub. No. 13739, Rev. v2.0.2, January 2005.

[BHA03]   V. Bhatia, W.-Y. Chen, and L. T. Metreaud, "Design of a Technique for Deployment of IEEE 802.11b/g WLANs," 2003, Major Qualifying Project, WPI.

[BRO93]   G. Bronson, K. Pahlavan, and H. Rotithor, "Performance Prediction of WLANs Based on Ray Tracing Algorithm," in *Proceedings of the IEEE PIMRC'93*. IEEE, September 1993.

[CIS05a]   *Cisco 7920 Wireless IP Phone Design and Deployment Guide: Appendix I*, Text Part Number: OL-6383-04, Cisco Systems, Inc., October 2005.

[CIS05b]   *Cisco Aironet 802.11a/b/g Wireless Cardbus Adapter Data Sheet*, Cisco Systems, Inc., 2005.

[FEI99]   J. Feigin and K. Pahlavan, "Measurement of Characteristics of VoIP in the WLAN Environment," in *IEEE MoMuC*, IEEE, November 1999.

[GOP04]   P. Gopalakrishnan, P. Spasojevic, L. Greenstein, and I. Seskar, "A Method for Predicting the Throughput Characteristics of Rate-Adaptive Wireless LANs," in *Proceedings of the 60th Bi-Annual Vehicular Technology Conference*. IEEE, Fall 2004.

[HEN01]   B. E. Henty, "Throughput Measurements and Empirical Prediction Models for IEEE 802.11b Wireless LAN (WLAN) Installations," M.S. Thesis, Virginia Polytechnic Institute and State University, Blacksburg, Virginia, USA, August 2001.

[IEE99a]   IEEE Working Group 802.11, *Part 11: Wireless LAN Medium Access Control (MAC) and Physical Layer (PHY) Specifications*, ANSI/IEEE, 1999 (Reaffirmed 2003).

[IEE99b]   IEEE Working Group 802.11a, *Part 11: Wireless LAN Medium Access Control (MAC) and Physical Layer (PHY) Specifications, High-Speed Physical Layer in the 5 GHz Band*, IEEE, 1999 (Reaffirmed 2003).

[IEE99c]   IEEE Working Group 802.11b, *Part 11: Wireless LAN Medium Access Control (MAC) and Physical Layer (PHY) Specifications, Higher-Speed Physical Layer Extension in the 2.4 GHz Band*, IEEE, 1999 (Reaffirmed 2003).

[IEE03]   IEEE Working Group 802.11g, *Part 11: Wireless LAN Medium Access Control (MAC) and Physical Layer (PHY) Specifications, Amendment 4: Further Higher Data Rate Extension in the 2.4 GHz Band*, IEEE, 2003.

[IEE04]   IEEE 802.11 Working Group, "TGn Channel Models," IEEE 802.11-03/940r4, May 2004.

[IEE06]   IEEE Working Group P802.11n™/D1.0 (Draft Amendment), *Part 11: Wireless LAN Medium Access Control (MAC) and Physical Layer (PHY) Specifications: Enhancements for Higher Throughput*, IEEE, March 2006.

[MET06]   L. T. Metreaud and K. Pahlavan, "RF-Isolated Real-Time Multipath Testbed for Performance Analysis of WLANs," presented at the 40th Annual Conference on Information Sciences and Systems, Princeton, NJ, 2006.

[PAH02]   K. Pahlavan and P. Krishnamurthy, *Principles of Wireless Networks: A Unified Approach*, 1st ed. Prentice Hill, 2002.

[PAH05]   K. Pahlavan and A. Levesque, *Wireless Information Networks*, 2nd ed. John Wiley & Sons, 2005.

[PRO02]   *PROPSim™ C8 Wideband Multichannel Simulator: Operational Manual*, August 2002 Edition, Elektrobit Group, Ltd., August 2002.

[SIL04]   A. Silvennoinen and T. Karhima, "IEEE 802.11b WLAN Capacity and Performance Measurements in Channel with Large Delay Spreads," in *Proceedings of the 2004 IEEE Military Communications Conference*, IEEE, 2004.

[STE03]   C. Steger, P. Radosavljevic, and J. P. Frantz, "Performance of IEEE 802.11b Wireless LAN in an Emulated Mobile Channel," in *Proceedings of the 57th IEEE Semiannual Vehicular Technology Conference*, IEEE, Spring 2003.

[WIJ05]   A. L. Wijesinha, Y. tae Song, M. Krishnan, V. Mathur, J. Ahn, and V. Shyamasundar, "Throughput Measurement for UDP Traffic in an IEEE 802.11g WLAN," in *Proceedings of the Sixth International Conference on Software Engineering, Artificial Intelligence, Networking, and Parallel/Distributed Computing and First ACIS International Workshop on Self-Assembling Wireless Networks*. IEEE, 2005.

[ZAH97]   A. Zahedi and K. Pahlavan, "Natural Hidden Terminal and Throughput of a WLAN," *IEEE Electronic Letters*, April 1997.

[ZAH00]   A. Zahedi and K. Pahlavan, "Capacity of a WLAN with Voice and Data Services," *IEEE Transactions on Communications*, July 2000.

[ZHA90]   K. Zhang and K. Pahlavan, "An Integrated Voice-Data System for WLANs," *IEEE Transactions on V.T.*, April 1990.